Inactivation of Protein Tyrosine Phosphatases by Dietary and Endogenous Agents

---

A Dissertation

Presented to

The Faculty of the Graduate School

University of Missouri

In partial Fulfillment

Of the Requirements for the Degree

Doctor of Philosophy

By

DERRICK R. SEINER

Dissertation Advisor: Dr. Kent Gates

MAY 2009

The undersigned, appointed by the Dean of The Graduate School, have examined the dissertation entitled:

INACTIVATION OF PROTEIN TYROSINE PHOSPHATASES BY ENDOGENOUS AND DIETARY AGENTS

presented by Derrick R. Seiner

a candidate for the degree of Doctor of Philosophy

and hereby certify that in their opinion it is worthy of acceptance.

_____

Professor Kent S. Gates

_____

Professor Timothy Glass

_____

Professor Silvia Jurisson

_____

Professor Susan Lever

_____

Professor Tom Quinn

To my family, with love.

I dedicate this dissertation to my family, whose love, encouragement, and support have made this all possible. I wish to thank my parents, Brent and Vesta Seiner for their tremendous level of support for my education, in all ways. I would also like to thank my brothers, Heath and Nick, and my Sisters-in-law, Lori and Danielle, for their encouragement and support. Together, all of this support has made this dream become a reality.

Most of all, I need to sincerely thank my fiancée, Brienne Nicole. She has made me a better scientist, but more importantly, she has made me a better person. I am very excited to spend the rest of my life in her company.

ACKNOWLEDGEMENTS

I have been blessed with several people in my life who have had an impact on my journey through graduate school. Although they all deserve more than one page in the beginning of this document, I hope they understand how grateful I truly am.

First, I need to thank my advisor, Kent Gates, for his unwavering patience and commitment toward developing young graduate students into real scientists. In his laboratory, I have learned how to design, execute, and most importantly, critically think about scientific research. I wish to sincerely thank him for all that he has done for me.

I wish to thank my dissertation committee members, who have taken time out of their busy schedules to provide me guidance over the years: Dr. Tim Glass, Dr. Susan Lever, Dr. Silvia Jurisson, and Dr. Tom Quinn.

I need to thank my colleagues in the Gates lab. My fellow labmates have made this experience a fun and exciting one. In addition, I need to thank my colleagues in the Chemistry department, several of you have made my time in and out of lab much more enjoyable.

I would also like to thank Beverly DaGue for helping me with the mass spectrometry work. Furthermore, Jerry Brightwell and Bill Vellema have been extremely helpful to me on a number of occasions, thank you both.

TABLE OF CONTENTS

CHAPTER 2. THE INACTIVATION OF PTP1B BY THE ENDOGENOUS/DIETARY ALDEHYDE ACROLIEN

List of Tables

Page

LIST OF FIGURES

Page

LIST OF SCHEMES

Page

ABSTRACT

Protein tyrosine phosphatases (PTPs) are cysteine dependent enzymes responsible for dephosphorylating phosphotyrosine residues through a phosphocysteine intermediate. PTPs work in tandem with protein tyrosine kinases to regulate a number of essential mammalian signal transduction pathways. These are critical cellular pathways and their disruption by inhibition or inactivation of these enzymes can lead to profound biological consequences.

The α,β-unsaturated aldehyde acrolein has been shown to have a wide variety of biological activity, and exposure to acrolein can come from a variety of sources. Acrolein is found in cigarette smoke, dietary sources, and is also produced endogenously through lipid peroxidation or oxidation of certain amino acids. This electrophilic aldehyde has been shown to covalently modify critical cysteine residues on a variety of proteins. PTPs are cysteine dependent enzymes, and we proposed that some of acroleins biological activity could derive from modification of PTPs.

We found that acrolein is indeed a potent, time-dependent, irreversible inactivator of the archetypal PTP, PTP1B. To explore the inactivation mechanism, we chose to perform MALDI TOF/TOF mass spectrometry on the tryptic-digested acrolein-inactivated enzyme. A major signal was identified that corresponded to the active site peptide modified by acrolein. Nanospray MS/MS-TOF was employed to identify which residue(s) were modified on the active site peptide. The data revealed acrolein primarily modified the peptide at the active site cysteine. To establish the mechanism of inactivation, a structure-activity study was undertaken with related aldehydes. We found

the aliphatic aldehydes such as propanal or acetaldehyde to be relatively poor inactivators of PTP1B. This provides evidence that the inactivation of PTP1B proceeds through a conjugate addition mechanism involving the carbon-carbon double bond of acrolein. This work has completely characterized the inactivation of PTP1B by acrolein, and provides evidence supporting the notion that some of acroleins biological activity comes from PTP inactivation.

Another project involves the effects of dietary phytochemicals on PTPs. Isothiocyanates (R-N=C=S), from cruciferous vegetables, have been reported to have a wide variety of biological activity. Similar to acrolein, isothiocyanates such as allyl and benzyl isothiocyanate, as well as sulforaphane, have been reported to modify functionally critical cysteine residues inside cells. We thought it was possible that some of isothiocyanates biological activity could be derived from the inactivation of PTPs.

We have found isothiocyanates to be time-dependent, reversible inactivators of PTP1B. The kinetics of inactivation has been characterized for sulforaphane, and allyl and benzyl isothiocyanate. Allyl isothiocyanate, being the most potent inactivator studied, was chosen for characterization by tryptic digestion mass spectrometry, and the mass spectrometry revealed modification at several cysteine residues of PTP1B, including the active site cysteine. PTPs are validated targets for many different diseases, and the dietary isothiocyanates activity against PTPs could be a chemical explanation for their biological activity. This work could provide a 'chemical bridge' between the immense evidence that diet can have a profound effect on disease.

Additionally, crystal structures of proteins can provide a vast amount of information about enzyme function, inhibition and mechanism. Toward this end, we sought to produce our own crystal structures of PTP1B. PTP1B was crystallized, based on a modified literature procedure, and the structure of PTP1B was solved to 1.85Å, with refinement in PHENIX and model building in COOT. Additionally, the structure of oxidized PTP1B, with a sulfenylamide in the active site was also solved at 2.3Å. Crystal structures of PTP1B inactivated by various agents are a continuing project, which holds a great deal of promise to deliver a vast amount of information.

PTPs share a common active site motif; however, we thought it would be prudent to have another PTP in our hands for both structural and kinetic comparisons besides PTP1B. Toward this end, SHP2, another PTP, was expressed by recombinant methods and purified by Ni-NTA and cationic exchange. We have assessed the kinetics of inactivation by H_2O_2, a known endogenous regulator of PTPs, and found it to be similar to PTP1B. Crystallization trials are currently underway with SHP2, with promising potential.

PTPs have been the focus of the majority of my graduate research, but I have also spent some time investigating DNA chemistry. Abasic sites are the most common DNA damage event inside cells, with calculations on the order of 10,000 abasic sites per cell, per day. This laboratory has previously reported a sequence involving an abasic site that produces a DNA intrastrand crosslink under biologically relevant conditions. DNA crosslinks are known to have profound biological consequences. Therefore, we set out to explore the effect of sequence context on the rate and yield of the DNA intrastrand crosslink formed by the abasic site.

We have calculated the rate of crosslink formation, using ^{32}P labeled DNA and monitoring the formation of the DNA crosslink by Polyacrylamide gel electrophoresis. We find that formation of the crosslink has a half-life on the order of hours, which is significant on a physiological time scale. Additionally, we found that sequence context does indeed have a significant impact on the formation of a DNA crosslink. For example, when guanine is placed opposite of the abasic site, the yield of crosslink more than doubled, over any other nucleotide. This sequence information is vital to understand how often this crosslink may be occurring inside cells. Further, the intrastrand crosslink has been shown previously to be stable to APE1, a DNA repair enzyme. As well as further sequence context investigation, the crosslink's stability will be tested against several DNA repair enzymes, to learn more about the viability of the crosslink inside cells.

Introduction to Protein Tyrosine Phosphatases

1.1 Background on Protein Tyrosine Phosphatases

Protein Tyrosine Phosphatases (PTPs) were once viewed as housekeeping enzymes, charged with the routine task of removing phosphoryl groups from phosphorylated protein tyrosine residues in a nonspecific fashion.[1] This idea, however, has been rendered obsolete. It has been shown that the human genome encodes about 100 different PTPs, each with specific substrate specificities.[2]

It has also been well established that the phosphorylation of protein tyrosine residues plays a central role in controlling a number of critical mammalian signal transduction pathways.[3] The phosphorylation of certain tryrosine residues serves as a biochemical "switch" that alters the function of many different proteins involved in these signal transduction pathways.[4] PTPs work in tandem with protein tyrosine kinases, which catalyze the addition of the phosphoryl groups, to control the phosphorylation status of tyrosine residues in these proteins (Figure 1-1).[2, 5] Together, protein tyrosine phosphatases and protein tyrosine kinases are responsible for both the "on" and "off" of many functionally critical signaling pathways.[2, 6]

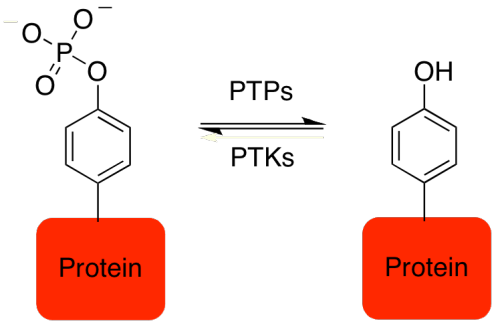

Figure 1-1 PTPs (Protein Tyrosine Phosphatases) and PTKs (Protein Tyrosine Kinases) work in tandem to control the phosphorylation status of tyrosine residues of proteins.

Given the important function that PTPs play in a number of signal transduction pathways, it is not surprising that the inhibition of PTPs can yield profound biological effects. For this reason, a number of groups have attempted to discover and produce novel PTP inhibitors, and thus, a new class of therapeutic agents.[7-12]

1.2 PTP Active Site Structure

We will describe the structure and catalytic mechanism in the context of protein tyrosine phosphatase 1B (PTP1B) because this enzyme has been identified as an archetypal member of this family of enzymes and is the focus of many experiments in this document.[13-17] PTPs share an active site sequence motif [I/V]HCXXGXXR[T/S], referred to as the phosphate-binding loop, or P-loop.[16, 18] The cysteine residue in this P-loop (Cys 215 in PTP1B) has an abnormally low pK_a of 5.7, versus about 8.5 for a normal cysteine thiol, and therefore, exists as the more nucleophilic thiolate (RS^-) form at physiological pH.[19] The thiolate charge of the active site cysteine is stabilized mostly by binding to a network of N-H groups of the P-loop (Figure 1-2).[20]

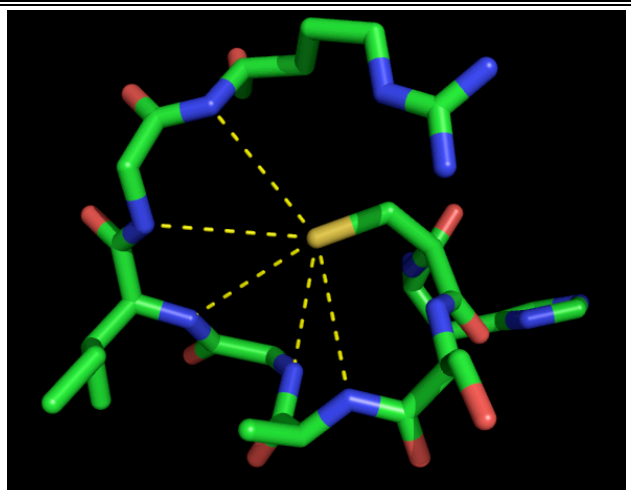

Figure 1-2. The active site cysteine thiolate, in PTP1B, interacts with several NH groups of the P-loop[21] in the crystal structure of the enzyme, the rest of the protein has been hidden for clarity.

In addition to the P-loop, another loop involved in the catalytic mechanism of PTP1B is the WPD loop. When the phosphorylated tyrosine substrate binds, the WPD loop (amino acids 79-187) closes the active site by moving approximately 12 Å forming a π-stacking interaction with the phenyl ring of the substrate (Figure 1-3).[22] This moves Asp 181 into position for catalysis, as described in the next section.

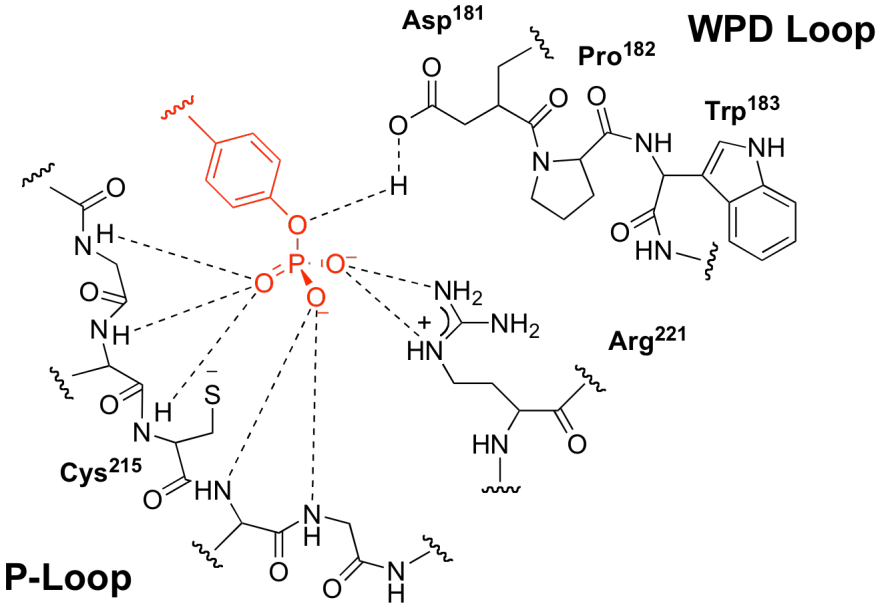

Figure 1-3. The active site of PTP1B with a phosphorylated tyrosine substrate bound, displaying only the P-loop, and the WPD loop, for clarity.[21]

1.3 PTP Catalytic Mechanism

The catalytic mechanism of PTPs has been well established. As mentioned above, upon binding of substrate, the WPD loop moves to close the active site pocket. In the first step, the nucleophilic active site thiolate residue (Cys 215) attacks the phosphoryl group of the substrate, forming a phosphoryl cysteine intermediate.[23] The leaving group, a phenolate ion, is stabilized in flight by the donation of a hydrogen atom from Asp 181 of the WPD loop.[24] This same residue, Asp 181, then activates a water molecule for nucleophilic attack on the phosphoryl cysteine intermediate in the final step of catalysis. Inorganic phosphate and active enzyme are then released, and the catalytic cycle is complete (Scheme 1-1).[24]

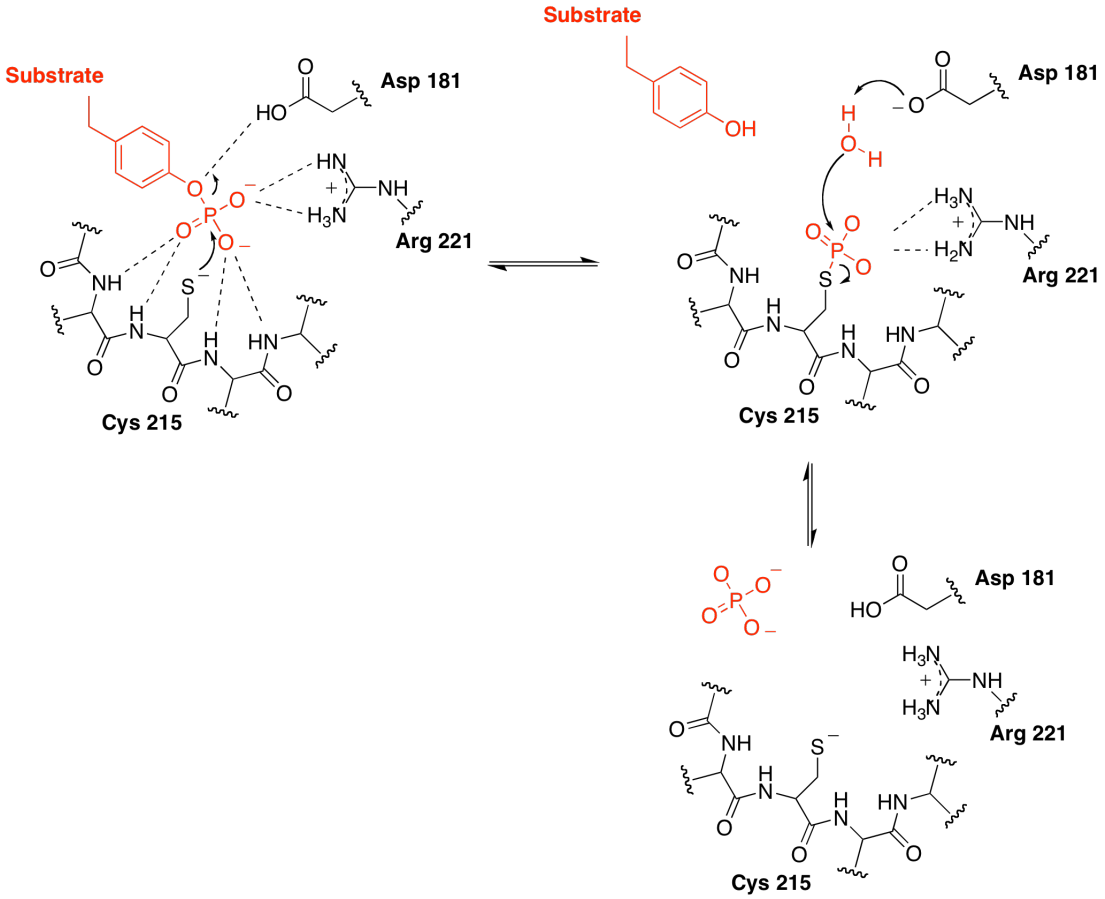

Scheme 1-1. The PTP catalytic mechanism for the dephosphorylation of a phosphorylated tyrosine residue, using PTP1B numbering of the amino acids.

1.4 PTP1B involvement in the Insulin Signaling Pathway

PTPs are involved in a number of mammalian signal transduction pathways. A prime example of this is the involvement of PTP1B in the insulin signaling cascade. PTP1B has been identified as the negative regulator of the insulin signaling cascade.[25] As illustrated in Figure 1-4, binding of insulin to the dimeric insulin receptor triggers the insulin signaling pathway inside the cell. Specifically, binding of insulin causes activation of the insulin receptor, causing both autophosphorylation of the insulin receptor and the insulin receptor subtrates (IRS) 1, 2, and 3. These phosphorylation events trigger a cascade of events inside the cell that ultimately lead to Glut 4 translocation to the cellular membrane and glucose uptake and utilization by the cell.[7, 22]

Activation of the insulin signaling pathway involves the phosphorylation of several tyrosine residues on both the insulin receptor and the IRS. Clearly, the dephosphorylation of these tyrosine residues would result in the termination of the insulin signaling pathway. PTP1B has been identified as the negative regulator of the insulin signaling pathway because it catalyzes the removal of the tyrosine phosphoryl groups from the insulin receptor and the IRS, thus abrogating the action of insulin.[9, 21, 26, 27]

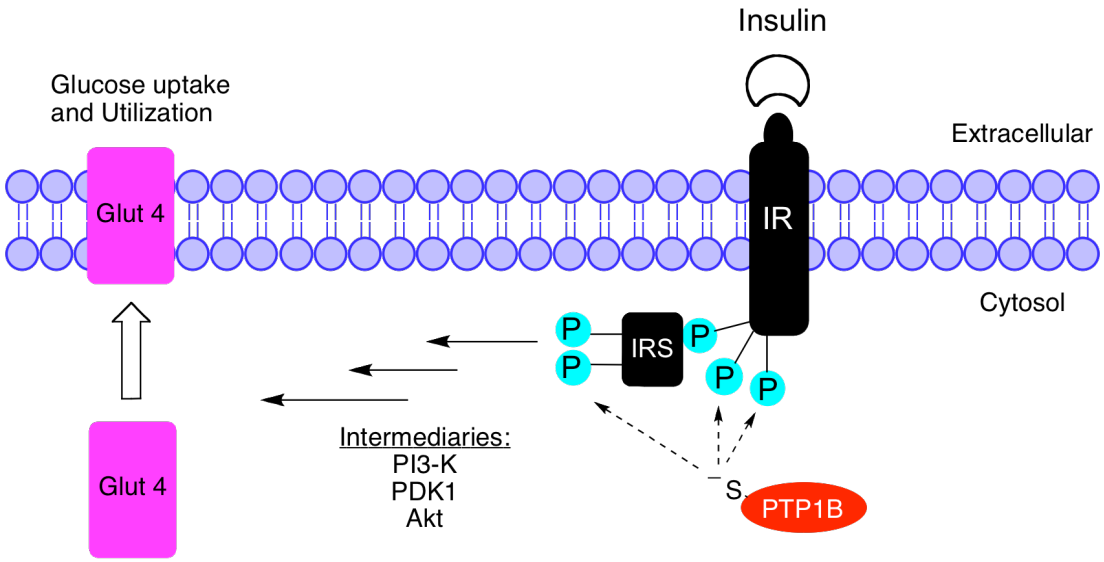

Figure 1-4. A simplified cartoon representation of the insulin signaling pathway, highlighting the involvement of the enzyme PTP1B. Modified from reference 22.

1.5 Regulation of PTP Activity

Of course, in order for a cell to function properly, PTP activity must be tightly regulated. The cellular regulation of PTPs involves several different mechanisms. One of these mechanisms involves the oxidation and reduction of the active site cysteine residue. Since PTPs possess an abnormally low pK_a active site cysteine, the PTPs are very susceptible to oxidation. Moreover, it has recently been discovered that the cell utilizes low levels of hydrogen peroxide as a signaling agent.[27] Indeed, it has been shown that insulin triggers a burst of H_2O_2 by the activation of NADPH oxidase enzymes.[4, 28]

In the case of PTP1B, oxidation of the active site cysteine thiolate results in formation of a sulfenic acid at the active site. The sulfenic acid is then attacked by the amide nitrogen of the neighboring residue (Ser 216), forming a five-membered ring, called a sulfenylamide, at the active site (Scheme 1-2).[29, 30]

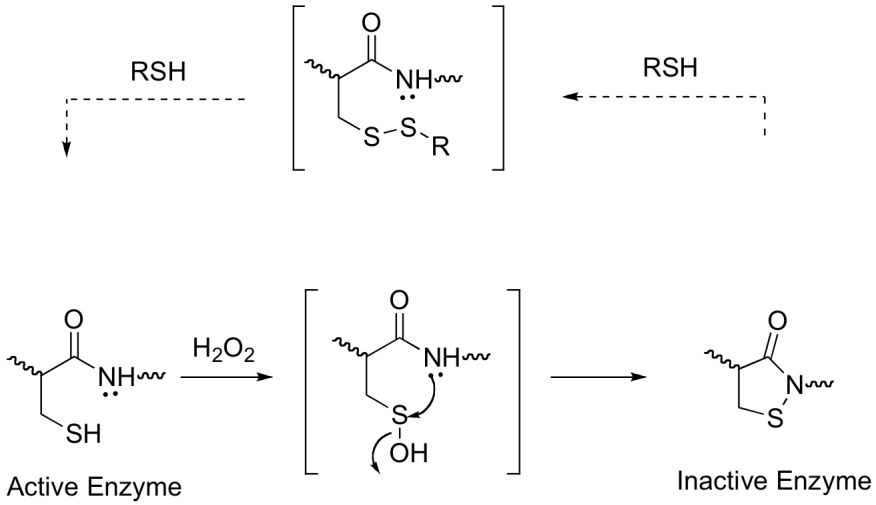

Scheme 1-2. The active site cysteine is oxidized to the sulfenic acid intermediate, leading to attack from the amide nitrogen of the neighboring residue, this forms a five-member ring, known as a sulfenylamide.

The inactivation by oxidation of the active site cysteine, and the resulting sulfenylamide formation, leads to many structural events that is beyond the scope of this Chapter, but will be discussed later in Chapter 4 of this document. As can be seen in Scheme 1-2 above, the oxidized, inactive enzyme is reduced by two units of the thiol to return to the active enzyme.[31]

Importantly, research over the last couple decades has shown that the inhibition or inactivation of PTPs by small molecules leads to significant biological effects.[7] Examination of all these efforts to develop selective, small molecule, inhibitors of PTPs is beyond the scope of this chapter, however, promising progress has been made to target PTPs in a wide variety of disease states, including cancer (multiple PTPs), diabetes (PTP1B and LAR), obesity (PTP1B and SHP2), inflammation (CD45 and PTP-ε), and infection (multiple PTPs).[7, 26, 32, 33] It is only a matter of time before these substantial efforts to develop inhibitors of PTPs produces a viable drug, and opens the door to new treatments of these diseases.

1.6 Goals of this Dissertation

When I started the PTP work, we had many intriguing questions about PTPs function, regulation, structure, and inhibition. Within this document, I have tried to address a few of those questions. In the following chapters, we will address the several different aspects of PTP function, and their possible involvement in the activity of endogenous and/or dietary small molecules.

1. In Chapter 2, the inactivation of PTPs by the dietary/endogenous aldehyde acrolein will be evaluated. We have defined the kinetics, mapped the adduct sites with MALDI TOF/TOF MS and MS/MS, and explored the mechanism of the inactivation by structure-activity studies.

2. In Chapter 3, the inactivation of PTPs by the dietary isothiocyanates will be discussed. The kinetics of the inactivation by several different isothiocyanates will be presented. In addition, the adduct sites of allyl isothiocyanate were mapped with mass spectrometry.

3. Chapter 4 will be an overview of the PTP structural work we have undertaken. The archetypal member of the PTP family, PTP1B, has been crystallized, and the structure solved. Also, the structure of the inactive, sulfenylamide, has been solved.

4. Chapter 5 discusses the work we have toward expanding to other PTPs, beside PTP1B. SHP2 (PTPN11) has been expressed and purified. The kinetics of inactivation by H_2O_2 has also been defined.

5. In addition to our PTP work, we have looked at the formation of DNA interstrand crosslinks generated from abasic sites in duplex DNA. We have explored the sequence

context necessary for the formation of the crosslink, and defined the kinetics of the crosslink reaction.

1.6 References

1. Tonks, N. K., Redox redux: revisiting PTPs and the control of cell signaling. *Cell* **2005,** 121, (June 3), 667-670.

2. Alonso, A.; Sasin, J.; Bottini, N.; Friedberg, I.; Friedberg, I.; Ostermann, A.; Godzik, A.; Hunter, T.; Dixon, J. E.; Mustelin, T., Protein tyrosine phosphatases in the human genome. *Cell* **2004,** 117, (June 11), 699-711.

3. Wang, S.; Yu, W.-M.; Zhang, W.; McCrae, K. R.; Neel, B. G.; Qu, C.-K., Noonan Syndrome/Leukemia-associated Gain-of-function Mutations in SHP-2 Phosphatase (PTPN11) Enhance Cell Migration and Angiogenesis. *J. Biol. Chem.* **2009,** 284, (2), 913-920.

4. Mahedev, K.; Zilbering, A.; Zhu, L.; Goldstein, B. J., Insulin-stimulated hydrogen peroxide reversibly inhibits protein-tyrosine phosphatase 1B in vivo and enhances the early insulin action cascade. *J. Biol. Chem.* **2001,** 276, (24), 21938-21942.

5. Hunter, T., Signaling - 2000 and beyond. *Cell* **2000,** 100, 113-127.

6. Manning, G.; Whyte, D. B.; Martinez, R.; Hunter, T.; Sudarsanam, S., The protein kinase component of the human genome. *Science* **2002,** 298, (Dec 6), 1912-1934.

7. Bialy, L.; Waldmann, H., Inhibitors of protein tyrosine phosphatases: next generation drugs? *Angew. Chem. Int. Ed. Eng.* **2005,** 44, 3814-3839.

8. Lueng, K. W. K.; Posner, B. I.; Just, G., Periodinates: a new class of protein tyrosine phosphatase inhibitors. *Bioorg. Med. Chem. Lett.* **1999,** 9, 353-356.

9. Hooft van Huijsduijnen, R.; Sauer, W. H. B.; Bombrun, A.; Swinnen, D., Prospects for inhibitors of protein tyrosine phosphatase 1B as antidiabetic drugs. *J. Med. Chem.* **2004,** 47, 4142-4146.

10. Arabaci, G.; Guo, X.-C.; Beebe, K. D.; Coggeshall, K. M.; Pei, D., alpha-Haloacetophenone derivatives as photoreversible covalent inhibitors of protein tyrosine phosphatases. *J. Am. Chem. Soc.* **1999,** 121, 5085-5086.

11. Fu, H.; Park, J.; Pei, D., Peptidyl adehydes as reversible covalent inhibitors of protein tyrosine phosphatases. *Biochemistry* **2002,** 41, (34), 10700-10709.

12. Park, J.; Fu, H.; Pei, D., Peptidyl aldehydes as slow-binding inhibitors of dual-specificity phosphatases. *Bioorg. Med. Chem.* **2004,** 14, (3), 685-687.

13. LaButti, J. N.; Chowdhury, G.; Reilly, T. J.; Gates, K. S., Redox regulation of protein tyrosine phosphatase 1B by peroxymonophosphate. *J. Am. Chem. Soc.* **2007,** 129, 5320-5321.

14. Stone, R. L.; Dixon, J. E., Protein-tyrosine phosphatases. *J. Biol. Chem.* **1994,** 269, (50), 31323-31326.

15. Zhang, Z.-Y., Protein tyrosine phosphatases: structure and function, substrate specificity, and inhibitor development. *Ann. Rev. Pharmacol. Toxicol.* **2002,** 42, (42), 209-234.

16. Jackson, M. D.; Denu, J. M., Molecular reactions of protein phosphatases - insights from structure and chemistry. *Chem. Rev.* **2001,** 101, 2313-2340.

17. Seiner, D. R.; Gates, K. S., Kinetics and mechanism of protein tyrosine phosphatase 1B inactivation by acrolein. *Chem. Res. Toxicol.* **2007,** 20, 1315-1320.

18. Zhang, Z.-Y., Chemical and mechanistic approaches to the study of protein tyrosine phosphatases. *Acc. Chem. Res.* **2003,** 36, 385-392.

19. Barford, D., Protein phosphatases. *Curr. Opin. Struct. Biol.* **1995,** 5, 728-734.

20. Pederson, C. T., 1,2-Dithiole-3-thiones and 1,2-dithiole-3-ones. *Adv. Hetercyclic Chem.* **1982, 31**, 63-113.

21. Nichols, A. J.; Mashal, R. D.; Balkan, B., Toward the discovery of small molecule PTP1B inhibitors for the treatment of metabolic diseases. *Drug Dev. Res.* **2006,** 67, (7), 559-566.

22. Johnson, T. O.; Ermolieff, J.; Jirousek, M. R., Protein tyrosine phosphatase 1B inhibitors for diabetes. *Nature Rev. Drug Discov.* **2002,** 1, (Sept), 696-709.

23. Denu, J. M.; Lohse, D. L.; Vijayalakshmi, J.; Saper, M. A.; Dixon, J. E., Visualization of intermediate and transition-state structures in protein-tyrosine phosphatase catalysis. *Proc. Natl. Acad. Sci. U. S. A.* **1996,** 93, (6), 2493-8.

24. Lohse, D. L.; Denu, J. M.; Santoro, N.; Dixon, J. E., Roles of aspartic acid-181 and serine-222 in intermediate formation and hydrolysis of the mammalian protein-tyrosine-phosphatase PTP1. *Biochemistry* **1997,** 36, 4568-4575.

25. Shrestha, S.; Bhattarai, B. R.; Cho, H.; Choi, J.-K.; Cho, H., PTP1B inhibitor Ertiprotafib is also a potent inhibitor of I[kappa]B kinase [beta] (IKK-[beta]). *Bioorganic & Medicinal Chemistry Letters* **2007,** 17, (10), 2728-2730.

26. Xie, J.; Comeau, A. B.; Seto, C. T., Squaric Acids: A New Motif for Designing Inhibitors of Protein Tyrosine Phosphatases. *Org. Lett.* **2004,** 6, (1), 83-86.

27. Goldstein, B. J.; Kalyankar, M.; Wu, X., Redox paradox: insulin action is facilitated by insulin-stimulated reactive oxygen species with multiple potential signaling targets. *Diabetes* **2004,** 54, (2), 311-321.

28. Mahadev, K.; Motoshima, H.; Wu, X.; Ruddy, J. M.; Arnold, R. S.; Cheng, G.; Lambeth, J. D.; Goldstein, B. J., The NAD(P)H oxidase homolog Nox4 modulates insulin-stimulated generation of H2O2 and plays an integral role in insulin signal transduction. *Mol. Cell. Biol.* **2004,** 24, (5), 1844-1854.

29. Salmeen, A.; Anderson, J. N.; Myers, M. P.; Meng, T.-C.; Hinks, J. A.; Tonks, N. K.; Barford, D., Redox regulation of protein tyrosine phosphatase 1B involves a sulphenyl-amide intermediate. *Nature* **2003,** 423, (June 12), 769-773.

30. van Montfort, R. L. M.; Congreeve, M.; Tisi, D.; Carr, R.; Jhoti, H., Oxidation state of the active-site cysteine in protein tyrosine phosphatase 1B. *Nature* **2003,** 423, (June 12), 773-777.

31. Denu, J. M.; Tanner, K. G., Specific and reversible inactivation of protein tyrosine phosphatases by hydrogen peroxide: evidence for a sulfenic acid intermediate and implications for redox regulation. *Biochemistry* **1998,** 37, 5633-5642.

32. Chan, G.; Kalaitzidis, D.; Neel, B. G., The tyrosine phosphatase Shp2 (PTPN11) in cancer. *Cancer Metastasis Rev.* **2008,** 27, (2), 179-192.

33. Tonks, N. K.; Muthuswamy, S. K., A brake becomes an accelerator: PTP1B - A new therapeutic target for breast cancer. *Cancer Cell* **2007,** 11, (Mar), 214-215.

THE INACTIVATION OF PTP1B BY THE ENDOGENOUS/DIETARY ALDEHYDE ACROLEIN

2.1 Endogenous Sources of Acrolein

Human cells are exposed to a variety of reactive aldehydes.[1] One group of these endogenous aldehydes is the Michael acceptors. One of the most biologically active of all the aldehydes in this group is the electrophilic, α, β-unsaturated aldehyde acrolein (Figure 2-1). Acrolein is a ubiquitous molecule, with human cells being exposed from a variety of sources, both endogenous and exogenous.[1]

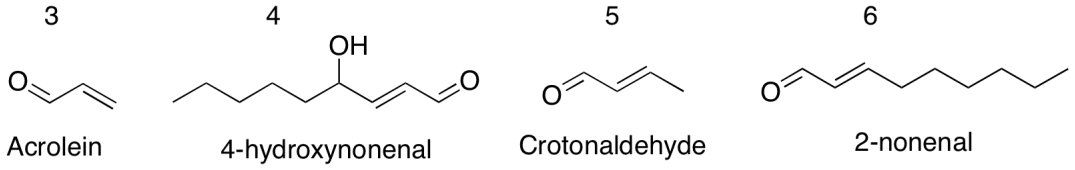

Figure 2-1. Acrolein (**3**) and other common endogenous α, β-unsaturated aldehydes.

Lipid peroxidation has been shown to produce acrolein inside cells, among many other reactive aldehydes.[2-4] Indeed, whenever cells in culture are exposed to oxidative stress, acrolein production was found to double, most likely from an increase in the oxidative degradation of lipids.[5] Furthermore, acrolein has also been shown to be produced endogenously by amine oxidases from spermine, as shown in Scheme 2-1.[1]

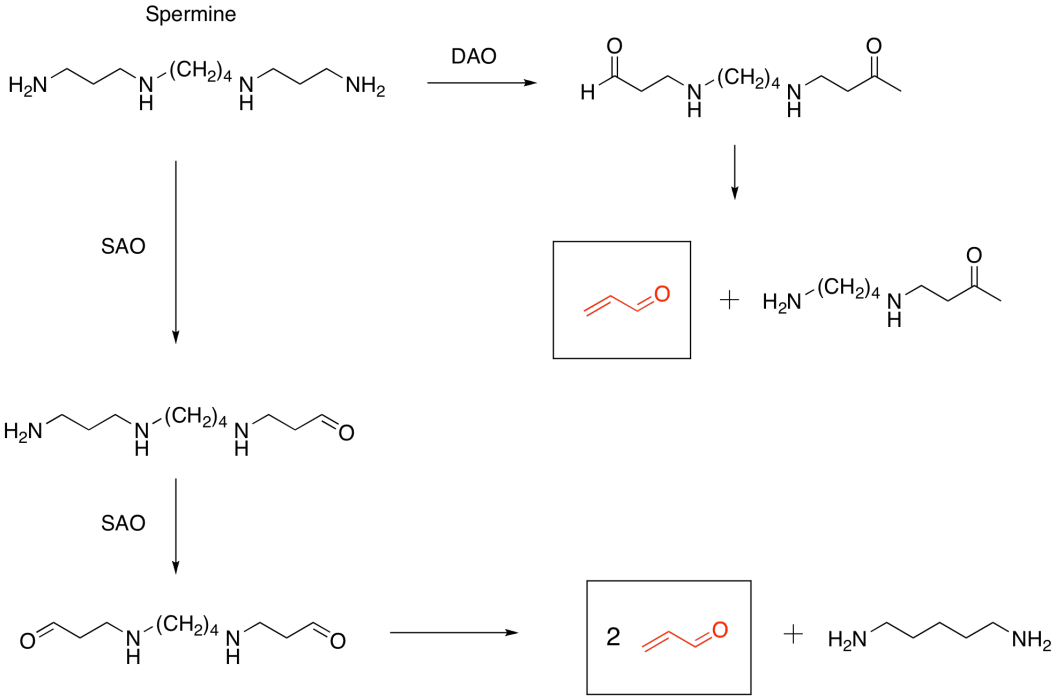

Scheme 2-1. Endogenous production of acrolein by amine oxidases.[1] SAO = serum amine oxidase; DAO = diamine oxidase.

In another example, acrolein has recently been shown to be produced by myeloperoxidase (MPO) in human neutrophils from threonine. (Scheme 2-2).[6]

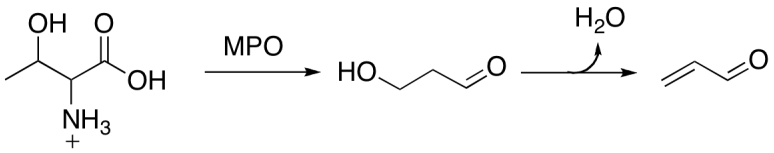

Scheme 2-2. Generation of acrolein by myeloperoxidase (MPO) from threonine.[6]

2.2 Dietary Sources of Acrolein

Additionally, acrolein is found in a variety of dietary sources.[1, 7, 8] It can be found in high concentrations in fried or over-cooked foods.[1, 9] Furthermore, cigarette smoke and car exhaust contain high amounts of acrolein.[1, 10] Cigarettes have been shown to contain

between 18-98 μg of acrolein (per cigarette), as well as a variety of other reactive aldehydes.[10]

2.3 Physiological Concentration of Acrolein.

Acrolein's reactivity has been detrimental to determining its biological concentration, however, Kato and coworkers recently reported that acrolein levels in human breast cancer cells in cell culture are around 0.5 μM.[5] Furthermore, they reported that whenever the cells were subjected to oxidative stress, by treatment with doxorubicin, the levels of acrolein increased by around two fold, owing to the endogenous production of acrolein under oxidative stress.[5] Recent analysis of aldehyde concentrations in saliva or airway secretions revealed that acrolein is present in the low micromolar range in nonsmokers (~2 μM).[11, 12] It is worth noting that heavy smokers saw an up to 10-fold increase in acrolein levels in airway secretions.[11]

2.4 Biological Activity of Acrolein.

Acrolein displays a wide range of biological activity. Importantly, acrolein has been shown to modify functionally critical cysteine residues on proteins inside cells. For example, acrolein has been shown to modify critical thiol side chain residues of cysteine proteases (capase-3).[12] In another example, TRPA1 ion channels and certain transcription factors (NF-κB, Keap1/Nrf2) have also been shown to be modified by acrolein at certain cysteine residues.[13-15]

2.5 Hypothesis: Acrolein May Have Activity Against PTPs.

As discussed in Chapter One, PTPs are cysteine-dependent enzymes that control important biological signal transduction pathways through regulation of phosphorylation levels of certain proteins. Importantly, acrolein has been shown to increase the phosphorylation levels of several proteins.[11, 16] This has been attributed to the activation of protein tyrosine kinases through different mechanisms.[11, 16] We thought it was also possible that acrolein could be producing an increase in the phosphorylation levels of some proteins through a decrease in the activity of protein tyrosine phosphatases. As can be seen in Figure 2-2, the phosphorylation status of cellular proteins can be increased by activation of protein tyrosine kinases, which would shift the equilibrium to the left.

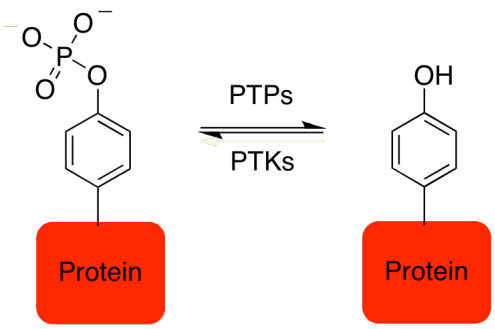

Figure 2-2. The equilibrium of tyrosine phosphorylation is controlled by tandem action of PTPs and PTKs.

It is also possible, that by decreasing the activity of cellular protein tyrosine phosphatases, the equilibrium would shift to the left in a similar way. This pathway to explain the increase of phosphorylation levels after cellular treatment with acrolein has not been well characterized.

We wanted to explore this possibility, since we knew that acrolein has been shown to modify functionally critical cysteine residues inside cells, and PTPs are cysteine

dependent enzymes. We utilized the catalytic subunit of human PTP1B (a.a. 1-322) as an archetypal member of the PTP family of enzymes.

2.6 Kinetics of PTP1B Inactivation by Acrolein.

We have found that acrolein is indeed a potent, time dependent inactivator of the enzyme PTP1B (Figure 2-3).

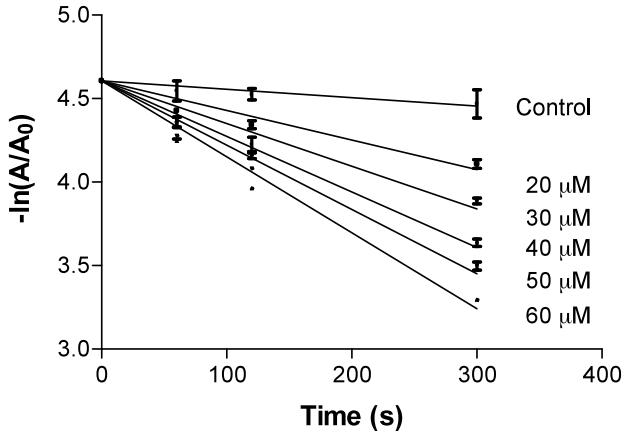

Figure 2-3. Semilog plot of time courses for the inactivation of PTP1B by various concentrations of acrolein. Points represent the mean with SD: n = 3.

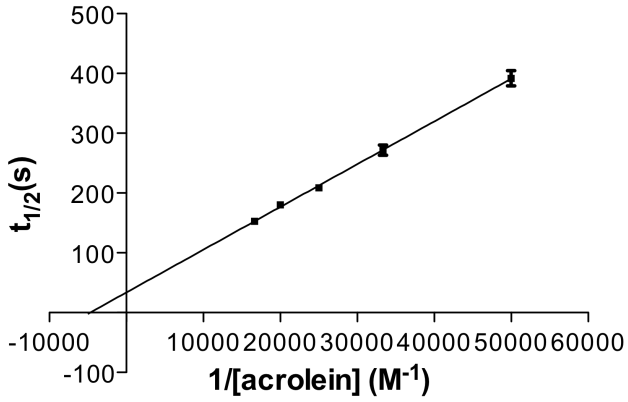

Figure 2-4. Kitz-Wilson replot of the inactivation time-course data. All points represent the mean with SD: n = 3.

The Kitz-Wilson replot of the inactivation data (Figure 2-4) reveals that the maximum rate of inactivation at saturating concentrations of acrolein, k_{inact}, is 0.020 ± 0.005 s^{-1}. Furthermore, the concentration of acrolein required to achieve a half-maximal rate of inactivation, K_I, is 2.3 ± 0.6 x 10^{-4} M. The apparent second-order rate constant for the inactivation of PTP1B by acrolein (k_{inact}/K_I = 87 $M^{-1}s^{-1}$) is comparable to the rate reported for the endogenous regulator of PTP1B activity, H_2O_2 (10 $M^{-1}s^{-1}$).[17, 18]

2.7 Examination of the inactivation process.

The time-dependent nature of the inactivation process points to a covalent modification of the enzyme by acrolein.[19] This idea is reinforced by the fact that the inactivation of PTP1B by acrolein is not reversed by gel filtration or dialysis of the inactivated enzyme. Figure 2-5 shows that after inactivation of PTP1B by acrolein (1 mM, 10 minutes), gel filtration of the enzyme shows no appreciable return of enzymatic activity.

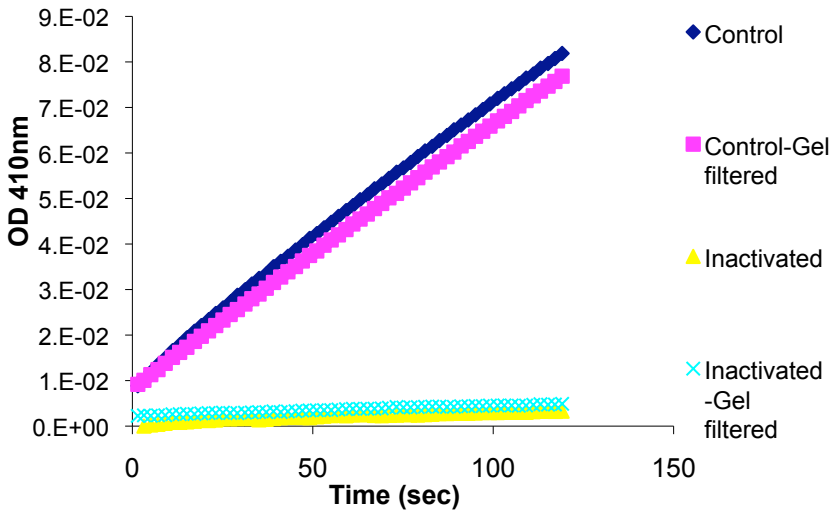

Figure 2-5. Gel filtration of the inactivated enzyme (1 mM Acrolein, 15 minutes) does not return enzyme activity, pointing towards covalent modification of the enzyme.

We wished to probe whether acrolein was inactivating PTP1B through modification of an amino acid residue within the active site pocket. An active site competition experiment was designed where the accessibility to the active site was hindered by the addition of the active site binder orthovanadate (Scheme 2-3). Vanadate is a known active site binder of PTPs.

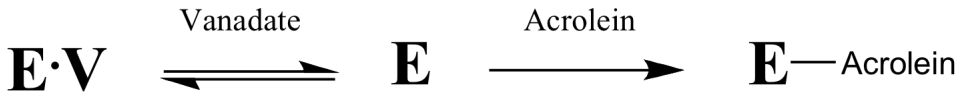

Scheme 2-3. The enzyme is in equilibrium with the active site binder vanadate, thus slowing an active site directed inactivator.

Indeed, whenever this active site competition experiment was performed, the inactivation of PTP1B activity by acrolein was significantly hindered (Figure 2-6).

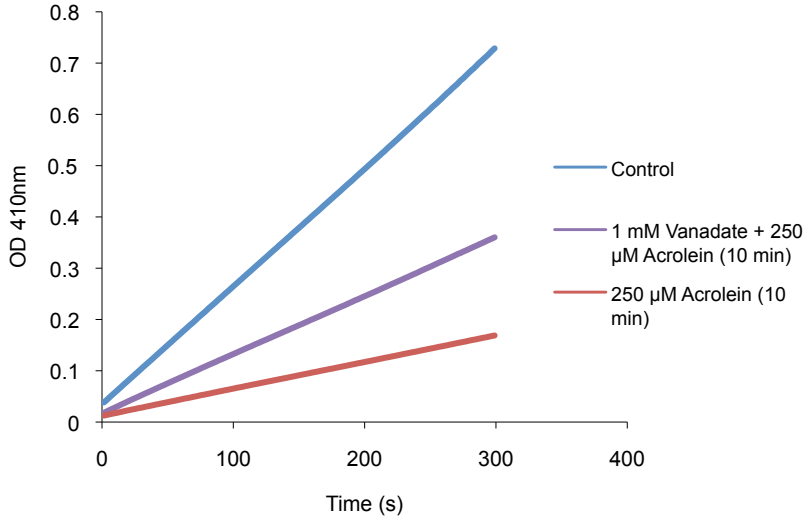

Figure 2-6. The inactivation of PTP1B by acrolein (250 µM, 10 minutes) is hindered by the active site binder orthovanadate (1 mM), providing evidence for an active site directed inactivation mechanism.

As mentioned previously in Chapter 1, PTPs are susceptible to inactivation by reactive oxygen species such as superoxide radical and hydrogen peroxide.[17, 18, 20] These agents inactivate PTP1B via oxidation of the active site cysteine-215 to the sulfenic acid oxidation state (Scheme 2-4).

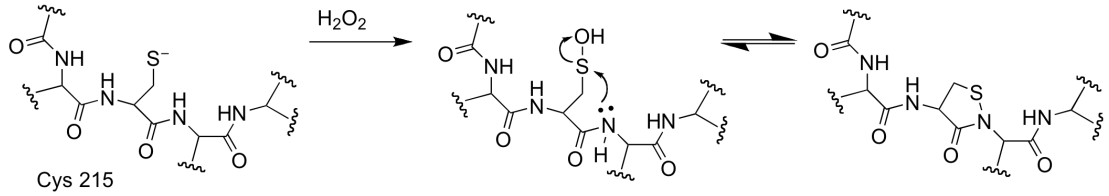

Scheme 2-4. The reactive oxygen species, H_2O_2, inactivates PTP1B by oxidation of the active site cysteine 215 to a sulfenic acid, which is attacked by the neighboring backbone amide nitrogen to produce a sulfenylamide.[21]

Importantly, aldehydes, through spontaneous autooxidation, have been shown to produce reactive oxygen species like hydrogen peroxide and superoxide radical in aerobic solution.[22] The involvement of reactive oxygen species in the inactivation of PTP1B by acrolein was ruled out by the observation that the presence of the superoxide-

and hydrogen peroxide-destroying enzymes superoxide dismutase (SOD) (Figure 2-7) and catalase[23] (Figure 2-8) has no effect on the rate of the inactivation reaction.

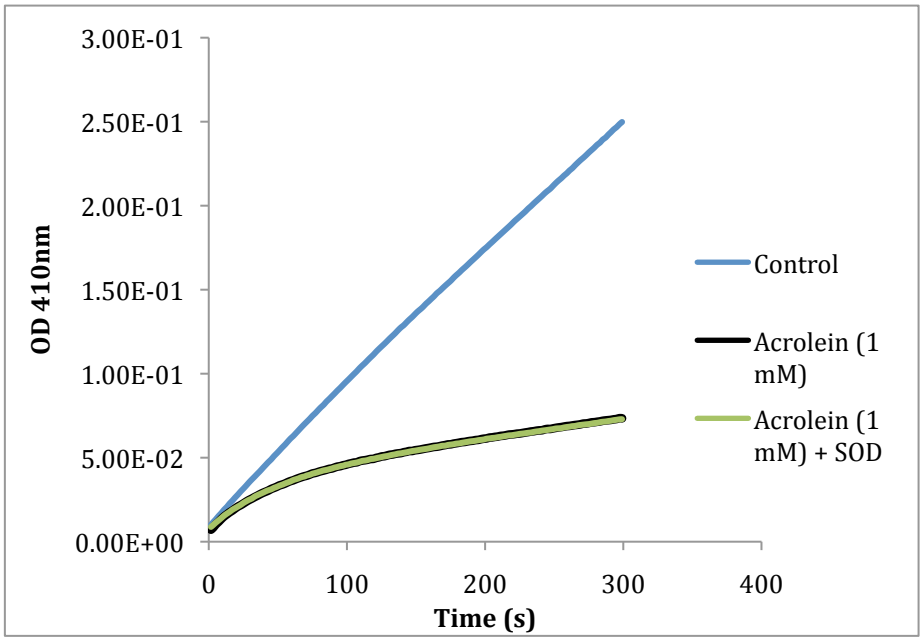

Figure 2-7. The inactivation of PTP1B by acrolein (1 mM) is not affected by the addition of Superoxide dismutase (SOD).

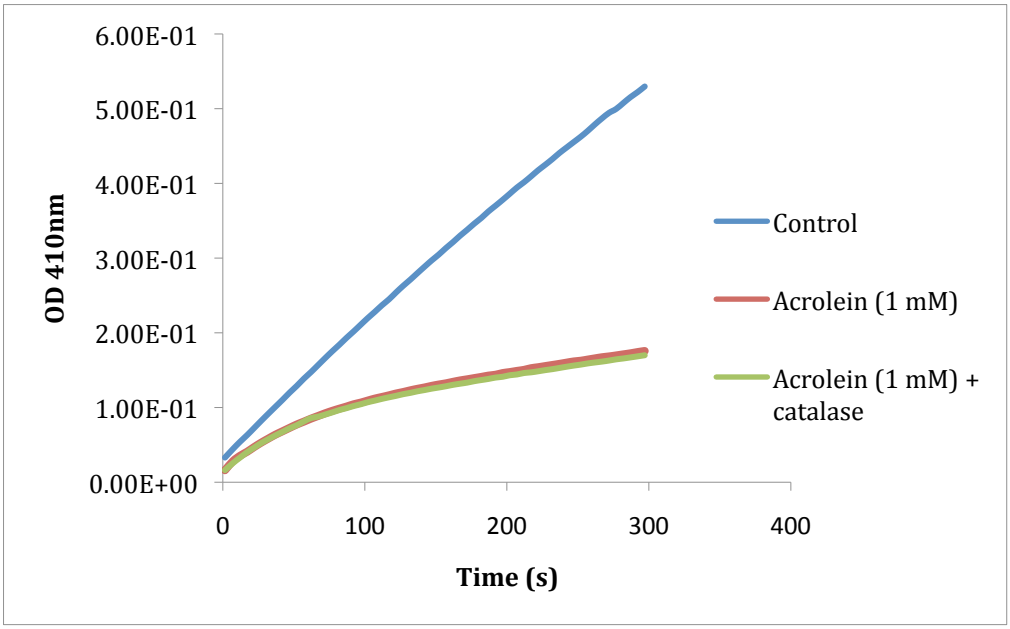

Figure 2-8. The inactivation of PTP1B by acrolein is not affected by the addition of catalase.

Furthermore, the oxidation of PTP1B by hydrogen peroxide is reversed by two units of ubiquitous thiol, returning enzymatic activity. On the other hand, when the acrolein-inactivated enzyme is incubated with the endogenous thiol glutathione, we observed no return of enzyme activity (Figure 2-9). This rules out the involvement of reactive oxygen species in the inactivation reaction.

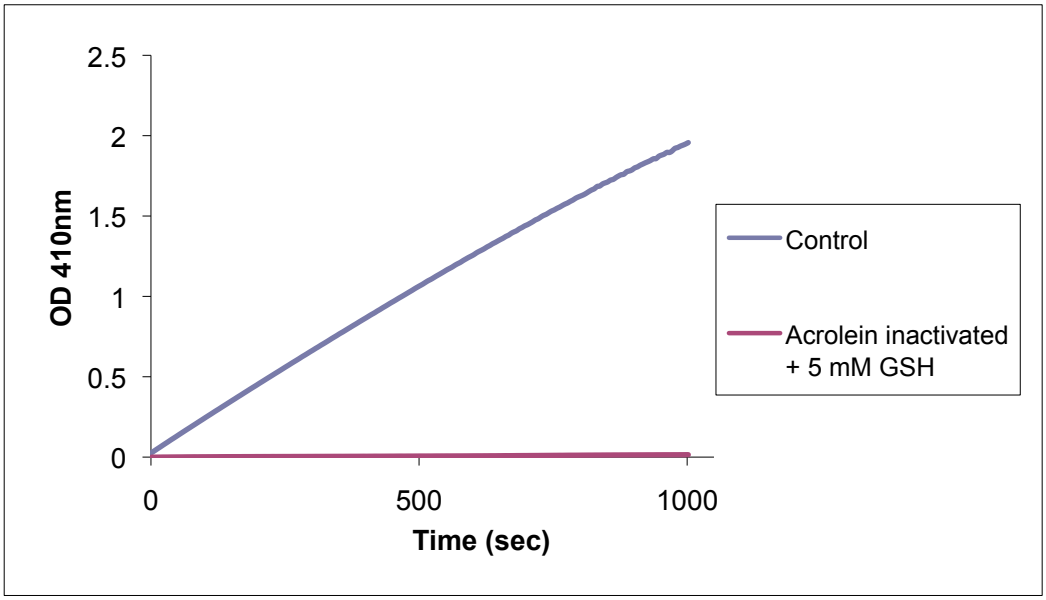

Figure 2-9. The acrolein-inactivated enzyme (1 mM, 15 min) is not reactivated by the endogenous thiol, glutathione (5 mM).

2.8 Mapping the Adduct site(s) with Mass Spectrometry

In order to probe what site(s) acrolein is modifying in the active site of PTP1B, we chose to carry out mass spectrometric studies on acrolein inactivated PTP1B. Acrolein has been shown to modify a number of amino acid residues in proteins, including histidine, lysine, and cysteine.[2, 7, 13, 14, 26-30] The active site of PTP1B contains

both a histidine (His 214) and a cysteine (Cys 215) that are essential to catalytic activity.[24]

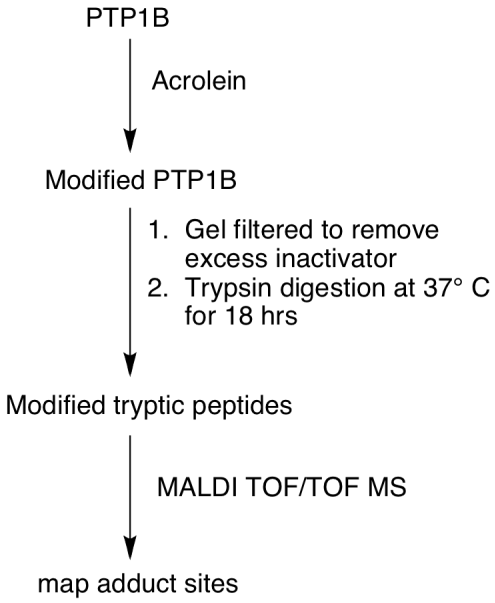

Scheme 2-5. The experimental order of the mass spectrometry experiments, a control sample not treated with acrolein was also prepared.

As can be seen in Scheme 2-5, PTP1B was inactivated by acrolein and subjected to digestion by the protease Trypsin. Trypsin cleaves peptides on the carboxyl side of every arginine or lysine residue.[25] Since trypsin is consistent in its cleavage pattern, it enables us to predict a tryptic peptide fingerprint for the enzyme. This makes the evaluation of the resulting mass spectra much easier to analyze.

After trypsin digestion, the resulting fragments were analyzed by MALDI-TOF-TOF mass spectrometry. As can be seen in Figure 2-10, in the active PTP1B (not reacted with acrolein) sample mass spectrometry, we were able to observe all of the cysteine containing tryptic peptides. In addition, most of the tryptic peptide mass ions were observed in both the control and modified digests, although these ions were not labeled

for clarity in Figure 2-10. However, all of the cysteine containing tryptic peptides, in the control (not inactivated by acrolein) mass spectra are pointed out in Figure 2-10.

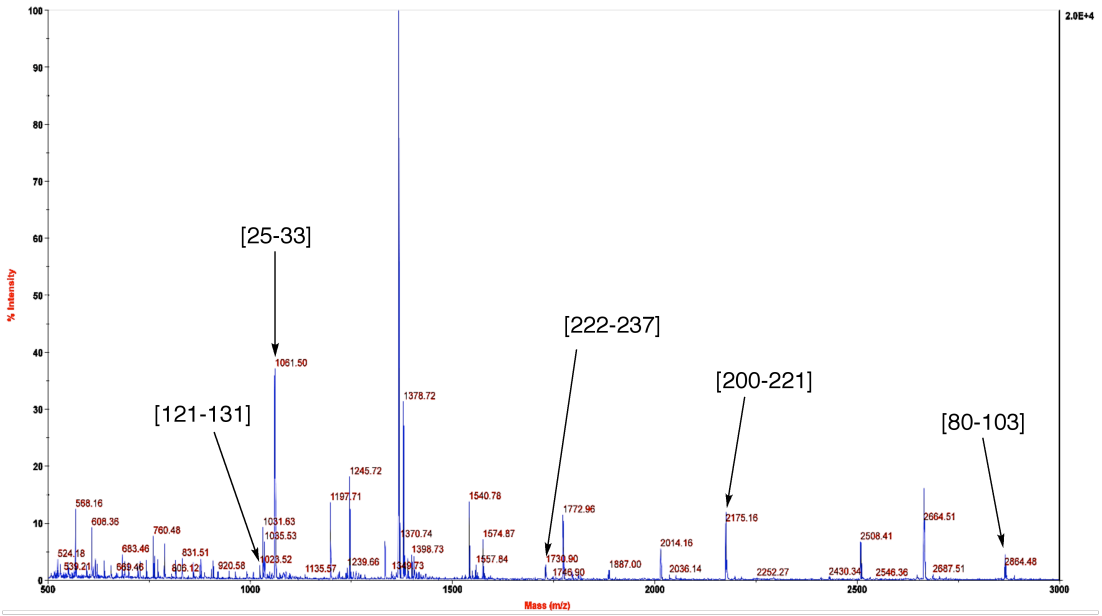

Figure 2-10. The MALDI TOF/TOF MS spectra of the PTP1B control experiment (without treatment of acrolein). The cysteine containing tryptic peptides have been labeled.

As can be seen in Figure 2-10 above, all of the cysteines containing tryptic fragments can be identified in the control experiment. The MALDI TOF/TOF MS of the inactivated enzyme can be seen in Figure 2-11. Notice that several of the cysteine containing tryptic peptides have been modified, at least to some extent.

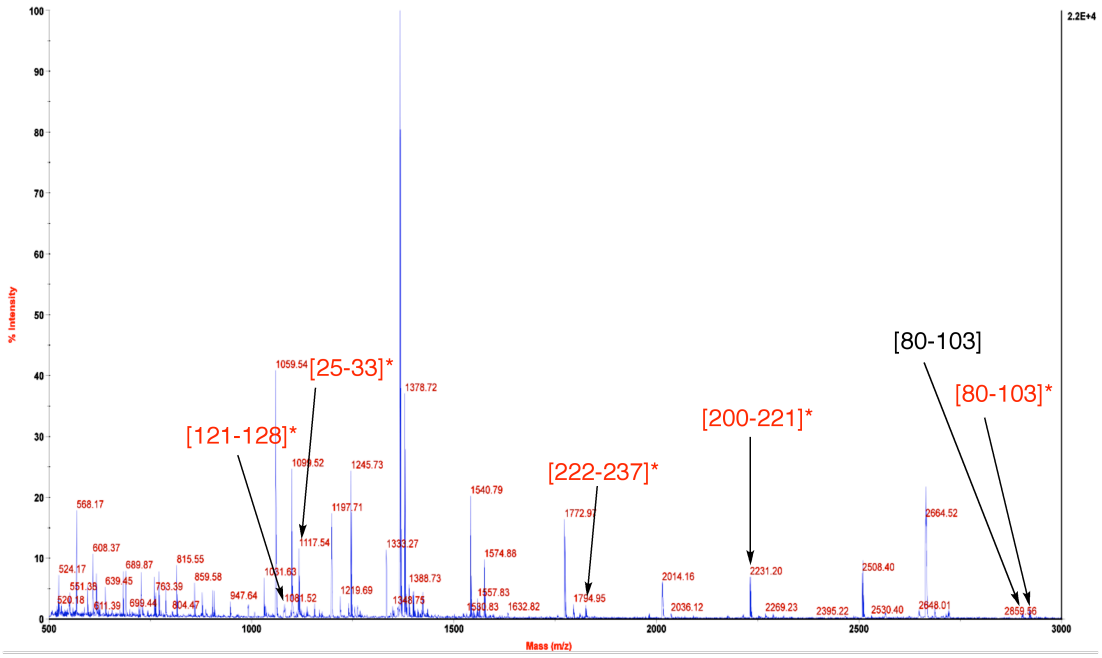

Figure 2-11. MALDI TOF/TOF MS spectra of the acrolein inactivated PTP1B. Modified peptides are labeled in red and with an asterisk(*).

The MALDI TOF/TOF MS spectra of acrolein inactivated PTP1B shows several modified tryptic peptides. Importantly, a major signal was observed at *m/z* 2231.09 corresponding to the acrolein-modified active site peptide a.a. 200-221. A very weak signal was observed for the unmodified active site peptide (*m/z* 2175.17). In addition, weak signals indicating at least some modification of four other cysteine-containing tryptic fragments corresponding to a.a. 25-33 (*m/z* 1117.47, Cys 32), 80-103 (*m/z* 2920.38, Cys 92), 121-128 (*m/z* 1079.66, Cys 121) and 222-237 (*m/z* 1824.80, Cys 232).

Nanospray MS/MS-TOF was employed to further characterize the site(s) of acrolein modification in all of the modified tryptic peptides. In the case of the active site peptide 200-221, we observed the unmodified b_{12}-b_{15} ions expected. However, on the other hand, we observed the b_{16}-b_{17} ions are increased by +56 Da, corresponding to one molecule of acrolein. Further, the masses for the y_5 and y_6 ions are consistent with those

expected for the unmodified peptide fragments, while the masses for the y_7-y_{13} ions are increased by +56 Da. Overall, the data suggest that acrolein inactivates PTP1B primarily via reaction with the active site cysteine-215. Additionally, weak signals corresponding to the acrolein-modified b_{15} and unmodified y_7 ions are also observed, suggesting that some modification also occurs at the histidine-214 of the active site peptide. The Nanospray MS/MS-TOF data for the modified active site peptide 200-221 can be seen in Figure 2-12.

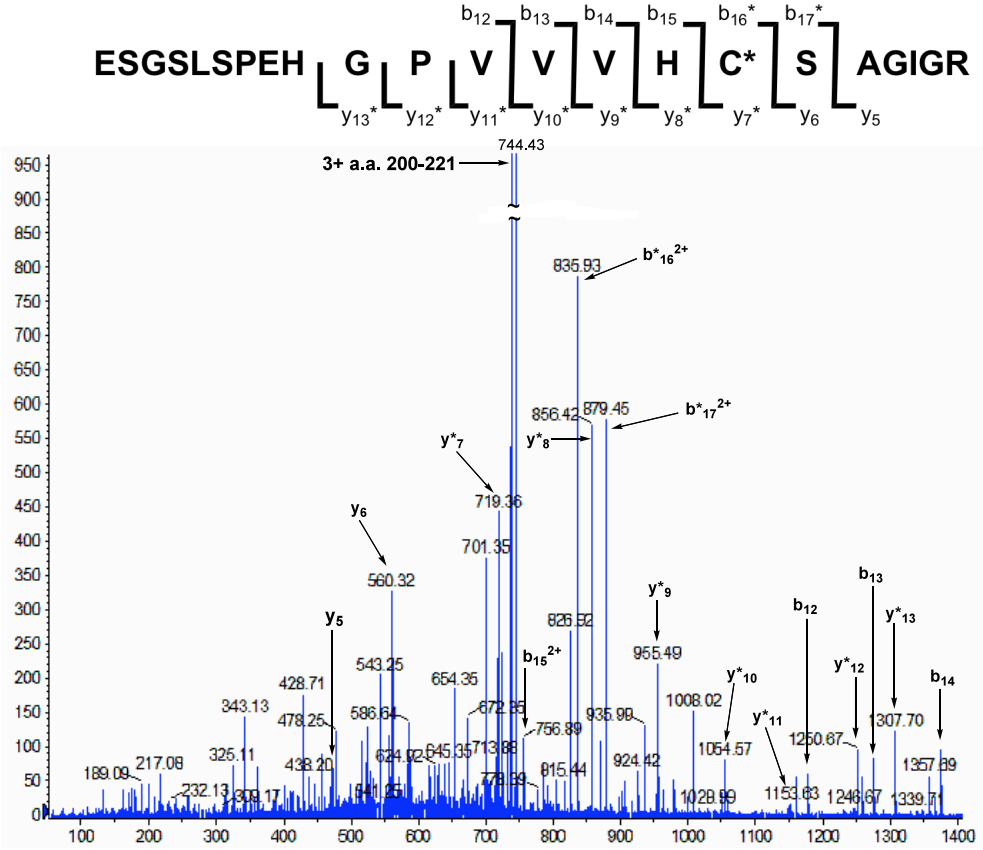

Figure 2-12. The Nanospray MS/MS-TOF of the active site peptide 200-221, the data indicate major modification occurring at the active site cysteine-215.

As shown in Figure 2-12, the Nanospray MS/MS-TOF for the [25-33] tryptic fragment (*m/z* 1117.47) shows modification of the peptide to be on Cys 32 by acrolein. We observed the unmodified b_2-b_6 ions as well as the unmodified y_1 ion. Additionally, we observed the y_9-y_7 and y_3-y_4 ions are modified by the addition of +56 Da. This data is consistent with some modification of the Cys 32 by acrolein.

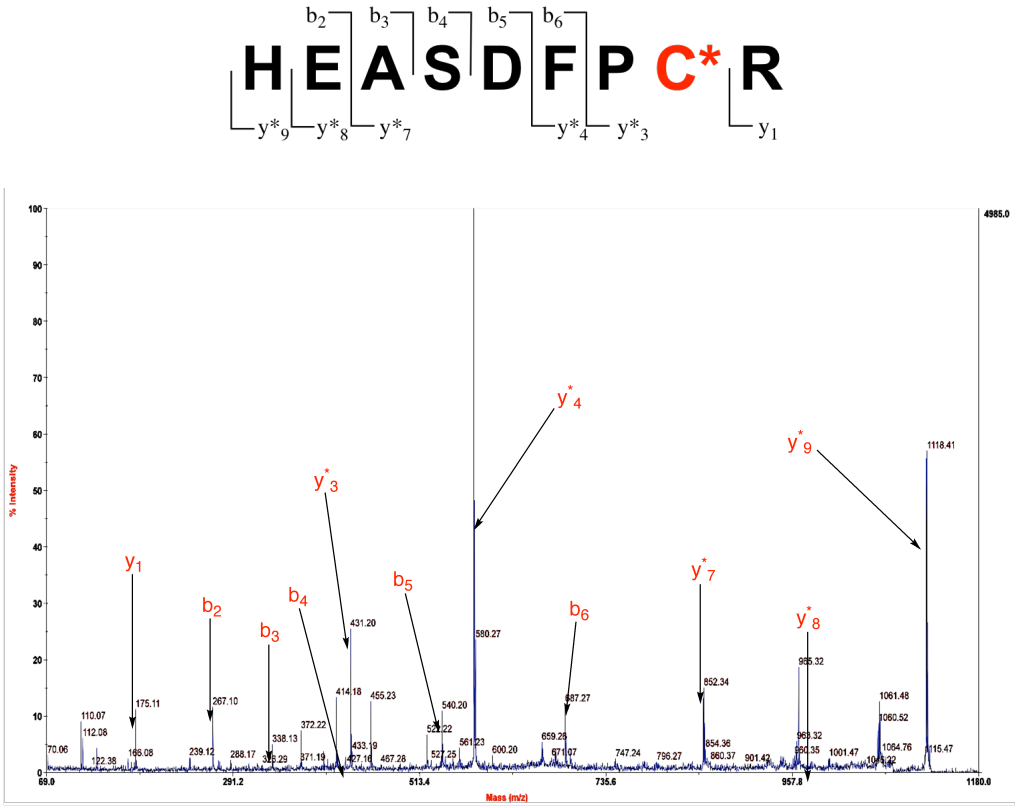

Figure 2-13. The MS/MS of the tryptic fragment [25-33] displaying modification of Cys 32 by acrolein.

Further, in the case of the tryptic fragment [80-103], we observed the unmodified y_{11}, y_8, y_6, and y_4 ions. We also observed y_{20}, y_{18}, y_{15}, y_{14}, and y_{13} ions all modified with the addition of 56 Da. On the other hand, we observed b_{20} also modified by the addition

of 56 Da. This data is overall consistent with partial modification of Cys 92 by one molecule of acrolein.

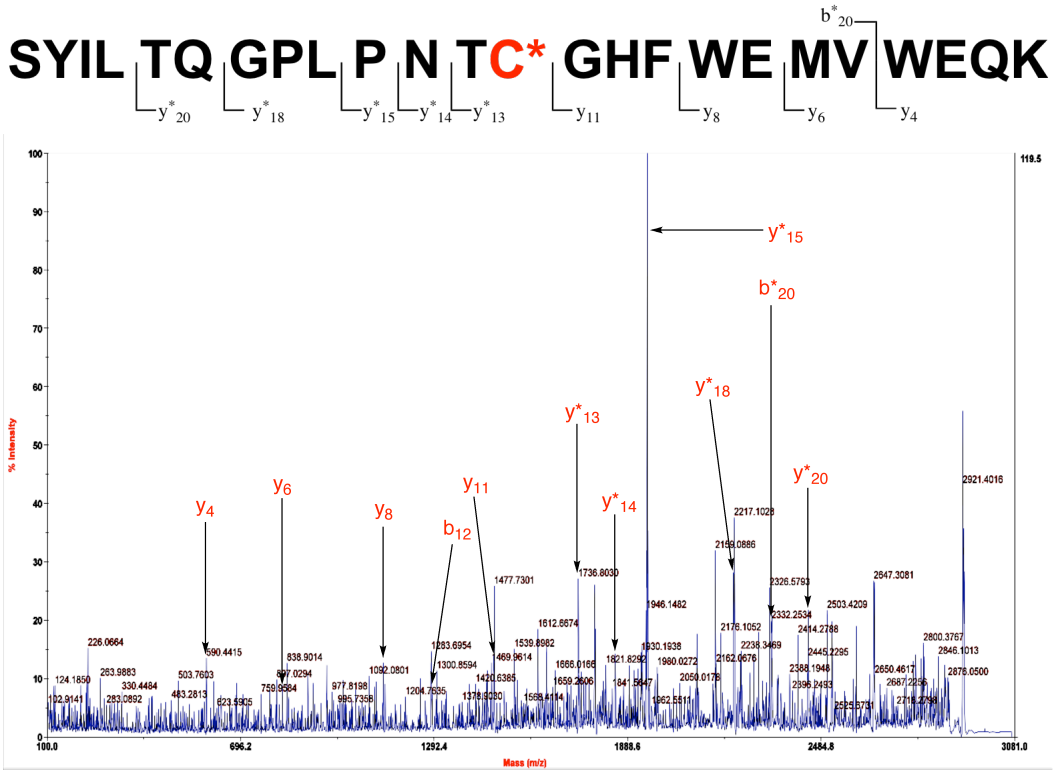

Figure 2-14. The MALDI TOF/TOF MS/MS spectra for the tryptic fragment [80-103] displays modification by acrolein at Cys 92.

Overall, the mass spectrometry data indicate that acrolein is inactivating PTP1B primarily through modification of the active site cysteine. In addition, acrolein is also modifying several other cysteine residues in the protein. MS/MS confirms that Cys 92 and Cys 32 were modified by acrolein. Two other cysteine containing tryptic fragments were identified in the MS as being modified by acrolein, however, these signals were too weak for tandem mass spectrometry. Based on the other data, it is likely that acrolein is

partially modifying the cysteine residues in those tryptic fragments, in this case Cys 121, and Cys 232.

2.9 Structure-Activity Studies with related aldehydes.

In aqueous solution, simple thiols react with acrolein via initial conjugate addition to the double bond of the α, β-unsaturated aldehyde, rather than by addition to the aldehyde moiety.[26] Thus, we anticipated that the inactivation of PTP1B by acrolein may proceed via the conjugate addition mechanism as shown at the top of Scheme 2-6.

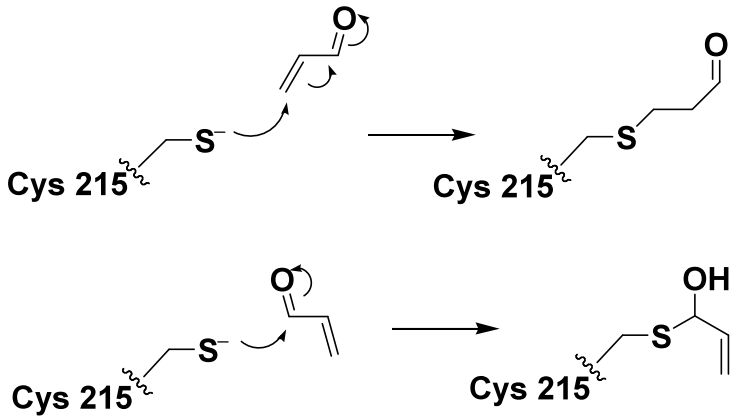

Scheme 2-6. Acrolein may react with the active site thiolate by two different mechanisms, either 1,4 (top) or 1,2 (bottom) addition.

A structure-activity study was undertaken and we observed that aliphatic aldehydes such as glyoxal, acetaldehyde, and propanal, lacking the unsaturation found in acrolein, are relatively poor inactivators of the enzyme (Figure 2-15). These results are in line with previous work that showed that simple aldehydes such as acetaldehyde do not effectively inactivate PTP1B.[27]

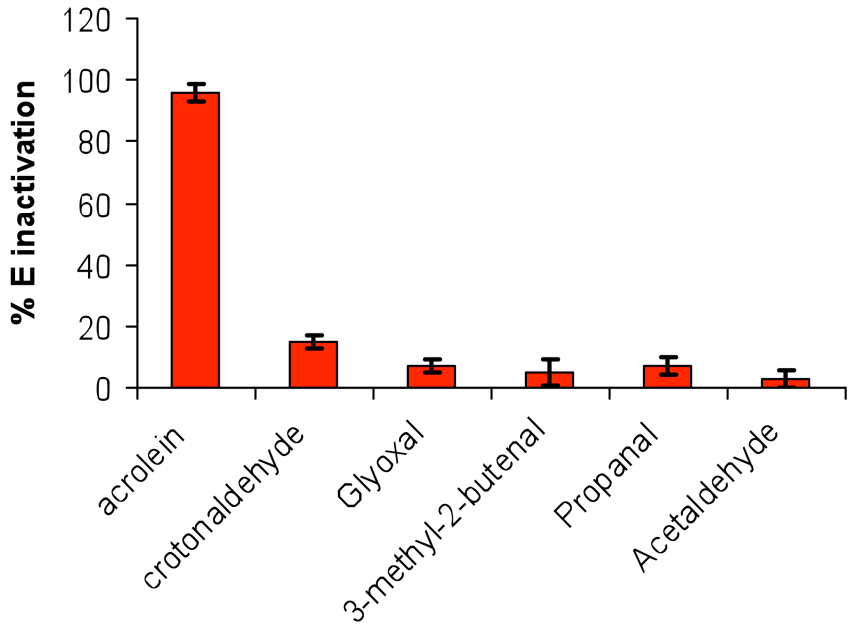

Figure 2-15. The inactivation of PTP1B by various aldehydes showed that saturation at the double bond of acrolein is essential to its reactivity. Bars represent mean with SD, N=3.

Also consistent with our favored conjugate addition mechanism for the inactivation of PTP1B by acrolein, we find that analogues such as crotonaldehyde and 3-methyl-2-butenal, possessing some added steric bulk at the terminal position of the double bond, are relatively weak inactivators of the enzyme (Figure 2-15), though they are better inactivators than the simple aldehydes.

2.10 Fluorescent Probe Studies.

As shown in Scheme 2-6, if the mechanism of inactivation of PTP1B by acrolein involves a 1,4 Michael-type addition, the protein will be left with a 'dangling aldehyde', on the modified cysteine residues. Aldehydes are not found in native proteins, and we thought we could exploit this difference to provide further evidence the inactivation of

PTP1B by acrolein involves a 1,4 Michael-type addition. We utilized a hydroxylamine tagged fluorescent probe, purchased from Molecular Probes (A-30629). Hydroxylamines are known to react readily with aldehydes in aqueous solution.[28, 29] Thus, the acrolein-inactivated protein would be tagged covalently to the fluorophore, and with removal of the excess fluorescent probe, we should see an increase in the level of fluorescence from the acrolein-inactivated sample, when compared to the control (active) sample (Scheme 2-7).

Scheme 2-7. The aldehyde from acrolein will react with the hydroxylamine to produce a fluorescent tagged protein.

Hydroxylamines have been used to tag aldehydes in damaged DNA previously.[30] As can be seen in Figure 2-16, when the fluorescent probe was allowed to react with both the acrolein-inactivated enzyme and active enzyme (as a control), and excess probe was removed by subsequent gel filtration, the inactivated protein retained a large amount of the probe, as evidenced by the large increase in absorbance at 494 nm. This suggests that the inactivation of PTP1B by acrolein is leaving a dangling aldehyde that is covalently reacting with the hydroxylamine probe.

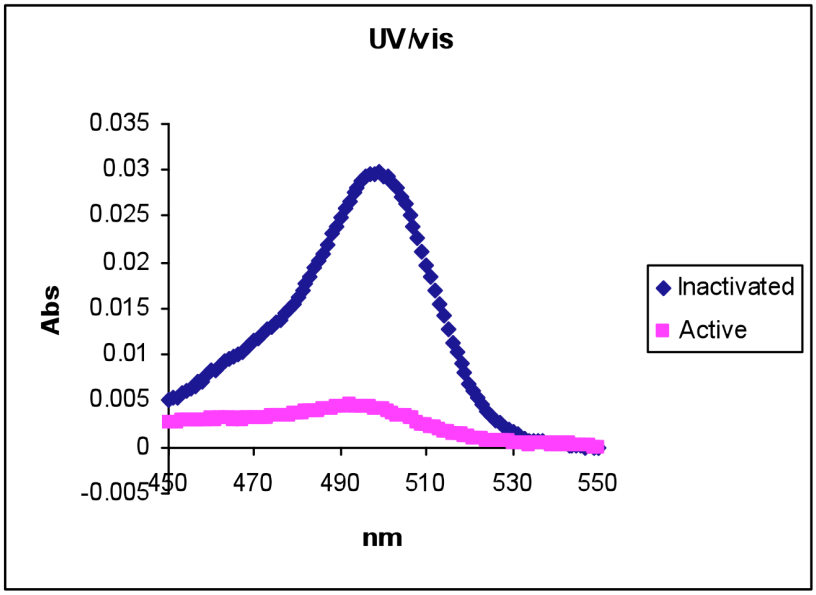

Figure 2-16. An overlay of the UV/vis spectra of both the control (active) and the acrolein-inactivated enzyme treated with the aldehyde-reactive fluorescent probe.

Further, the fluorescence of both samples was tested, and we observed a strong fluorescence signal at Em of 518 nm from the acrolein-inactivated enzyme, although the control (active) enzyme did still retain some fluorescence, it was significantly less than the acrolein-inactivated enzyme. It is possible that side reactions are taking place between the fluorescent probe and the active enzyme, leading to residual tagging of the fluorescent probe to the enzyme. Importantly, we observed a clear increase in fluorescence from the acrolein-inactivated enzyme. The fluorescence data is shown in Figure 2-17, below.

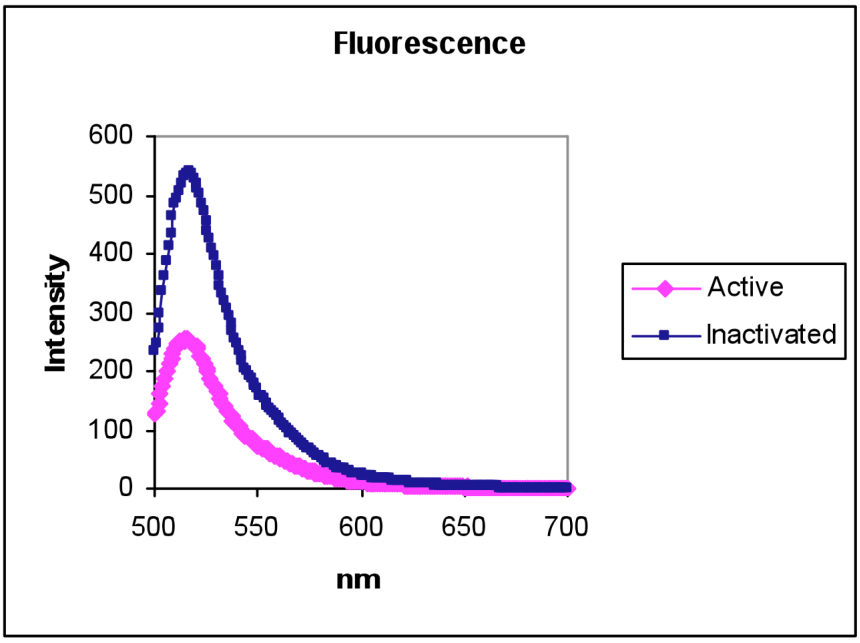

Figure 2-17. An overlay of the fluorescence spectra of both control (active) and acrolein-inactivated PTP1B.

Overall, both the structure-activity relationship study and the aldehyde tagging with the fluorescent probe confirm that the inactivation of PTP1B by acrolein proceeds through the 1,4-Michael type reaction with the carbon-carbon double bond of acrolein.

2.11 Discussion.

We have provided evidence that acrolein is a potent irreversible inactivator of the enzyme PTP1B (k_{inact} = 0.020 ± 0.005 s^{-1}, K_I = 2.3 ± 0.6 x 10^{-4}M). The apparent second-order rate constant for the inactivation of PTP1B by acrolein (87 $M^{-1}s^{-1}$) is comparable to that reported previously for hydrogen peroxide (10 $M^{-1}s^{-1}$), a known endogenous regulator of PTP1B.[17, 18, 31, 32] The inactivation of PTP1B by acrolein is considerably slowed by the addition of an active site binder to the inactivation reaction, providing evidence that the inactivation is active-site directed in nature. Indeed, we have confirmed

this by mass spectrometry of the inactivated enzyme, which indicated that the active site cysteine-215 residue is modified by acrolein. In addition, in the mass spectrometry of acrolein inactivated PTP1B, we see at least some modification of a few other cysteine residues outside the active site. Such allosteric modifications can alter activity, however, clearly modification of the active site cysteine is involved so this is unlikely in this case.

Examination of a series of structurally related aldehydes shows that the double bond of acrolein is central to its properties as a phosphatase inactivator. This fact is revealed by the observation that simple aliphatic aldehydes, like acetaldehyde, propanal or glyoxal, do not significantly inactivate PTP1B under the conditions employed for these studies. Furthermore, steric bulk at the alkene terminus, like in 3-methyl-2-butenal, or crotonaldehyde, diminishes the PTP1B-inactivated properties of compounds in this series. To further confirm our mechanistic conclusions, we have shown that the hydroxylamine tagged fluorescent probe binds more readily to the acrolein-inactivated enzyme when compared to the control, active enzyme reaction. Together, these observations support an inactivation mechanism involving conjugate addition of the active site cysteine-215 to the carbon-carbon double bond of acrolein.

In conclusion, inactivation of PTPs can yield profound biological consequences arising from the disruption of cellular signaling pathways.[33-37] Acrolein has been shown to modify functionally critical cysteine residues inside cells, leading to a number of different biological activities. The results reported here indicate that inactivation of PTPs can be considered as a possible contributor to the diverse biological activities of acrolein and structurally related α, β-unsaturated aldehydes.

2.12 Materials and Methods.

2.12.1 Chemicals and Reagents.

Reagents were purchased from the following suppliers: Buffer salts, *p*-nitrophenyl phosphate (pNPP), thiols, trifluoroacetic acid (TFA), sodium orthovanadate, acetaldehyde, 3-methyl-2-butenal, Diethylenetriaminepentaacetic acid (DTPA), Tergitol (NP-40) and crotonaldehyde were obtained from Sigma-Aldrich (St. Louis, MO). Catalase (catalog number 106810) and SOD (catalog number 837113) were obtained from Roche Bioscience (Palo Alto, CA). Acrolein and Glyoxal were obtained from Acros Organics. Sequencing grade modified trypsin (catalog number V5111) was obtained from Promega. Ammonium bicarbonate was obtained from Fisher Scientific. Hydroxlyamine-tagged fluorescent probe was obtained from Molecular Probes (catalog number A30629). Recombinant PTP1B (a.a. 1-322) was prepared in our laboratory as reported previously.[20] The concentration of active PTP1B in the samples was determined as described previously.[20]

2.12.2 Time-Dependent Inactivation of PTP1B.

Inactivation kinetics assays were performed using modifications of existing literature protocols.[19, 38, 39] Free thiols were removed from a stock solution of purified PTP1B using Zeba mini centrifugal buffer exchange columns (Pierce, catalog number 89882) according to manufacturer's protocol. The exchange buffer contained 100 mM TRIS-HCl, 10 mM DTPA, 0.05% NP-40, pH 7.4. In the inactivation reactions, acrolein was added as a stock solution in water to a mixture containing PTP1B in TRIS-HCl (100 mM, pH 7.4), DTPA (10 mM), and NP-40 (0.05%) at 30°C (final concentrations, acrolein: 60 μM, 50 μM, 40 μM, 30 μM, and 20 μM, PTP1B: ~75 ηmol, final volume:

100 μL). Aliquots (10 μL) were removed at various time points (1 min, 2 min, 5 min, and 10 min) and placed in 490 μL of PTP1B assay buffer consisting of Bis-Tris (50 mM, pH 6.0), NaCl (100 mM), DTPA (10 mM) and pNPP (20 mM) at 30°C for 10 minutes. The enzymatic reaction was quenched by addition of NaOH (500 μL of 2 N solution in water), and the amount of p-nitrophenol released during the assay was determined at 25°C by measuring the absorbance at 410 nm using a UV-vis spectrometer.

2.12.3 Gel Filtration of Acrolein-Inactivated PTP1B.

A solution of acrolein in water (10 μL of a 5 mM solution) was added to PTP1B (40 μL of a 4 μM solution in TRIS-HCl (100 mM, pH 7.4), DTPA (10 mM), and NP-40 (0.05% v/v). After 10 minutes, an aliquot (10 μL) was removed and tested for activity to confirm that the enzyme was completely inactivated. An Aliquot of the remaining solution (12 μL) was gel filtered through a Zeba micro spin column according to manufacturer's protocol. The exchange buffer contained 100 mM TRIS-HCl, 10 mM NaCl, 10 mM DTPA, 0.05% NP-40, pH 7.4. Following buffer exchange, an aliquot (10 μL) was tested for PTP1B activity as described above. No measurable return of PTP1B activity was observed (compared to a control sample treated in an identical manner except without inactivation by acrolein).

2.12.4 Time-Dependent Inactivation in the Presence of a Competitive PTP1B Inhibitor or Superoxide Dismutase or Catalase.

An aliquot of thiol-free enzyme (20 μL of a 4 μM solution in 100 mM TRIS-HCl, 10 mM NaCl, 10 mM DTPA, 0.05% NP-40, pH 7.4) was combined with an aqueous

solution of acrolein and orthovanadate (20 μL of 500 μM acrolein in H_2O containing 1 mM orthovanadate) at 25°C (Final concentrations: PTP1B, 2 μM; acrolein, 250 μM; orthovanadate, 500 μM). After 5 min, a 10 μL aliquot was removed and added to a cuvette containing a three component PTP1B assay buffer (990 μL) consisting of sodium acetate (100 mM), Bis-TRIS (50 mM), and TRIS (50 mM) at pH 7.0 (final volume of 1 mL). Immediately following addition of enzyme to the cuvette, the assay was mixed by repeated inversion, and enzyme catalyzed release of *p*-nitrophenol was monitored at 25°C by measuring the increase in absorbance at 410 nm. In the assays designed to probe the potential role of reactive oxygen species in the inactivation of PTP1B by acrolein, thiol-free PTP1B (18 pmol) was added to a cuvette containing the assay buffer (sodium acetate (100 mM), Bis-TRIS (50 mM), and TRIS (50 mM) pH 7.0), 10 mM *p*-Nitro phenylphosphate (pNPP), 1 mM acrolein, and 10 μg/mL SOD or 0.5 μg/mL catalase. PTP1B activity was monitored as described above. The presence of catalase or superoxide dismutase exerted no measurable effect on the inactivation reaction.

2.12.5 Matrix-Assisted Laser Desorption/Ionization Time-of-Flight (MALDI TOF/TOF MS and Nanospray MS/MS Analysis of Acrolein-Modified PTP1B.

Thiol free PTP1B (~14 pmol/μL) in 50 μL buffer (100 mM TRIS-HCl, 10 mM NaCl, 10 mM DTPA, 0.05% NP-40, pH 7.4) containing 2 mM acrolein was incubated at 25°C for 30 minutes. The reaction was followed side by side with a control with no acrolein. After incubation, both solutions were subjected to a Zeba mini centrifugal buffer exchange column. 50 μL of sequence grade modified trypsin (1μg/50μL) in 50

mM ammonium bicarbonate was added to the solution. The digestion was incubated at 37°C for 18 hours then quenched with 5 μL of 10% TFA (aq). 20 μL of each solution was frozen with liquid nitrogen and lyophilized dry. The residue was resuspended in 10 μL of water and lyophilized dry a second time. The final dried sample was reconstituted in 5 μL 700/290/10 (V/V/V) acetonitrile/water/88% formic acid. For MALDI TOF/TOF MS analysis, a 0.6 μL portion of diluted sample was mixed with an equal volume of alpha-cyano-4-hydroxycinnamic acid (CHCA) matrix solution (5 mg CHCA/mL 500/455/20/25 (V/V/V/V) acetronitrile/water/10% TFA/400 mM (aq) ammonium dihydrogen phosphate). Aliquots (0.4 μL) of the mixture were deposited on a polished stainless steel target. Crystallization of the mixture proceeded under ambient conditions. Mass spectra were acquired on an Applied Biosystems Inc. 4700 MALDI TOF/TOF mass spectrometer with a 355 nm Nd:YAG laser (200 Hz) in the positive ion delayed extraction reflector MS mode. The MS spectra (2000 laser shots summed/averaged) were acquired over the mass range 700-4000 Da. Each MS spectrum was re-calibrated internally using the masses (monoisotopic $[M+H]^+$) for the PTP1B Tryptic fragments observed at 1366.675 Da ([13-24]) and 2508.2881 Da ([293-314]). For Nanospray MS/MS of the active site peptide 200-221, ziptip cleanup of sample with fractions of 50/940/10, 100/890/10, and 200/790/10 (V/V/V) acetonitrile/water/88% formic acid (AWF) were pooled then lyophilized dry. The sample was reconstituted in 4 μL 700/290/10 AWF for nanospray QqTOF MS analysis on an Applied Biosystems/MDS Sciex (Foster City, CA, USA) QStar/Pulsar/I instrument fitted with a Proxeon (Odense, Denmark) nanospray source. A pulsar frequency of 6.99 kHz was used for MS/MS mass range 50-2000 Da. MS/MS spectra were obtained with N_2 collision gas. The MS/MS of

the 3^+ ion at 744.37 Da for the peptide of interest was obtained with a collision energy of 35 volts. The instrument software was Analyst QS and the data analysis software was BioAnalyst 1.1.

2.12.6 Hydroylamine Fluorescent Probe Tagging of Acrolein-Modified PTP1B.

A solution of acrolein in water (5 μL of a 18 mM solution, final concentration = 1.8 mM) was combined with a solution of thiol-free PTP1B (45 μL of a 15 μM solution in TRIS-HCl (100 mM, pH 7.4), DTPA (10 mM), and NP-40 (0.05% v/v) at 25°C. A control, with no acrolein, was also run side by side. After 30 min, the solution was gel filtered through a Zeba mini spin column according to manufacturer's protocol to remove excess acrolein. The exchange buffer contained 100 mM TRIS-HCl, 10 mM NaCl, 10 mM DTPA, 0.05% NP-40, pH 7.4. The gel filtered solution was combined with a solution of Alexa Fluor 488 hydroxylamine fluorescent probe (50 μL of a 80 μM solution, final concentration = 40 μM) at 37°C. After 1 hour, the resultant solution was gel filtered through a Zeba mini spin column according to manufacturer's protocol to remove excess fluorescent probe. The solution was then subjected to a second Zeba mini spin column to remove as much excess probe as possible, to aid analysis. The resultant solution was combined with 900 μL 100 mM TRIS-HCl, 10 mM NaCl, 10 mM DTPA, 0.05% NP-40, pH 7.4 (Final volume = 1000 uL). The absorbance of the control and acrolein-modified solutions was determined at 494 nm by a Uv/vis spectrometer. The fluorescence at an Em of 518 nm was determined on a fluorescence spectrometer.

2.13 References

1. O'Brien, P. J.; Siraki, A. G.; Shangari, N., Aldehyde sources, metabolism, molecular toxicity, and possible effects on human health. *Crit. Rev. Toxicol.* **2005,** 35, 609-662.

2. Uchida, K.; Kanematsu, M.; Sakai, K.; Matsuda, T.; Hattori, N.; Mizuno, Y.; Suzuki, D.; Miyata, T.; Noguchi, N.; Niki, E.; Osawa, T., Protein-bound acrolein: potential markers for oxidative stress. *Proc. Nat. Acad. Sci. USA* **1998,** 95 (9), 4882-4887.

3. Montine, T. J.; Neely, M. D.; Quinn, J. F.; Beal, M. F.; Markesbery, W. R.; Roberts, L. J.; Morrow, J. D., LIpid peroxidation in aging brain and Alzheimer's. *Free Rad. Biol. Med.* **2002,** 33 (5), 620-626.

4. Arlt, S.; Beisiegel, U.; Kontush, A., Lipid peroxidation in neurodegeneration: new insights into Alzheimer's disease. *Curr. Opin. Lipidology* **2002,** 13 (3), 289-294.

5. Kato, S.; Post, G. C.; Bierbaum, V. M.; Koch, T. H., Chemical Ionization Mass Spectrometric Determination of Acrolein in Human Breast Cancer Cells. *Analytical Biochemistry* **2002,** 305 (2), 251-259.

6. Anderson, M. M.; Hazen, S. L.; Hsu, F. F.; Heinecke, J. W., Human neutrophils employ the myeloperoxidase-hydrogen peroxide-chloride system to convert hydroxy-amino acids into glycolaldehyde, 2-hydroxypropanal, and acrolein. *J. Clin. Investig.* **1997,** 99 (3), 424-432.

7. Carbone, D. L.; Doorn, J. A.; Kiebler, Z.; Petersen, D. R., Cysteine Modification by Lipid Peroxidation Products Inhibits Protein Disulfide Isomerase. *Chem. Res. Toxicol.* **2005,** 18 (8), 1324-1331.

8. Feron, V. J.; Til, H. P.; De Vrijer, F., Aldehydes in food: occurrence, carcinogenic activity, and risks. *Voeding* **1992,** 53 (1), 2-8.

9. Lane, R. H.; Smathers, J. L., Monitoring aldehyde production during frying by reversed-phase liquid chromatography. *J. - Assoc. Off. Anal. Chem.* **1991,** 74 (6), 957-60.

10. Hecht, S. S., Smoking and lung cancer - a new role for an old toxicant? *Proc. Nat. Acad. Sci. USA* **2006,** 103 (43), 15725-15726.

11. Finkelstein, E. I.; Ruben, J.; Koot, C. W.; Hristova, M.; van der Vliet, A., Regulation of constitutive neutrophil apoptosis by the α,β-unsaturated aldehydes acrolein and 4-hydroxynonenal. *Am. J. Physiol.* **2005,** 289 (6, Pt. 1), L1019-L1028.

12. Kern, J. C.; Kehrer, J. P., Acrolein-induced cell death: a caspase-influenced decision between apoptosis and oncosis/necrosis. *Chem. Biol. Interact.* **2002,** 139 (1), 79-95.

13. Macpherson, L. J.; Dubin, A. E.; Evans, M. J.; Marr, F.; Schultz, P. G.; Cravatt, B. F.; Patapoutian, A., Noxious compounds activate TRPA1 ion channels through covalent modification of cysteines. *Nature* **2007,** 445 (7127), 541-545.

14. Horton, N. D.; Biswal, S. S.; Corrigan, L. L.; Bratta, J.; Kehrer, J. P., Acrolein causes inhibitor kB-independent decreases in nuclear factor kB activation in human lung adenocarcinoma (A549) cells. *J. Biol. Chem.* **1999,** 274 (14), 9200-9206.

15. Tirumalai, R.; Rajesh Kumar, T.; Mai, K. H.; Biswal, S., Acrolein causes transcriptional induction of phase II genes by activation of Nrf2 in human lung type II epithelial (A549) cells. *Toxicol. Lett* **2002,** 132 (1), 27-36.

16. Pugazhenthi, S.; Phansalkar, K.; Audesirk, G.; West, A.; Cabell, L., Differential regulation of c-jun and CREB by acrolein and 4-hydroxynonenal. *Free Radical Biol. Med.* **2006,** 40 (1), 21-34.

17. Barrett, W. C.; DeGnore, J. P.; Keng, Y.-F.; Zhang, Z.-Y.; Yim, M. B.; Chock, P. B., Roles of superoxide radical anion in signal transduction mediated by reversible regulation of protein-tyrosine phosphatase 1B. *J. Biol. Chem.* **1999,** 274 (49), 34543-34546.

18. Denu, J. M.; Tanner, K. G., Specific and reversible inactivation of protein tyrosine phosphatases by hydrogen peroxide: evidence for a sulfenic acid intermediate and implications for redox regulation. *Biochemistry* **1998,** 37, 5633-5642.

19. Silverman, R. B., *Mechanism-Based Enzyme Inactivation: Chemistry and Enzymology*. CRC Press: Boca Raton, 1988; Vol. I.

20. LaButti, J. N.; Chowdhury, G.; Reilly, T. J.; Gates, K. S., Redox regulation of protein tyrosine phosphatase 1B by peroxymonophosphate. *J. Am. Chem. Soc.* **2007,** 129, 5320-5321.

21. Salmeen, A.; Anderson, J. N.; Myers, M. P.; Meng, T.-C.; Hinks, J. A.; Tonks, N. K.; Barford, D., Redox regulation of protein tyrosine phosphatase 1B involves a sulphenyl-amide intermediate. *Nature* **2003,** 423 (June 12), 769-773.

22. Thornalley, P.; Wolff, S.; Crabbe, J.; Stern, A., The autooxidation of glyceraldehyde and other simple monosaccharides under physiological conditions catalysed by buffer ions. *Biochim. Biophys. Acta* **1984,** 797, 276-287.

23. Halliwell, B.; Gutteridge, J. M. C., Role of free radicals and catalytic metal ions in human disease: an overview. *Methods Enzymol.* **1990,** 186, 1-85.

24. Zhang, Z.-Y., Protein tyrosine phosphatases: structure and function, substrate specificity, and inhibitor development. *Ann. Rev. Pharmacol. Toxicol.* **2002,** 42 (42), 209-234.

25. Keil-Dlouh·, V.; Zylber, N.; Imhoff, J. M.; Tong, N. T.; Keil, B., Proteolytic activity of pseudotrypsin. *FEBS Letters* **1971,** 16 (4), 291-295.

26. Esterbauer, H.; Ertl, A.; Scholz, N., The reaction of cysteine with a,b-unsaturated aldehydes. *Tetrahedron* **1976,** 32, 285-289.

27. Hernandez-Hernandez, A.; Sanchez-Yague, J.; Martin-Valmaseda, E. M.; Llanillo, M., Oxidative inactivation of human and sheep platelet membrane-associated phosphotyrosine phosphatase activity. *Free Rad. Biol. Med.* **1999,** 26 (9/10), 1218-1230.

28. Dutta, S.; Chowdhury, G.; Gates, K. S., Interstrand crosslinks generated by abasic sites in duplex DNA. *J. Am. Chem. Soc.* **2007,** 129, 1852-1853.

29. clayden, J.; Greeves, N.; Warren, S.; Wothers, P., *Organic Chemistry*. Oxford University Press: New York, 2001.

30. Fundador, E.; Rusling, J., Detection of labeled abasic sites in damaged DNA by capillary electrophoresis with laser-induced fluorescence. *Analytical and Bioanalytical Chemistry* **2007,** 387 (5), 1883-1890.

31. Mahedev, K.; Zilbering, A.; Zhu, L.; Goldstein, B. J., Insulin-stimulated hydrogen peroxide reversibly inhibits protein-tyrosine phosphatase 1B in vivo and enhances the early insulin action cascade. *J. Biol. Chem.* **2001,** 276 (24), 21938-21942.

32. Tonks, N. K., Redox redux: revisiting PTPs and the control of cell signaling. *Cell* **2005,** 121 (June 3), 667-670.

33. Bialy, L.; Waldmann, H., Inhibitors of protein tyrosine phosphatases: next generation drugs? *Angew. Chem. Int. Ed. Eng.* **2005,** 44, 3814-3839.

34. Johnson, T. O.; Ermolieff, J.; Jirousek, M. R., Protein tyrosine phosphatase 1B inhibitors for diabetes. *Nature Rev. Drug Discov.* **2002,** 1 (Sept), 696-709.

35. Hoffman, B. T.; Nelson, M. R.; Burdick, K.; Baxter, S. M., Protein tyrosine phosphatases: strategies for distinguishing proteins in a family containing multiple drug targets and anti-targets. *Curr. Pharm. Des.* **2004,** 10, 1161-1181.

36. Bridges, A. J., Therapeutic challenges of kinase and phosphatase inhibition and use in anti-diabetic strategy. *Biochem. Soc. Trans* **2005,** 33 (2), 343-345.

37. Julien, S. G.; Dubé, N.; Read, M.; Penney, J.; Paquet, M.; Han, Y.; Kennedy, B. P.; Muller, W. J.; Tremblay, M. L., Protein tyrosine phosphatase 1B deficiency or inhibition delays Erb2-induced mammary tumorigenesis and protects from lung metastasis. *Nat. Genetics* **2007,** 39 (3), 338-346.

38. Arabaci, G.; Guo, X.-C.; Beebe, K. D.; Coggeshall, K. M.; Pei, D., alpha-Haloacetophenone derivatives as photoreversible covalent inhibitors of protein tyrosine phosphatases. *J. Am. Chem. Soc.* **1999,** 121, 5085-5086.

39. Montalibet, J.; Skorey, K. I.; Kennedy, B. P., Protein tyrosine phosphatase: enzymatic assays. *Methods* **2005,** 35, 2-8.

THE MECHANISM OF INACTIVATION OF PTP1B BY THE DIETARY ISOTHIOCYANATES

3.1 Isothiocyanate dietary sources

Isothiocyanates, such as allyl isothiocyanate, benzyl isothiocyanate, and sulforaphane (Figure 3-1), are found in a wide variety of plants in the Brassicaceae family, such as Brussels sprouts, broccoli, cabbage, cauliflower, mustard, and horseradish.[1-5] Allyl isothiocyanate is believed to be responsible for the spicy flavor of horseradish and mustard, as well as the 'bite' of raw cabbage.[6]

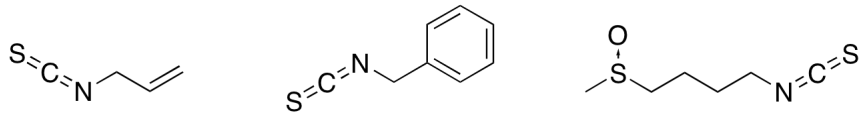

Figure 3-1. Three examples of commonly found dietary isothiocyanates, allyl isothiocyanate, benzyl isothiocyanate, and sulforaphane.

Isothiocyanates are formed from glucosinolates by enzymatic hydrolysis by the plant enzyme myrosinase.[7] Myrosinase is released as a plant defense mechanism upon crushing of the plant cell wall, such as during chewing or cutting, leading to conversion of the glucosinolate precursors to a variety of different isothiocyanates.[8] The most commonly found glucosinolate in cruciferous vegetables, with the exception of broccoli, is sinigrin, which upon enzymatic hydrolysis by myrosinase forms the previously mentioned allyl isothiocyanate (Scheme 1-1).[6]

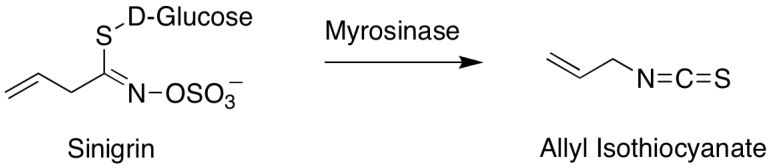

Scheme 3-1. Sinigrin is converted to allyl isothiocyanate by the plant enzyme myrosinase.[6]

3.2 Level of human exposure to isothiocyanates

The isothiocyanates have been shown in several studies to be readily absorbed by cells, both from raw and cooked vegetables, although boiling the vegetables decreases the overall absorption due to the inactivation of myrosinase.[9] In cell culture, isothiocyanates have been shown to rapidly accumulate inside cells, probably due to their rapid conjugation with cellular thiols.[9]

The glucosinolate precursors to isothiocyanates are found in high concentrations in certain foods.[10, 11] The cruciferous vegetables have been shown to contain between 10 and 940 μmol/kg of the glucosinolate precursors, depending on the vegetable.[11] Interestingly, some condiments have been shown to contain high levels of isothiocyanates; mustard and horseradish, for example, have been shown to contain between 830 μmol/kg and 1880 μmol/kg of allyl isothiocyanate, respectively, contributing to their spiciness.[11]

3.3 Biological activity of Isothiocyanates

Isothiocyanates display a wide array of biological activity.[3, 12-18] Sulforaphane, found especially in broccoli, has potent anti-cancer and anti-inflammatory properties.[2, 13,

[19] Importantly, sulforaphanes biological activity is directly derived from modification of functionally critical cysteine residues on proteins (Scheme 3-2).[15]

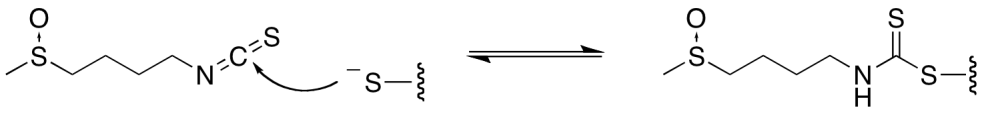

Scheme 3-2. Protein thiol side chains react reversibly with the electrophilic carbon of the isothiocyanate moiety of sulforaphane.[14]

For a widely explored example of its biological activity, sulforaphane has been shown to modify several sensor cysteines on Kelch-like ECH-associated protein 1 (Keap1), which leads to activation of the transcription factor nuclear factor-E2-related factor 2 (Nrf2).[14, 15] Activation of Nrf2 leads to induction of phase II enzymes and antioxidant gene products, and results in the majority of the widely reported chemopreventative effects of sulforaphane.[14] In addition, sulforaphane has been shown to inactivate Cytochrome P450 enzymes, leading to further chemopreventative effects by inhibiting the metabolism of certain procarcinogens.[20, 21]

Sulforaphane has received a lot of attention; however, it is not the only isothiocyanate with biological activity. Benzyl isothiocyanate and allyl isothiocyanate, the more commonly found isothiocyanates in cruciferous vegetables, also display a wide range of biological activity.[4, 6, 21-24] Like sulforaphane, allyl and benzyl isothiocyanate have also been shown to have anticarcinogenic properties.[22] Allyl and benzyl isothiocyanate have been shown to induce phase II detoxification enzymes in cultured cells and when fed to mice and rats.[6, 23] Further, both allyl and benzyl isothiocyanate have been shown to inactivate Cytochrome P450 enzymes in rat liver microsomes when fed orally to rats.[24]

3.4 Hypothesis: Isothiocyanates are inactivators of PTPs

As noted earlier, isothiocyanates' biological activity is derived from modification of functionally critical cysteine side chains.[15] Furthermore, isothiocyanates have been shown to modulate cellular phosphorylation levels.[25, 26] Since protein tyrosine phosphatases are cysteine dependent enzymes, we thought it was possible that part of isothiocyanates wide range of biological activity could be derived from the inactivation of protein tyrosine phosphatases. We chose to explore this possibility and study the mechanism of inactivation to obtain a better understanding of isothiocyanates biological activity.

We utilized the catalytic subunit of human PTP1B (a.a. 1-322) as an archetypal member of the PTP family of enzymes. We decided to focus on the three previously mentioned, commonly found, dietary isothiocyanates, allyl isothiocyanate, benzyl isothiocyanate and sulforaphane.

3.5 Kinetics of Inactivation of PTP1B by Isothiocyanates

We have found that isothiocyanates are, indeed, time-dependent inactivators of PTP1B. We initially tested the most common isothiocyanate in cruciferous vegetables, allyl isothiocyanate (AITC), and found it to be a potent, time-dependent inactivator of PTP1B (Figure 3-2).

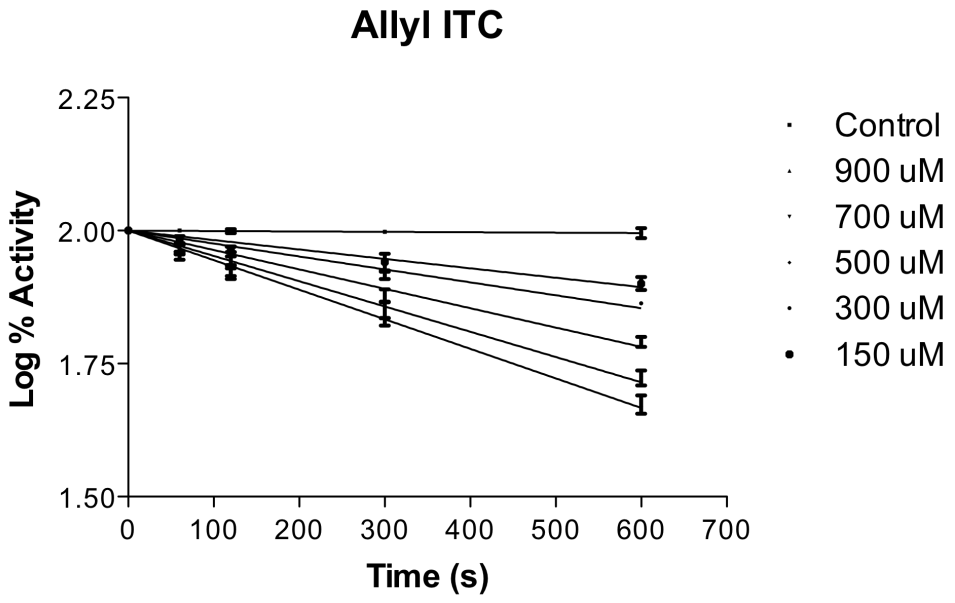

Figure 3-2. Semilog plot of time courses for the inactivation of PTP1B by various concentrations of allyl isothiocyanate (AITC). Points represent mean with SD, N=3.

The Kitz-Wilson replot of the inactivation data (Figure 3-3) revealed that the maximum rate of inactivation under saturating concentrations of allyl isothiocyanate, k_{inact} is 0.0020 ± 0.0002 s^{-1}. Furthermore, the concentration of acrolein required to achieve a half-maximal rate of inactivation, K_I, is 54 ± 3 x 10^{-5} M. It is worth noting, that the apparent second-order rate constant for the inactivation of PTP1B by allyl isothiocyanate (k_{inact}/K_I = 3.0 ± 0.5 $M^{-1}s^{-1}$) is comparable to the rate reported for the endogenous regulator of PTP1B activity, H_2O_2 (10 $M^{-1}s^{-1}$).[27-30]

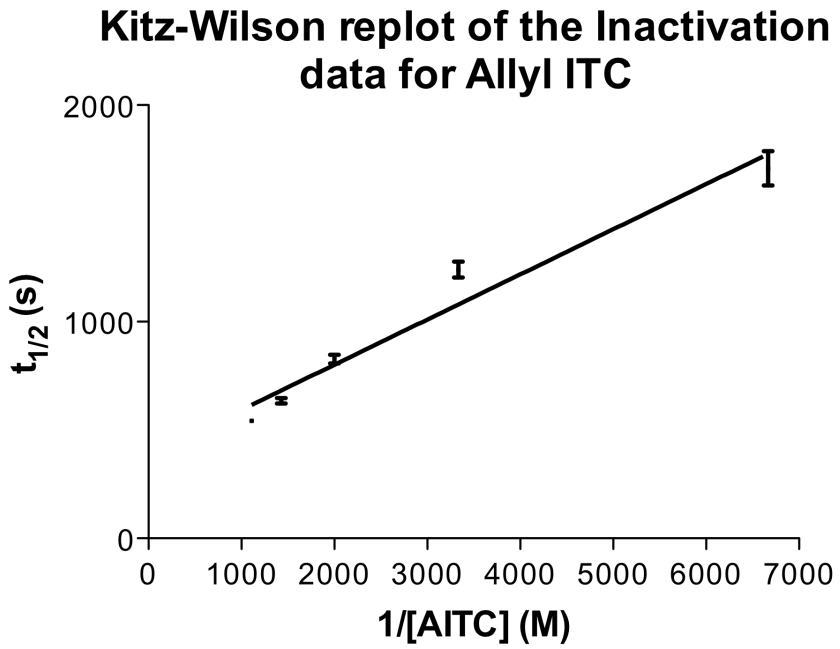

Figure 3-3. The Kitz-Wilson replot of the inactivation data for allyl isothiocyanate. Points represent mean with SD, N=3.

Next, we explored the kinetics of other isothiocyanates to probe whether different functional groups off of the isothiocyanate moiety would affect their activity against this enzyme. We decided to test sulforaphane, the major isothiocyanate found in broccoli, which has been shown to have significant biological activity.[31] We found that sulforaphane was indeed a time-dependent inactivator of PTP1B (Figure 3-4).

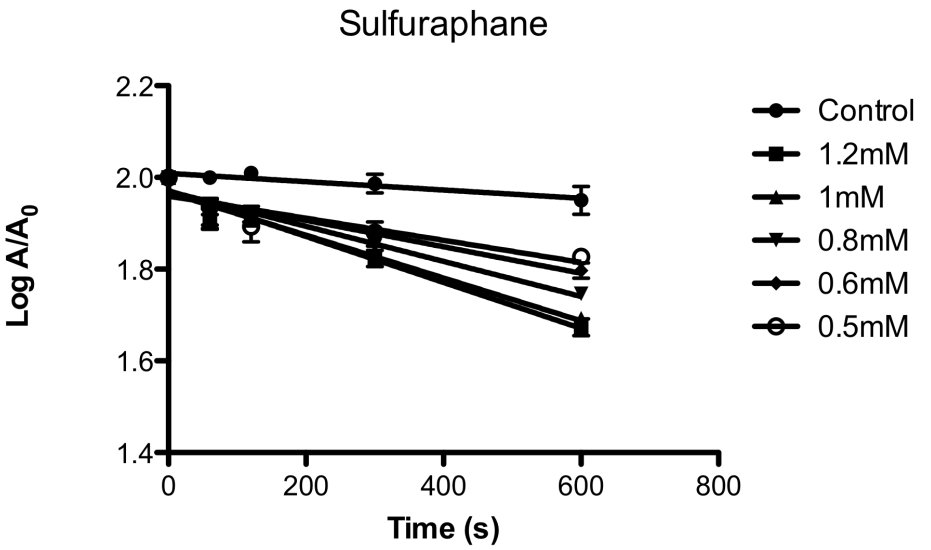

Figure 3-4. Semilog plot of the time courses for the inactivation of PTP1B by various concentrations of sulforaphane. Points represent mean with SD, N=3.

The Kitz-Wilson replot of the inactivation data (Figure 3-5) showed that the maximum rate of inactivation at saturating concentration of sulforaphane, k_{inact} is 0.010 ± 0.003 s^{-1}. Moreover, the concentration of sulforaphane required to achieve a half-maximal rate of inactivation, K_I, is 8.7 ± 5 x 10^{-3} M. As noted previously, the apparent second-order rate constant for the inactivation of PTP1B by sulforaphane (k_{inact}/K_I = 1.0 ± 0.1 $M^{-1}s^{-1}$) is comparable to the rate reported for the endogenous regulator of PTP1B activity, H_2O_2 (10 $M^{-1}s^{-1}$).

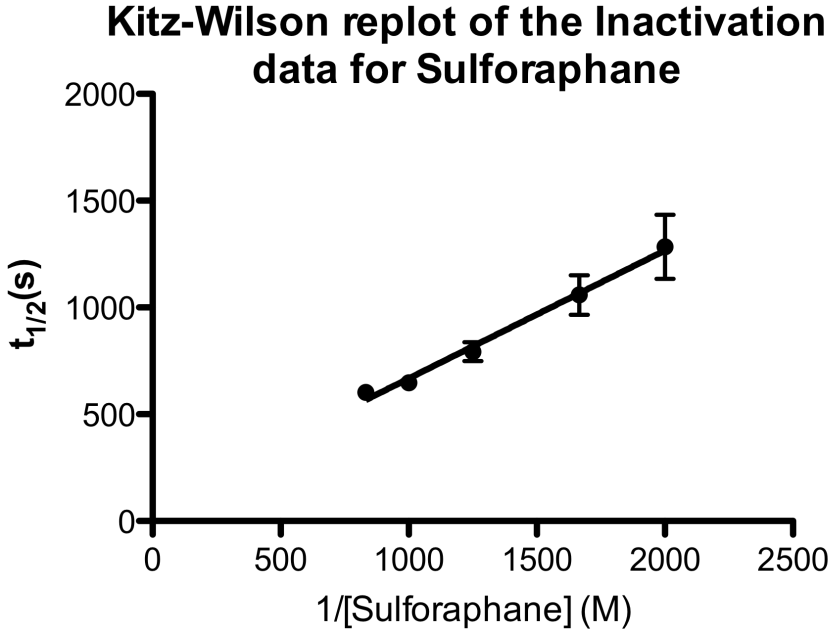

Figure 3-5. The Kitz-Wilson replot of the inactivation data for sulforaphane. Points represent mean with SD, N=3.

Next, we explored the isothiocyanates further by testing the activity of benzyl isothiocyanate. Benzyl isothiocyanate is another commonly found dietary isothiocyanate, and has shown some biological activity, as mentioned previously. We found that benzyl isothiocyanate is, indeed, a time-dependent inactivator of PTP1B (Figure 3-6).

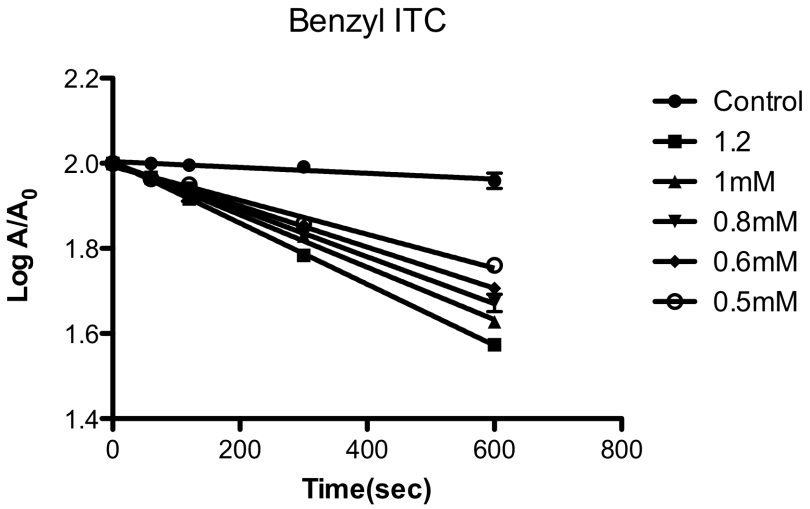

Figure 3-6. Semilog plot of time courses for the inactivation of PTP1B by various concentrations of benzyl isothiocyanate. Points represent mean with SD, N=3.

The Kitz-Wilson replot of the inactivation data (Figure 3-7) revealed that the maximum rate of inactivation at saturating concentration of benzyl isothiocyanate, k_{inact} is 0.0030 ± 0.0003 s^{-1}. Moreover, the calculated concentration of benzyl isothiocyanate required to achieve a half-maximal rate of inactivation, K_I, is 1.10 ± 0.04 x 10^{-3} M. Therefore, the apparent second-order rate constant for the inactivation of PTP1B by benzyl isothiocyanate (k_{inact}/K_I = 2.8 ± 0.2 $M^{-1}s^{-1}$) is comparable to the rate reported for the endogenous regulator of PTP1B activity, H_2O_2 (10 $M^{-1}s^{-1}$).

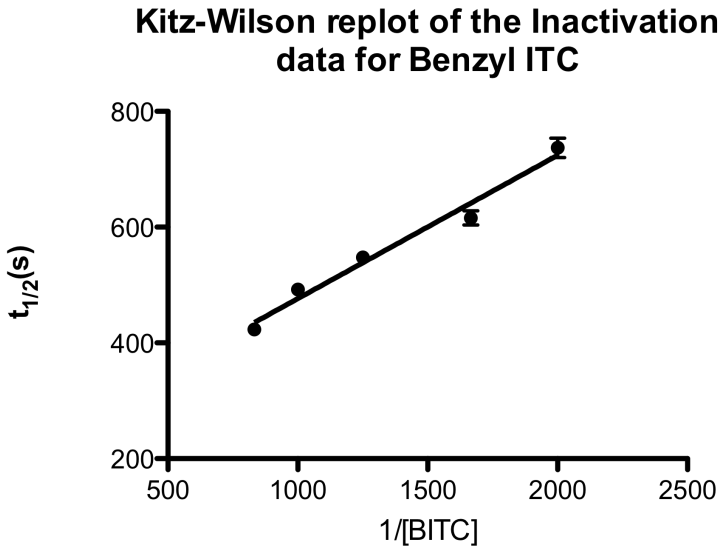

Figure 3-7. The Kitz-Wilson replot of the inactivation of PTP1B by benzyl isothiocyanate. Points represent mean with SD, N=3.

We explored the mechanism of inactivation by isothiocyanates further, and as mentioned previously, allyl isothiocyanate is the most commonly found isothiocyanate in cruciferous vegetables (with the only exception being broccoli).[6] Since the kinetics of inactivation were not largely dissimilar, we chose to continue our studies focusing on allyl isothiocyanate.

3.6 Inactivation of PTP1b by Allyl Isothiocyanate is Active-Site Directed

Arsenate has been identified as a active site binding ligand of PTP1B, with a reported K_I of 150 μM.[32, 33] We utilized this property of arsenate to explore whether allyl isothiocyanate inactivation of PTP1B is active site directed (Figure 3-8).

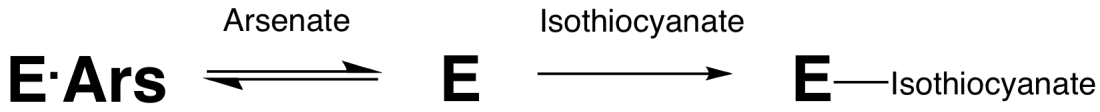

Figure 3-8. The active site directed experiments utilize the active site binder, arsenate, to compete for the active site of the enzyme with the inactivator.

Indeed, whenever 100 μM of arsenate was added to the inactivation reaction, the inactivation process was considerably slowed when compared to the 'standard' inactivation (without the active site binder present), as can be seen in Figure 3-9. This provides evidence that the inactivation of PTP1B involves reaction at the active site.

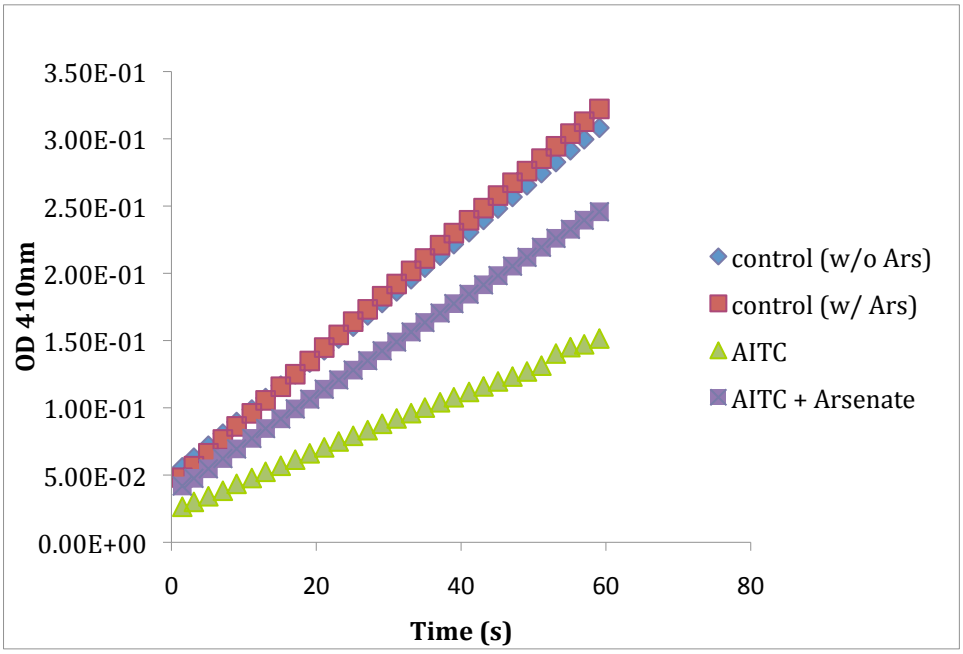

Figure 3-9. The inactivation of PTP1B by allyl isothiocyanate (AITC) is considerably slowed by the addition of 100 μM arsenate, an active site binder of PTP1B.

We sought to confirm these findings, so we decided to increase the amount of the active site 'competitor' in the inactivation reaction. Indeed, whenever we increased the arsenate in the inactivation reaction to 500 μM, we observed virtually complete quenching of the inactivation of PTP1B by allyl isothiocyanate (Figure 3-10).

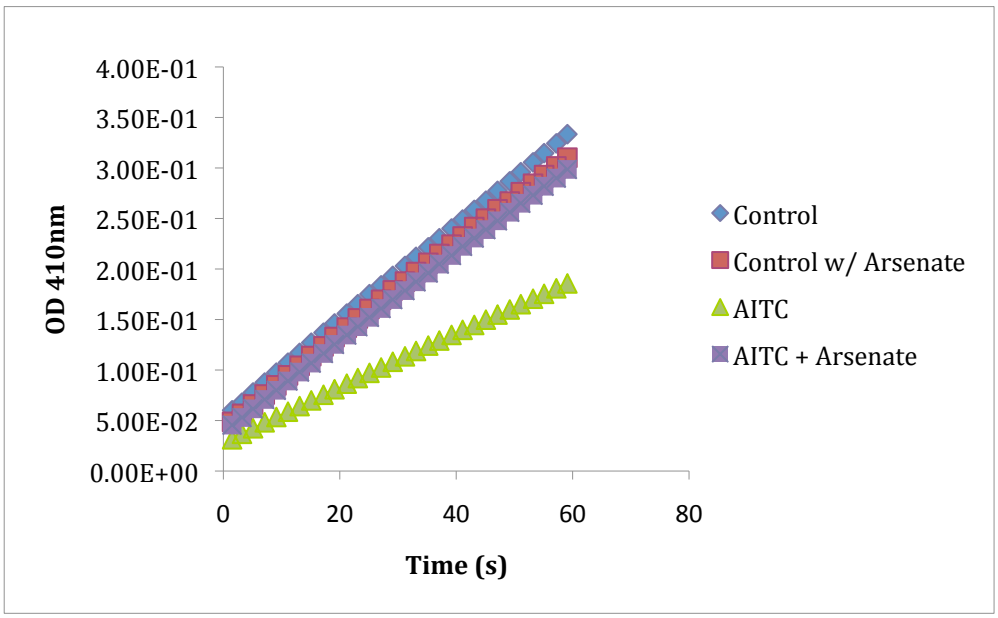

Figure 3-10. The inactivation of PTP1B is virtually quenched by the addition of 500 μM of the active site binder arsenate, providing further evidence the inactivation is active site directed in nature.

Next, we explored if the inactivation of PTP1B by allyl isothiocyanate was a reversible process since isothiocyanates have been identified as being reversible with thiol side chains on proteins.[34] First, we noticed that the inactivation of PTP1B by allyl isothiocyanate, even at high concentrations, did not completely inactivate the enzyme (Figure 3-11).

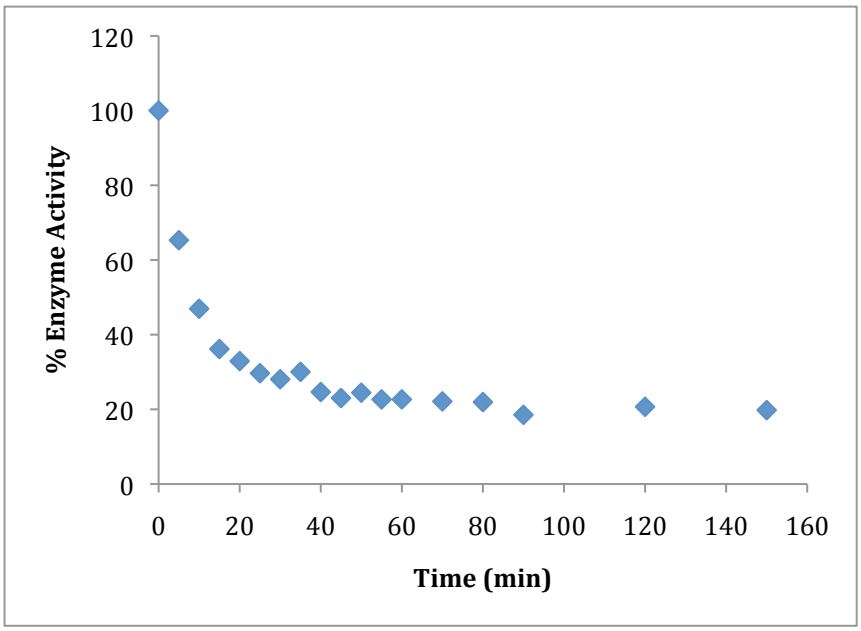

Figure 3-11. PTP1B is not completely inactivated by allyl isothiocyanate, even at high concentrations (1mM). This experiment was performed once, so error bars cannot be calculated.

Furthermore, whenever excess isothiocyanate is removed by gel filtration, we see a slow, time-dependent return of enzymatic activity, as can be seen in Figure 3-12. In this experiment, PTP1B was inactivated by allyl isothiocyanate as done before (1 mM allyl isothiocyanate, 30 min), then the reaction (along with the active control sample) was subjected to gel filtration to remove excess allyl isothiocyanate. As shown below, we see a doubling of enzymatic activity over the course of 4 hours. Notice that the control, non-inactivated enzyme, is slowly losing activity, probably due to background oxidation of the enzyme.

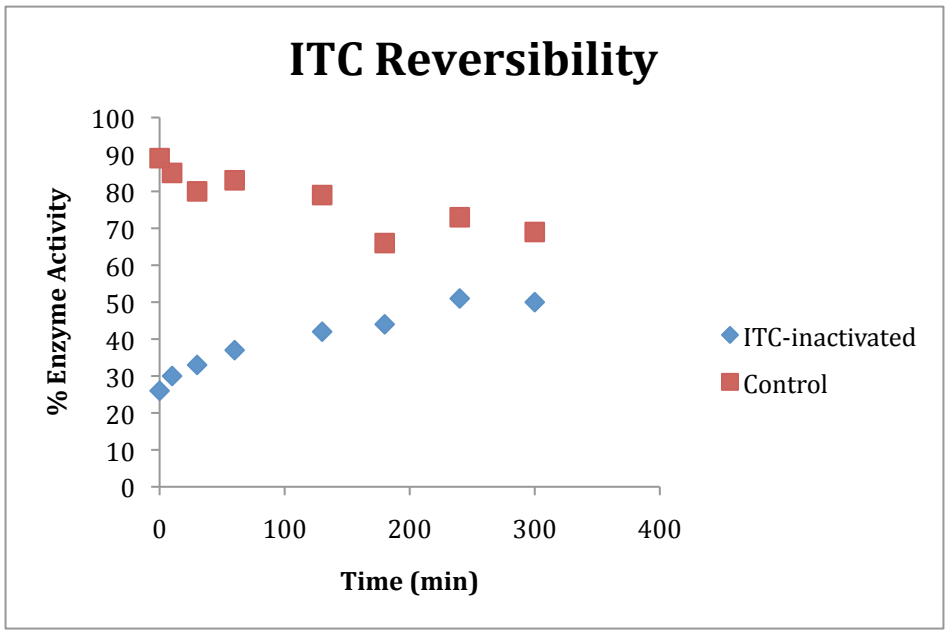

Figure 3-12. Enzymatic activity of allyl isothiocyanate-inactivated PTP1B returns upon removal of excess allyl isothiocyanate.

This data provides more evidence that the inactivation of PTP1B by allyl isothiocyanate involves a reversible covalent modification, possibly with the active site cysteine of PTP1B (Scheme 3-3).

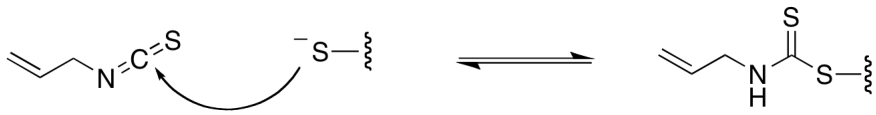

Scheme 3-3. Allyl isothiocyanate is reversible with protein thiols.

3.7 MALDI TOF/TOF MS and MS/MS Analysis of Allyl Isothiocyanate-Inactivated PTP1B

Isothiocyanates have been shown to react with a number of different amino acids.[35-38] It is worth noting that PTP1B has both a cysteine and a histidine in the active site pocket that are required for catalytic activity.[39] We used mass spectrometry to probe which site(s) the allyl isothiocyanate was modifying in the active site of PTP1B. Toward this end, we inactivated PTP1B with allyl isothiocyanate (2 mM, 1 hr) and subjected the inactivated protein to trypsin digestion. The resulting fragments were analyzed by MALDI-TOF-TOF mass spectrometry (Scheme 3-4).

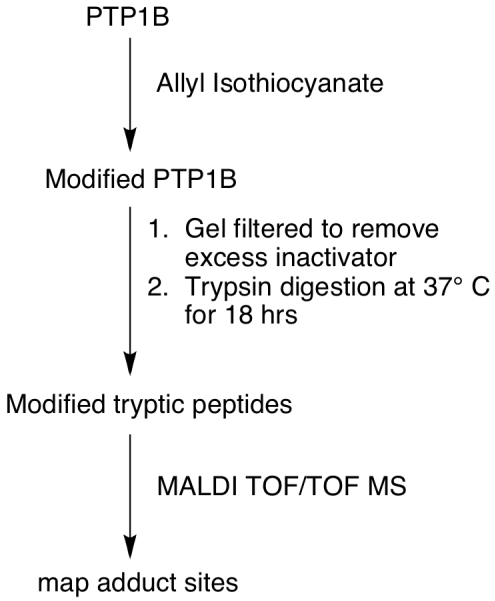

Scheme 3-3. The experimental order of the mass spectrometry experiments, a control sample containing no allyl isothiocyanate was also prepared.

A control experiment with active (no allyl isothiocyanate) was also run side by side. In the control (active enzyme) experiment, we were able to observe all of the cysteine containing tryptic fragments, as pointed out in Figure 3-13. Importantly, we

were able to observe a strong signal for the active site tryptic peptide [200-221] at *m/z* 2175.13.

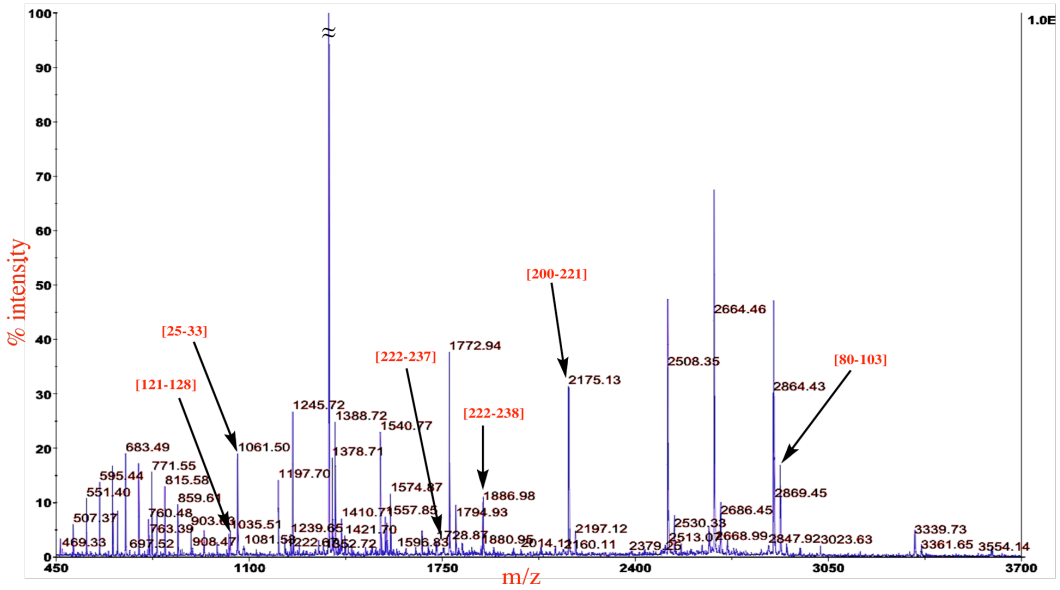

Figure 3-13. The control MALDI-TOF-TOF mass spectrum for the unmodified PTP1B. The cysteine containing tryptic fragments have been highlighted.

As can be seen in Figure 3-13, all of the cysteines containing tryptic fragments can be identified in the control experiment. The MALDI TOF/TOF MS of the inactivated enzyme can be seen in Figure 3-14. Notice that several of the cysteine containing tryptic peptides have been modified, at least to some extent.

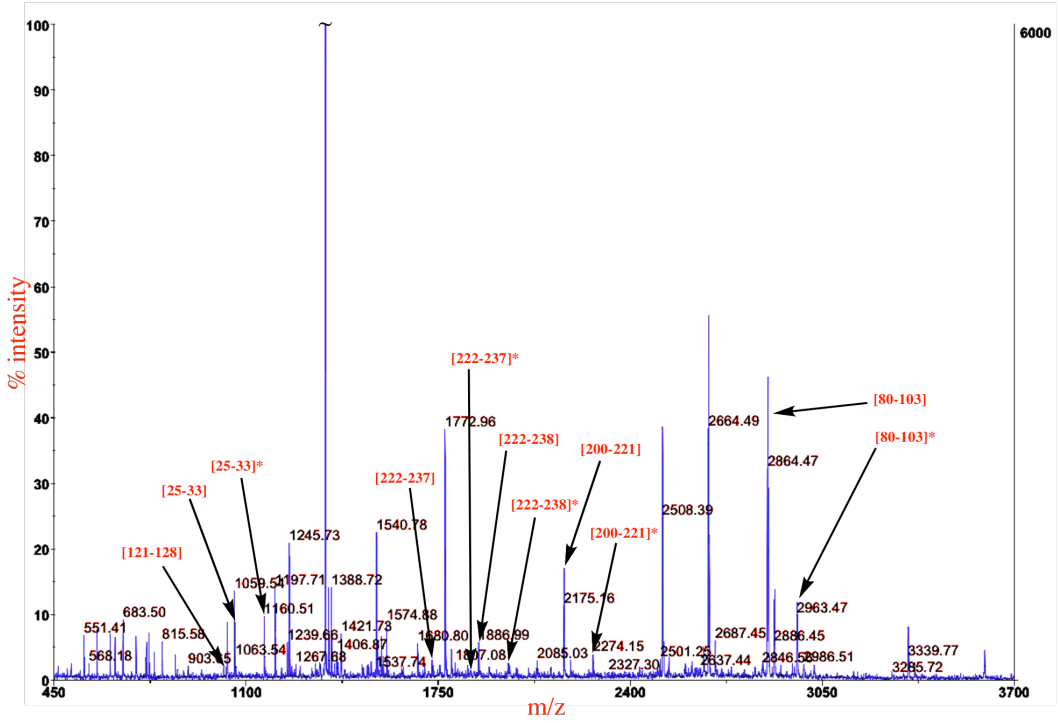

Figure 3-14. MALDI TOF/TOF MS spectra of the allyl isothiocyanate-inactivated PTP1B. Modified peptides are labeled in red with an asterisk(*).

The MALDI TOF/TOF MS spectrum of allyl isothiocyanate-inactivated PTP1B show several modified tryptic peptides. Importantly, a major signal was observed at *m/z* 2274.15 corresponding to the allyl isothiocyanate-modified active site peptide a.a. [200-221]. Also as expected, we observed the unmodified active site tryptic peptide at *m/z* 2175.16, since the cysteine-isothiocyanate adduct has been identified as being labile under trypsin digestion conditions.[34]

Furthermore, the MALDI TOF/TOF MS also showed at least some modification of a few other cysteine containing tryptic fragments. We observed the ions corresponding to allyl isothiocyanate modification of the tryptic peptides [80-103], [25-33], and [222-238]. These tryptic peptides correspond to Cys 92, Cys 32, and Cys 231 in PTP1B. However, we still needed to identify specifically which residue on the tryptic

peptides were being modified by allyl isothiocyanate. Toward this end, we chose to perform MALDI TOF/TOF MS/MS on each ion of interest.

First, we looked at the ion (*m/z* 2274.15) corresponding to the allyl isothiocyanate-modified active site peptide [200-221]. We observed the unmodified y_6 ion, whereas, we observed $y_{7,}$ y_{10}, y_{11}, y_{13}, and y_{14} all modified by +99 Da, corresponding to modification by one molecule of allyl isothiocyanate (Figure 3-15). Overall, this data shows that allyl isothiocyanate is modifying the active site cysteine residue of PTP1B, thus, shutting down the activity of the enzyme.

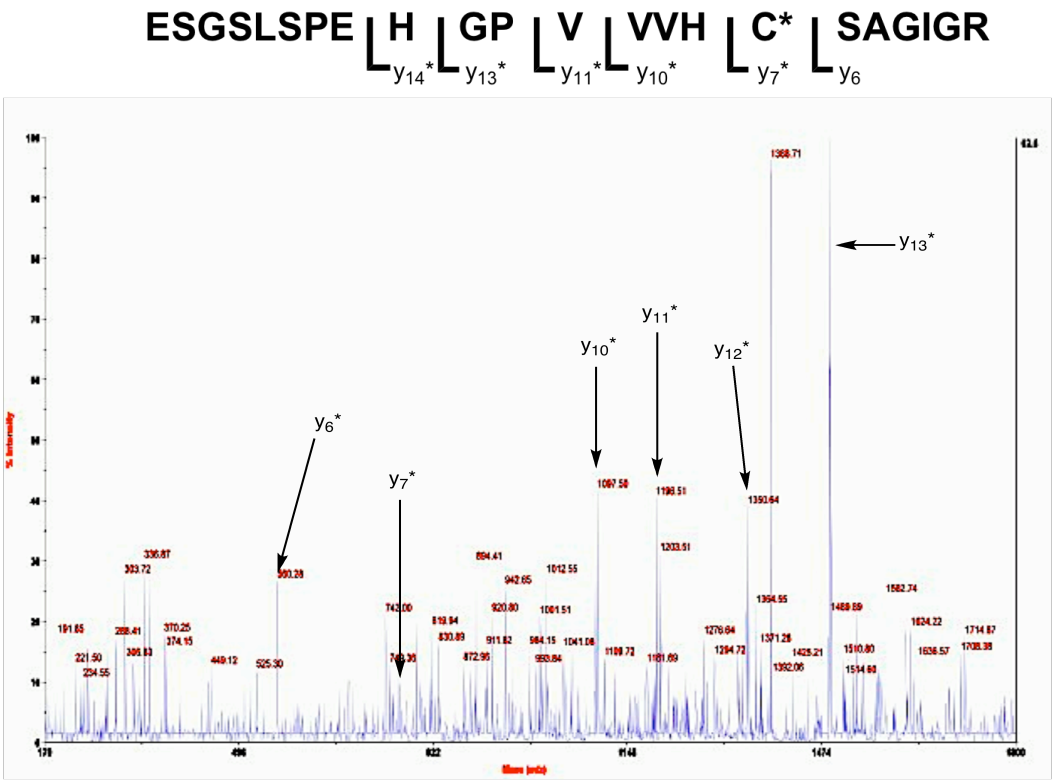

Figure 3-15. MALDI TOF/TOF MS/MS spectra for the active site tryptic peptide [200-221] with ions of interest highlighted. Modified ions are represented with an asterisk.

Next, we subjected the 2963.47 *m/z* ion, corresponding to modified tryptic peptide [80-103], to MALDI TOF/TOF MS/MS analysis to further quantify the sites of

modification by allyl isothiocyanate. The data showed the unmodified y_9-y_{11} ions, whereas the ions y_{12}-y_{13}, y_{15}, y_{17}-y_{18}, y_{20}, and y_{24}, were all modified by +99 Da, corresponding to the addition of one molecule of allyl isothiocyanate (Figure 3-16). However, we observed the b_{15}-b_{22} ions all increased by +99 Da, again corresponding to the addition of one molecule of allyl isothiocyanate. This data clearly shows that allyl isothiocyanate is modifying cysteine 92 of PTP1B.

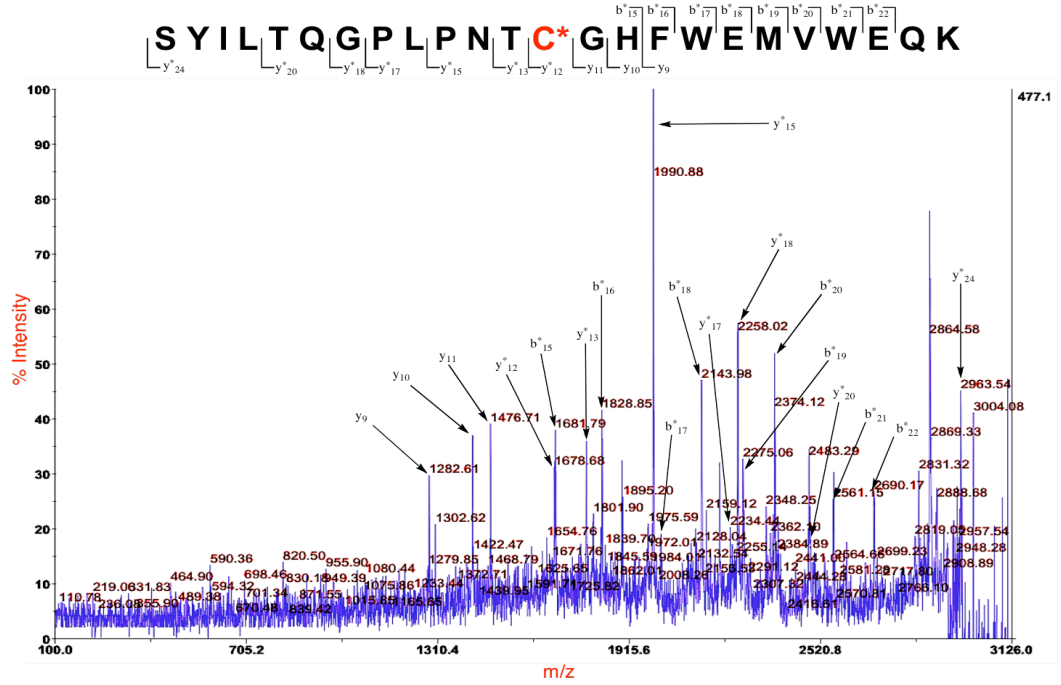

Figure 3-16. MALDI TOF/TOF MS/MS of the tryptic peptide [80-103] modified by one molecule of allyl isothiocyanate. The peptide has been modified by allyl isothiocyanate at Cys 92.

Lastly, we looked at the ion at *m/z* 1160.51, corresponding to the modified tryptic peptide [25-33]. We observed the unmodified y_1 ion, and the modified y_3-y_7, and y_8 ions all increased by +99 Da. Furthermore, we observed the b_2-b_7 ions all increased by +99 Da. This data clearly shows that allyl isothiocyanate is modifying the peptide at Cys 32 (Figure 3-17).

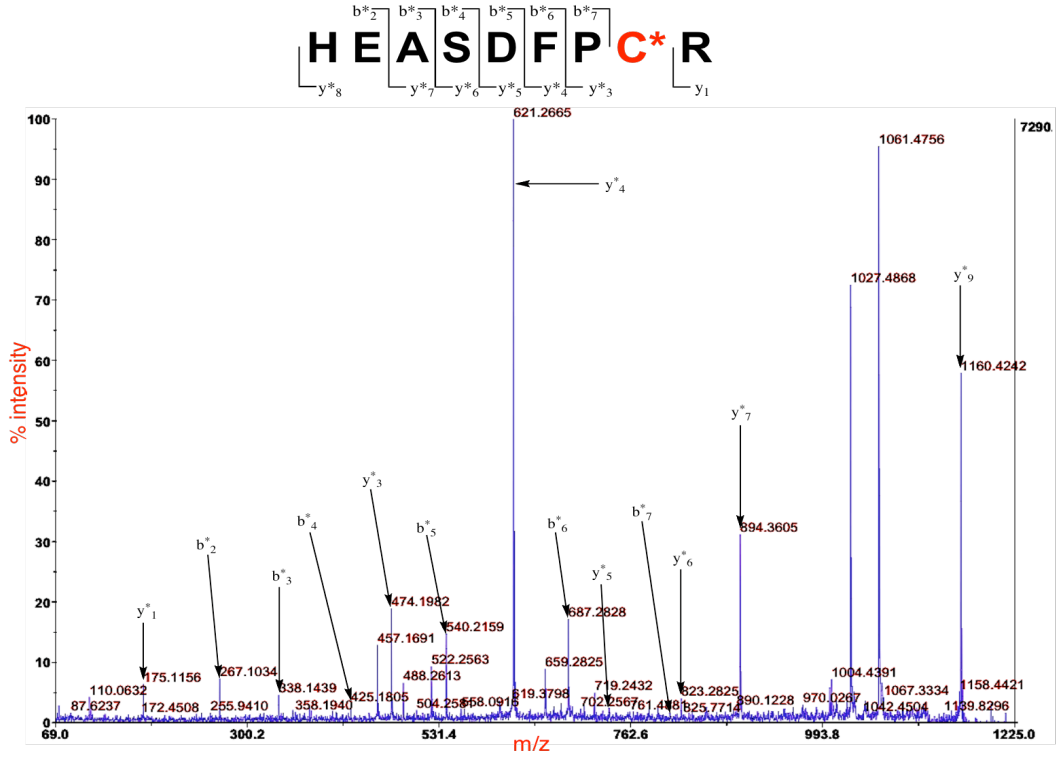

Figure 3-17. The MALDI TOF/TOF MS/MS spectrum showing that allyl isothiocyanate has modified PTP1B at Cys 32.

Overall, the mass spectrometry of the allyl isothiocyanate-inactivated PTP1B clearly shows that allyl isothiocyanate modifies the active site cysteine of PTP1B, thus shutting down the activity of the enzyme. As pointed out above, the mass spectrometry also shows that allyl isothiocyanate is modifying a few of the other solvent exposed cysteines of PTP1B, at least to some extent, including Cys 92 and Cys 32. We also observed in the MALDI TOF/TOF MS that one other cysteine containing tryptic peptide was modified by allyl isothiocyanate, [231-237] or [231-238]. However, the signal for this peptide was too weak to obtain tandem mass spectrum data. Of course, we can propose based on our other data that allyl isothiocyanate is slightly modifying the solvent exposed cysteine found in that tryptic peptide, Cys 231.

3.8 Discussion and Conclusions

We have found that the dietary isothiocyanates are time dependent inactivators of PTP1B. We have determined the kinetics of the inactivation for allyl isothiocyanate (k_{inact}/K_I = 3 $M^{-1}s^{-1}$), benzyl isothiocyanate (k_{inact}/K_I = 3 $M^{-1}s^{-1}$), and sulforaphane (k_{inact}/K_I = 1 $M^{-1}s^{-1}$). It is worth noting that the isothiocyanates explored in this effort inactivate PTP1B with a comparable potency to the identified endogenous regulator of PTPs, H_2O_2 (10 $M^{-1}s^{-1}$).[27, 29, 30]

We have found the enzymatic activity slowly returns after removal of excess isothiocyanate, indicative of a reversible covalent modification of the enzyme. In addition, the inactivation of PTP1B is considerably slowed by the addition of the active site binder, arsenate. This indicates the inactivation of PTP1B by the isothiocyanates is active site directed. Indeed, we confirmed this by subjecting the allyl isothiocyanate inactivated trypsin digested enzyme to MALDI TOF/TOF MS and MS/MS. We observed modification of the active site cysteine 215 by the isothiocyanate.

As mentioned previously, isothiocyanates have been shown to exert their wide range of biological activity from the modification of functionally critical cysteine residues inside cells. The results reported here indicate that inactivation of PTPs could be considered as a possible contributor to their diverse biological activities. Specifically, it is possible that PTPs are inactivated by isothiocyanates in order to exert part of their widely reported chemopreventative and anticancer properties.

3.9 Materials and Methods.

3.9.1 Chemicals and Reagents.

Reagents were purchased from the following suppliers: Buffer salts, *p*-nitrophenyl phosphate (pNPP), thiols, trifluoroacetic acid (TFA), dimethyl sulfoxide (DMSO), Sodium arsenate dibasic heptahydrate, allyl isothiocyanate, benzyl isothiocyanate, and sulforaphane were obtained from Sigma-Aldrich (St. Louis, MO). Sequencing grade-modified trypsin (catalog number V5111) was obtained from Promega. Ammonium bicarbonate was obtained from Fisher Scientific. Recombinant PTP1B (a.a. 1-322) was prepared in our laboratory as reported previously.[40, 41] The concentration of active PTP1B in the samples was determined as described previously.[40, 41]

3.9.2 Time-Dependent Inactivation of PTP1B by isothiocyanates

Inactivation kinetics assays were performed using modifications of existing literature protocols.[42-44] Free thiols were removed from a stock solution of purified PTP1B using Zeba mini centrifugal buffer exchange columns (Pierce, catalog number 89882) according to manufacturer's protocol. The exchange buffer contained 100 mM TRIS-HCl, 10 mM DTPA, 0.05% NP-40, pH 7.4. In the inactivation reactions, allyl isothiocyanate was added as a stock solution in DMSO to a mixture containing PTP1B in TRIS-HCl (100 mM, pH 7.4), DTPA (10 mM), and NP-40 (0.05%) at 30°C (final concentrations, allyl isothiocyanate: 150 μM, 300 μM, 500 μM, 700 μM, and 900 μM, PTP1B: ~75 ηmol, final volume: 100 μL). Aliquots (10 μL) were removed at various time points (1 min, 2 min, 5 min, and 10 min) and placed in 490 μL of PTP1B assay

buffer consisting of Bis-Tris (50 mM, pH 6.0), NaCl (100 mM), DTPA (10 mM) and pNPP (20 mM) at 30°C for 10 minutes. The enzymatic reaction was quenched by addition of NaOH (500 μL of 2 N solution in water), and the amount of p-nitrophenol released during the assay was determined at 25°C by measuring the absorbance at 410 nm using a UV-vis spectrometer.

3.9.3 Reversibility of ITC inactivated PTP1B.

An aliquot of thiol free enzyme (150 μL of 16 μM solution in 100 mM TRIS-HCl, 10 mM NaCl, 10 mM DTPA, 0.05% Tween 80, pH 7) was combined with 15 μL of a 10 mM solution of allyl isothiocyanate in DMSO at 25°C (Final concentrations: PTP1B, 15 μM; allyl isothiocyanate, 1 mM; DMSO, 10% v/v). A control, adding DMSO with no allyl isothiocyanate, was also run side by side. After 30 minutes, a 10 μL aliquot was removed and added to a cuvette containing a three component PTP1B assay buffer (990 μL) consisting of sodium acetate (100 mM), Bis-TRIS (50 mM), and TRIS (50 mM) at pH 7.0 (final volume of 1 mL). Immediately following addition of enzyme to the cuvette, the assay was mixed by repeated inversion, and enzyme catalyzed release of *p*-nitrophenol was monitored at 25°C by measuring the increase in absorbance at 410 nm. After 30 minutes, the inactivation was judged to be complete, and the sample was subjected to a Zeba mini centrifugal buffer exchange column (Pierce, catalog number 89882) according to manufacturer's protocol. The exchange buffer contained 100 mM TRIS-HCl, 10 mM DTPA, 0.05% Tween 80, pH 7.0. The gel filtered samples were incubated at 25°C and aliquots were removed and tested for enzymatic activity as described above at the designated time points.

3.9.4 Time-Dependent Inactivation in the Presence of a Competitive PTP1B Inhibitor

An aliquot of thiol-free enzyme (20 μL of a 4 μM solution in 100 mM TRIS-HCl, 10 mM NaCl, 10 mM DTPA, 0.05% Tween 80, pH 7) was combined with a 1:1 H_2O:DMSO (v/v) solution of allyl isothiocyanate and arsenate (10 μL of 500 μM allyl isothiocyanate containing 100 or 500 μM arsenate) at 25°C (Final concentrations: PTP1B, 2 μM; acrolein, 250 μM; arsenate, 100 or 500 μM). After 5 min, a 10 μL aliquot was removed and added to a cuvette containing a three component PTP1B assay buffer (990 μL) consisting of sodium acetate (100 mM), Bis-TRIS (50 mM), and TRIS (50 mM) at pH 7.0 (final volume of 1 mL). Immediately following addition of enzyme to the cuvette, the assay was mixed by repeated inversion, and enzyme catalyzed release of *p*-nitrophenol was monitored at 25°C by measuring the increase in absorbance at 410 nm.

3.9.5 Matrix-Assisted Laser Desorption/Ionization Time-of-Flight (MALDI TOF/TOF MS) Analysis of Allyl Isothiocyanate-Modified PTP1B.

Thiol free PTP1B (~14 pmol/μL) in 50 μL buffer (100 mM TRIS-HCl, 10 mM NaCl, 10 mM DTPA, 0.05% NP-40, pH 7.4) containing 2 mM allyl isothiocyanate was incubated at 25°C for 60 minutes. The reaction was followed side by side with a control with no allyl isothiocyanate. After incubation, both solutions were subjected to a Zeba mini centrifugal buffer exchange column. 50 μL of sequence grade modified trypsin (1μg/50μL) in 50 mM ammonium bicarbonate was added to the solution. The digestion was incubated at 37°C for 18 hours then quenched with 5 μL of 10% TFA (aq). For MALDI TOF/TOF MS analysis, the procedure used was a modified version of existing literature protocols.[45] A 2 μL portion of sample (with or without dilution) was mixed with an equal volume of alpha-cyano-4-hydroxycinnamic acid (CHCA) matrix solution (5 mg CHCA/mL 500/455/20/25 (V/V/V/V) acetonitrile/water/10% trifluoracetic acid (aq)/400 mM (aq) ammonium dihydrogen phosphate). Aliquots (0.4 μL) of the mixtures were deposited on a polished stainless steel target (ABI01-192-6-AB). Crystallization of the mixture proceeded under ambient conditions. The crystals were not washed.

Mass spectra were acquired on an Applied Biosystems Inc. 4700 MALDI TOF/TOF mass spectrometer with a 355 nm Nd:YAG laser (200 Hz) in the positive ion, delayed-extraction, reflector MS or positive ion MS/MS mode. The mMS spectra (100 20-shot spectra, first 10 shots discarded each time) were acquired over the mass range 500-4500 Da. The mass resolution was 9000-16000 across the mass range with the focus

mass set at 2000. Both the MS and MS/MS spectra were calibrated by the external method using commercially available peptide standards (Applied Biosystems, Inc.). The 1-kV peptide unimolecular decomposition spectra, or MS/MS were obtained without CID gas and with metastable ion suppression. The mass gate for precursor ion selection was set to allow into the collision cell ions from 2.0 Da below to 2.0 Da above the precursor ion mass. Calibration of the MS/MS spectra was based on the extermal default calibration obtained from MS/MS analysis of the peptide standard ACTF[1-17] at $[M+H]^+$ 2465.1989 Da. Spectra were processed with Applied Biosystems' 4000 Series Explorer software (version 3.0 RC1).

3.10 References

1. Mullin, W. J.; Sahasrabudhe, H. R., An estimate of the average daily intake of glucosinolates (precursors to isothiocyanates). *Nutr. Rep. Int.* **1978,** 18, 273-279.

2. Gamet-Payrestre, L.; Li, P.; Lumeau, S.; Cassar, G.; Dupont, M.-A.; Chevolleau, S.; Gasc, N.; Tulliez, J.; Terce, F., Sulforaphane, a naturally occurring isothiocyanate, induces cell cycle arrest and apoptosis in HT29 human colon cancer cells. *Cancer Res.* **2000,** 60, 1426-1433.

3. Bhamre, S.; Sahoo, D.; Tibshirani, R.; Dill, D. L.; Brooks, J. D., Temporal changes in gene expression induced by sulforaphane in human prostate cancer cells. *Prostate (Hoboken, NJ, U. S.)* **2009,** 69 (2), 181-190.

4. Sahu, R. P.; Srivastava, S. K., The Role of STAT-3 in the Induction of Apoptosis in Pancreatic Cancer Cells by Benzyl Isothiocyanate. *J. Natl. Cancer Inst.* **2009,** 101, (3) 176-193.

5. Lam, T. K.; Gallicchio, L.; Lindsley, K.; Shiels, M.; Hammond, E.; Tao, X.; Chen, L.; Robinson, K. A.; Caulfield, L. E.; Herman, J. G.; Guallar, E.; Alberg, A. J., Cruciferous Vegetable Consumption and Lung Cancer Risk: A Systematic Review. *Cancer Epidemiol., Biomarkers Prev.* **2009,** 18 (1), 184-195.

6. Hwang, E. S.; Jeffery, E. H., Evaluation of urinary N-acetyl cysteinyl allyl isothiocyanate as a biomarker for intake and bioactivity of Brussels sprouts. *Food and Chemical Toxicology* **2003,** 41 (12), 1817-1825.

7. Kissen, R.; Rossiter, J.; Bones, A., The 'mustard oil bomb': not so easy to assemble?! Localization, expression and distribution of the components of the myrosinase enzyme system. *Phytochemistry Reviews* **2009,** 8 (1), 69-86.

8. Burow, M.; Wittstock, U., Regulation and function of specifier proteins in plants. *Phytochemistry Reviews* **2009,** 8 (1), 87-99.

9. Zhang, Y., Cancer-preventive isothiocyanates: measurement of human exposure and mechanism of action. *Mutat. Res.* **2004,** 555 (1-2), 173-190.

10. Bellostas, N.; Kachlicki, P.; Soerensen, J. C.; Soerensen, H., Glucosinolate profiling of seeds and sprouts of B. oleracea varieties used for food. *Sci. Hortic. (Amsterdam, Neth.)* **2007,** 114 (4), 234-242.

11. Vermeulen, M.; Van den Berg, R.; Freidig, A. P.; Van Bladeren, P. J.; Vaes, W. H. J., Association between consumption of cruciferous vegetables and condiments and excretion in urine of isothiocyanate mercapturic acids. *J. Agric. Food Chem.* **2006,** 54 (15), 5350-5358.

12. Zhang, Y.; Talalay, P.; Cho, C. G.; Posner, G. H., A major inducer of anticarcinogenic protective enzymes from broccoli: isolation and elucidation of structure. *Proc. Natl. Acad. Sci. U. S. A.* **1992,** 89 (6), 2399-403.

13. Basten, G. P.; Bao, Y.; Williamson, G., Sulforaphane and its glutathione conjugate but not sulforaphane nitrile induce UDP-glucuronosyl transferase (UGT1A1) and glutathione transferase (GSTA1) in cultured cells. *Carcinogenesis* **2002,** 23 (8), 1399-1404.

14. Hong, F.; Freeman, M. L.; Liebler, D. C., Identification of Sensor Cysteines in Human Keap1 Modified by the Cancer Chemopreventive Agent Sulforaphane. *Chemical Research in Toxicology* **2005,** 18 (12), 1917-1926.

15. Juge, N.; Mithen, R.; Traka, M., Molecular basis for chemoprevention by sulforaphane: a comprehensive review. *Cellular and Molecular Life Sciences (CMLS)* **2007,** 64 (9), 1105-1127.

16. Azarenko, O.; Okouneva, T.; Singletary, K. W.; Jordan, M. A.; Wilson, L., Suppression of microtubule dynamic instability and turnover in MCF7 breast cancer cells by sulforaphane. *Carcinogenesis* **2008,** 29 (12), 2360-2368.

17. Antosiewicz, J.; Ziolkowski, W.; Kar, S.; Powolny, A. A.; Singh, S. V., Role of reactive oxygen intermediates in cellular responses to dietary cancer chemopreventive agents. *Planta Med.* **2008,** 74 (13), 1570-1579.

18. Ramirez, M. C.; Singletary, K., Regulation of estrogen receptor Œ± expression in human breast cancer cells by sulforaphane. *J. Nutr. Biochem.* **2009,** 20 (3), 195-201.

19. Fahey, J. W.; Haristoy, X.; Dolan, P. M.; Kensler, T. W.; Scholtus, I.; Stephenson, K. K.; Talalay, P.; Lozniewski, A., Sulforaphane inhibits extracellular,

intracellular, and antibiotic resistant strains of Helicobacter pylori and prevents benzo[a]pyrene-induced stomach tumors. *Proc. Nat. Acad. Sci. USA* **2002,** 99 (11), 7610-7615.

20. Conaway, C. C.; Krzeminski, J.; Amin, S.; Chung, F. L., Decomposition rates of isothiocyanate conjugates determine their activity as inhibitors of cytochrome P450 enzymes. *Chem. Res. Toxicol.* **2001,** 14, 1170-1176.

21. Conaway, C. C.; Jiao, D.; Chung, F. L., Inhibition of rat liver cytochrome P-450 isoenzymes by isothiocyanates and their conjugates: a structure-activity relationship study. *Carcinogenesis* **1996,** 17 (11), 2423-2427.

22. Bollard, M.; Stribbling, S.; Mitchell, S.; Caldwell, J., The Disposition of Allyl Isothiocyanate in the Rat and Mouse. *Food and Chemical Toxicology* **1997,** 35, 933-943.

23. Bogaards, J. J. P.; Van Ommen, B.; Falke, H. E.; Willems, M. I.; Van Bladeren, P. J., Glutathione S-transferase subunit induction patterns of Brussels sprouts, allyl isthiocyanate and goitrin in liver and small intestinal mucosa: a new approach for the identification of inducing xenobiotics. *Food and Chemical Toxicology* **1990,** 28, 8-88.

24. Plass, R.; Lewerenz, H. J.; Macholz, R. M., Effect of allyl isothiocyanate on cytochrome P-450 from rat liver microsomes. *Nahrung* **1983,** 27 (10), 1003-8.

25. Hu, J.; Straub, J.; Xiao, D.; Singh Shivendra, V.; Yang, H.-S.; Sonenberg, N.; Vatsyayan, J., Phenethyl isothiocyanate, a cancer chemopreventive constituent of cruciferous vegetables, inhibits cap-dependent translation by regulating the level and phosphorylation of 4E-BP1. *Cancer Res* **2007,** 67 (8), 3569-73.

26. Kalkunte, S.; Swamy, N.; Dizon, D. S.; Brard, L., Benzyl isothiocyanate (BITC) induces apoptosis in ovarian cancer cells in vitro. *J. Exp. Ther. Oncol.* **2006,** 5 (4), 287-300.

27. Denu, J. M.; Tanner, K. G., Specific and reversible inactivation of protein tyrosine phosphatases by hydrogen peroxide: evidence for a sulfenic acid intermediate and implications for redox regulation. *Biochemistry* **1998,** 37, 5633-5642.

28. Barrett, W. C.; DeGnore, J. P.; Keng, Y.-F.; Zhang, Z.-Y.; Yim, M. B.; Chock, P. B., Roles of superoxide radical anion in signal transduction mediated by reversible

regulation of protein-tyrosine phosphatase 1B. *J. Biol. Chem.* **1999,** 274 (49), 34543-34546.

29. Mahedev, K.; Zilbering, A.; Zhu, L.; Goldstein, B. J., Insulin-stimulated hydrogen peroxide reversibly inhibits protein-tyrosine phosphatase 1B in vivo and enhances the early insulin action cascade. *J. Biol. Chem.* **2001,** 276 (24), 21938-21942.

30. Tonks, N. K., Redox redux: revisiting PTPs and the control of cell signaling. *Cell* **2005,** 121 (June 3), 667-670.

31. Jeffery, E. H.; Araya, M., Physiological effects of broccoli consumption. *Phytochem. Rev.* **2009,** 8 (1), 283-298.

32. Zhang, Y.-L.; Zhang, Z.-Y., Low-affinity binding determined by titration calorimetry using a high-affinity coupling ligand: a thermodynamic study of ligand binding to protein tyrosine phosphatase 1B. *Anal. Biochem.* **1998,** 261 (2), 139-148.

33. Juszczak, L. J.; Zhang, Z.-Y.; Wu, L.; Gottfried, D. S.; Eads, D. D., Rapid loop dynamics of Yersinia protein tyrosine phosphatases. *Biochemistry* **1997,** 36 (8), 2227-2236.

34. Hong, F.; Freeman, M. L.; Liebler, D. C., Identification of Sensor Cysteines in Human Keap1 Modified by the Cancer Chemopreventive Agent Sulforaphane. *Chem. Res. Toxicol.* **2005,** 18 (12), 1917-1926.

35. Podhradsky, D.; Drobnica, L.; Kristian, P., Kinetics of reactions of isothiocyanates with diglycine, cystine, lysine, alpha-N-acetyllysine and oxidized glutathione. *Collect. Czech. Chem. Commun.* **1977,** 42 (1), 384-9.

36. Drobnica, L.; Augustin, J., Reactions of isothiocyanates with amino acids, peptides, and proteins. III. Kinetics and mechanism of the reaction of aromatic isothiocyanates with thioglycolic acid. . *Coll. Czech. Chem. Comm.* **1965,** 30, 1618-25.

37. Drobnica, L.; Augustin, J., Reaction of isothiocyanates with amino acids, peptides, and proteins. I. Kinetics of the reaction of aromatic isothiocyanates with glycine. *Coll. Czech. Chem. Commun.* **1965,** 30, 99-104.

38. Drobnica, L.; Augustin, J., Reactions of isothiocyanates with amino acids, peptides, and proteins. II. Kinetics of the reaction of aromatic isothiocyanates with amino acids and cyclization of the addition products. *Coll. Czech. Chem. Commun.* **1965,** 30 (4), 1221-8.

39. Zhang, Z.-Y., Protein tyrosine phosphatases: structure and function, substrate specificity, and inhibitor development. *Ann. Rev. Pharmacol. Toxicol.* **2002,** 42 (42), 209-234.

40. Seiner, D. R.; Gates, K. S., Kinetics and mechanism of protein tyrosine phosphatase 1B inactivation by acrolein. *Chem. Res. Toxicol.* **2007,** 20, 1315-1320.

41. LaButti, J. N.; Chowdhury, G.; Reilly, T. J.; Gates, K. S., Redox regulation of protein tyrosine phosphatase 1B by peroxymonophosphate. *J. Am. Chem. Soc.* **2007,** 129, 5320-5321.

42. Silverman, R. B., *Mechanism-Based Enzyme Inactivation: Chemistry and Enzymology*. CRC Press: Boca Raton, 1988; Vol. I.

43. Arabaci, G.; Guo, X.-C.; Beebe, K. D.; Coggeshall, K. M.; Pei, D., alpha-Haloacetophenone derivatives as photoreversible covalent inhibitors of protein tyrosine phosphatases. *J. Am. Chem. Soc.* **1999,** 121, 5085-5086.

44. Montalibet, J.; Skorey, K. I.; Kennedy, B. P., Protein tyrosine phosphatase: enzymatic assays. *Methods* **2005,** 35, 2-8.

45. Smirnov, I. P.; Zhu, X.; Taylor, T.; Huang, Y.; Ross, P.; Papayanopoulos, I. A.; Martin, S. A.; Pappin, D. J., Suppression of alpha-Cyano-4-hydroxycinnamic Acid Matrix Clusters and Reduction of Chemical Noise in MALDI-TOF Mass Spectrometry. *Anal. Chem.* **2004,** 76 (10), 2958-2965.

CRYSTALLIZATION OF NATIVE AND OXIDIZED PTP1B

4.1 Crystallography of PTPs

Protein tyrosine phosphatases (PTPs) have been readily crystallized over the past few years.[1] PTP1B, in particular, has received a lot of attention because of its targeting for the treatment of type 2 diabetes, as discussed in Chapter 1. PTP1B is also structurally interesting. Salmeen et. al. reported in 2003 the crystal structure of oxidized PTP1B with a sulfenylamide at the active site (Scheme 1).[2] The sulfenylamide is essentially a five membered intrastrand crosslink of the P-loop, which causes conformational changes to three different loops (P, WPD, and 40s).[2, 3]

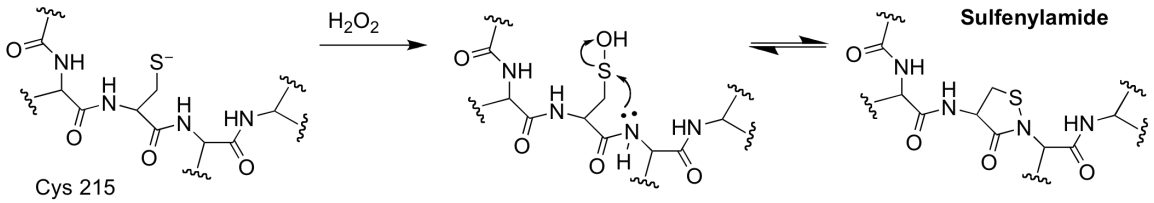

Scheme 4-1. Oxidation of the active site cysteine results in a sulfenylamide species at the active site of PTP1B.

We wanted to crystallize PTP1B in this laboratory with the aim of gaining the ability to structurally characterize inactivated PTPs and PTP-inhibitor complexes. Toward this end, we expressed and purified PTP1B, as done previously,[4, 5] for the purpose of obtaining structural data. Initial crystallization conditions were determined by crystallographic screens using the sitting drop method of vapor diffusion at 4°C. As can be observed in Figure 4-1, we obtained promising crystals from index screen 82-84, which contain $MgCl_2$ (200 mM), 25% PEG3350, and Bis-Tris buffer (pH 5.5-7.5).

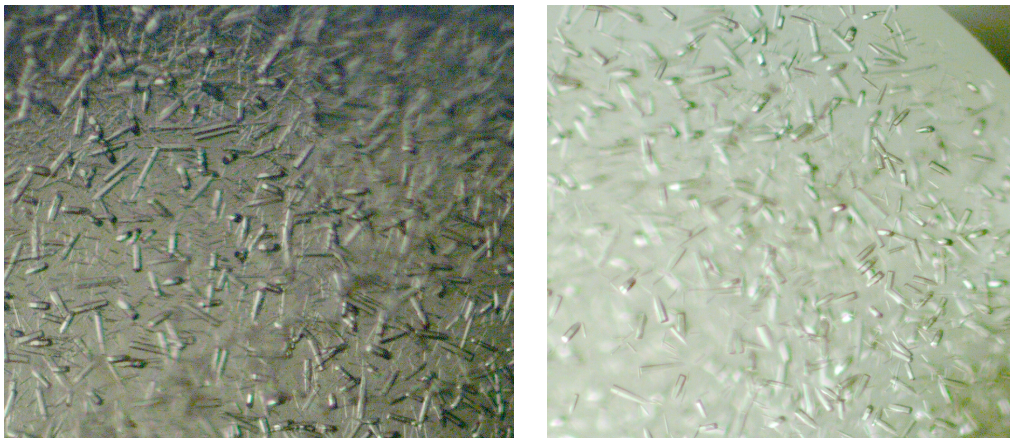

Figure 4-1. Promising crystals obtained from Index screen 83 (left) and Index screen 82 (right)

Based on our crystal screen hits, we optimized those crystallization conditions to obtain large diffraction quality crystals of PTP1B, with the best conditions being $MgCl_2$ (100 mM), 27% PEG3350, and Bis-Tris (100 mM) pH 6.0 (Figure 4-2).

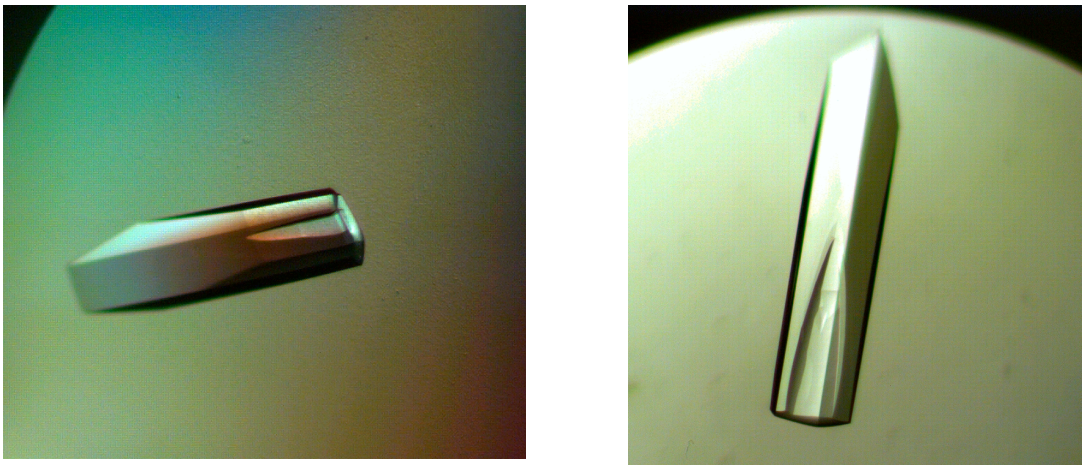

Figure 4-2. Crystals of PTP1B grown by sitting drop vapor diffusion at 4°C in the presence of $MgCl_2$, PEG 3350, and Bis-Tris, pH 6.0.

4.2 Crystal Soaking Experiments

As mentioned previously, the oxidized PTP1B contains an intrastrand crosslink of the P-loop as a result of a reaction between the oxidized cysteine and the neighboring amide nitrogen group. This forms a five membered ring at the active site that has been

previously seen in the literature.[2, 3] Next, we wanted to obtain the crystal structure of the oxidized, inactive PTP1B. Toward this end, we soaked crystals of native PTP1B with 50 μM of H_2O_2 in cryobuffer for 3 hours at room temperature (~25°C) and obtained a structure of the inactivated PTP1B as detailed in the next section.

4.3 Crystal Preparation and Data Collection

All crystals were prepared for low temperature data collection by soaking them in cryobuffer that contained 100 mM $MgCl_2$, 27% PEG3350, 15% PEG200, and 100 mM Bis-Tris pH 6.0. We collected the diffraction data from the crystals at beamline 4.2.2 of the Advanced Light Source in Berkley, CA. The data collection and refinement statistics for both the native and oxidized PTP1B structure are listed in Table 4-1.

	Active PTP1B	Oxidized PTP1B
Wavelength (Å)	1.00	1.00
Space group	$P3_121$	$P3_121$
Unit cell dimensions (Å)	a = 88.3, c = 104.1	a = 87.8, c = 103.4
Diffraction resolution	36 – 1.85 (1.92 – 1.85)	44 – 2.30 (2.38 – 2.30)
No. of observations	120971	88989
No. of unique reflections	40461	20840
Completeness (%)	99.7 (99.6)	99.6 (99.9)
Multiplicity	3.0 (3.0)	4.3 (4.4)
Average I/σ	6.9 (2.2)	10.5 (2.8)
R_{merge}	0.085 (0.419)	0.063 (0.365)
No. of protein chains	1	1
No. of protein residues	297	281
No. of protein atoms	2435	2253
No. of water molecules	177	46
R_{cryst}	0.207 (0.239)	0.231 (0.239)
R_{free}	0.230 (0.250)	0.273 (0.267)
RMSD bonds (Å)	0.007	0.005
RMSD bond angles(°)	1.1	0.9
Ramachandrand plot (No. of residues)		
Favored	288 / 5 / 2	271 / 6 / 2
Average B-factors (Å^2)		
Protein	29 / 26	49 / 41

Table 4-1. Data collection and refinement statistics for PTP1B structures.

An overlay of the native and oxidized enzyme structures is found in Figure 4-3. The loops that change conformation in the oxidized form are highlighted. As expected, we observe movement of the WPD, P, and 40s loops in the oxidized enzyme.

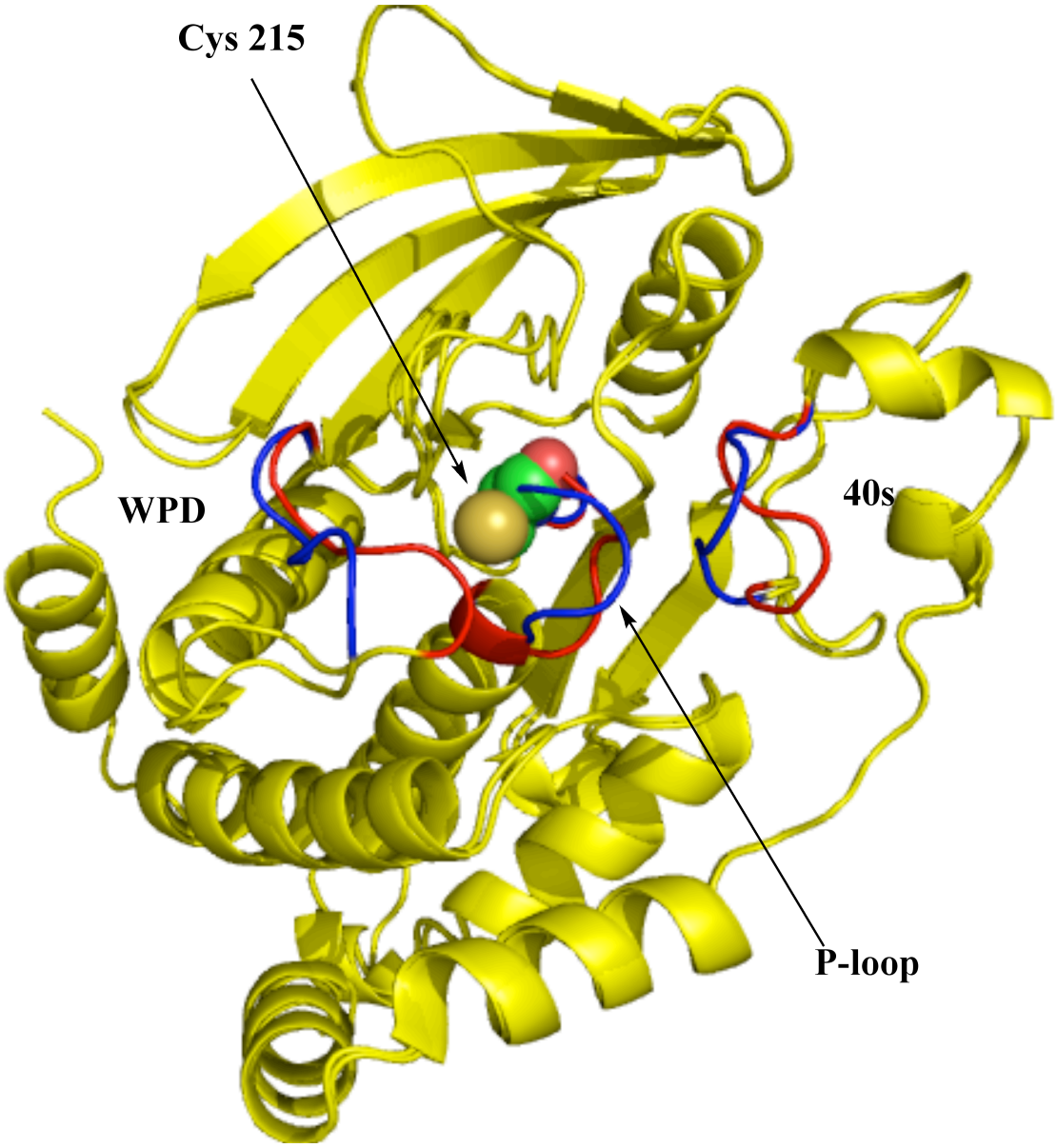

Figure 4-3. Overlay of the native and oxidized (inactive) PTP1B structures. Loops that change conformation upon formation of the sulfenylamide are labeled (P, WPD, and 40s). The highlighted loops are colored red in the native enzyme, and blue in the oxidized, the rest of the protein is colored yellow.

4.4 Discussion and Conclusions

We have shown that we are able to crystallize PTP1B and obtain high-resolution structures of both the native and the oxidized inactivate form. We found that the oxidation of the active site cysteine imparts structural changes to the enzyme, including movements of the P, WPD, and 40s loops, confirming the literature reports. These results coincide with the literature reports on the structures of inactivated PTP1B.

Although no novel PTP1B structures were obtained, I have been able to establish a new crystallography collaboration with the Tanner laboratory in the Chemistry department, and hope to obtain many novel protein structures in the near future, of both PTP1B and other phosphatases. This work has the possibility of providing a vast amount of information in the near future.

4.5 Materials and Methods

4.5.1 Chemicals and Reagents

Reagents were purchased from the following suppliers: Buffers and salts were obtained from Sigma Aldrich (St. Louis, MO). PEG3350 and PEG200 were obtained from Fisher Scientific. Sitting-Drop crystal trays, Index Crystallography Screen, and Hampton loops were obtained from Hampton Research. PTP1B was prepared in our laboratory as described previously.[5] For all crystallography trials, PTP1B was used at a concentration of approximately 10 mg/mL.

4.5.2 Crystallization of PTP1B

Freshly purified PTP1B was subjected to Index crystallography screen by a sitting drop method. PTP1B was diluted 1:1 (v/v) with each index reagent in the drop. The trays were allowed to equilibrate by vapor diffusion at 4°C. After approximately 5 days, crystals were observed over index reagents 82-84, which contained 0.2 M $MgCl_2$, 25% PEG3350, and Bis-Tris buffer over the range of pH 5.5-7.5. Optimization of these crystallographic conditions by varying the percent of PEG3350, concentration of the $MgCl_2$, and the pH yielded the best crystallographic conditions at 0.1 M $MgCl_2$ 27% PEG3350, and 0.1M Bis-Tris pH 6.0.

The crystals were prepared for data collection by soaking them in cryobuffer (0.1 M Bis-Tris pH 6.0, 0.1 M $MgCl_2$, 27% PEG3350, and 15% PEG 200) for 5-10 minutes. The cryoprotected crystals were picked up by Hampton loops and plunged into liquid nitrogen.

4.5.3 Oxidation of PTP1B crystals

PTP1B crystals were oxidized by washing the crystals with cryobuffer (0.1 M Bis-Tris pH 6.0, 0.1 M $MgCl_2$, 27% PEG3350, and 15% PEG 200) for 1-2 minutes. After washing, cryobuffer (0.1 M Bis-Tris pH 6.0, 0.1 M $MgCl_2$, 27% PEG3350, and 15% PEG 200) containing 50 μM H_2O_2 was slowly soaked into the crystal over the course of 1-2 minutes. The crystal was allowed to soak at 4°C for 4 hours. The crystals were immediately picked up with Hampton loops and plunged into liquid nitrogen.

4.5.3 Solving the PTP1B structures

Both PTP1B structures were solved by molecular replacement using a search model derived form a 1.5Å resolution structure of a PTP1B/inhibitor complex (PBD entry 2f71). Prior to molecular replacement, non-protein residues were removed and the occupancies of active site loops whose conformation is known to depend on the status of the active site were set to zero. Simulated annealing was performed on the structures by PHENIX. The model was improved with model building in COOT followed by refinement in PHENIX.

4.6 References

1. Barr, A. J.; Ugochukwu, E.; Lee, W. H.; King, O. N. F.; Filippakopoulos, P.; Alfano, I.; Savitsky, P.; Burgess-Brown, N. A.; Muller, S.; Knapp, S., Large-scale structural analysis of the classical human protein tyrosine phosphatome. *Cell (Cambridge, MA, U. S.)* **2009,** 136 (2), 352-363.

2. Salmeen, A.; Anderson, J. N.; Myers, M. P.; Meng, T.-C.; Hinks, J. A.; Tonks, N. K.; Barford, D., Redox regulation of protein tyrosine phosphatase 1B involves a sulphenyl-amide intermediate. *Nature* **2003,** 423 (June 12), 769-773.

3. van Montfort, R. L. M.; Congreeve, M.; Tisi, D.; Carr, R.; Jhoti, H., Oxidation state of the active-site cysteine in protein tyrosine phosphatase 1B. *Nature* **2003,** 423 (June 12), 773-777.

4. Seiner, D. R.; Gates, K. S., Kinetics and mechanism of protein tyrosine phosphatase 1B inactivation by acrolein. *Chem. Res. Toxicol.* **2007,** 20, 1315-1320.

5. LaButti, J. N.; Chowdhury, G.; Reilly, T. J.; Gates, K. S., Redox regulation of protein tyrosine phosphatase 1B by peroxymonophosphate. *J. Am. Chem. Soc.* **2007,** 129, 5320-5321.

EXPRESSION, PURIFICATION, AND OXIDATIVE INACTIVATION OF SHP2

5.1 Background on SHP2

The Src homology-2 domain-containing phosphatases (SHP) are a small subfamily of the non-receptor protein tyrosine phosphatases.[1] The subfamily contains two human members, SHP1 (endcoded by the gene PTPN6) and SHP2 (encoded by PTPN11).[1] SHP2 is a ubiquitous enzyme that has been shown to be involved in a multitude of different cellular signal transduction pathways.[1-11] Importantly, PTPN11 mutations are responsible for about half of all cases of Noonan Syndrome, a common developmental disorder.[2] Furthermore, SHP2 has been identified as being involved in several oncogene signaling pathways.[3]

Since SHP2 function is involved in several disease states, we wanted to obtain SHP2 for kinetic analysis, and to have structural and functional comparison capabilities to our original protein tyrosine phosphatase, PTP1B. Toward this end, we have expressed and purified SHP2, and initial kinetic analysis of oxidative inactivation have been performed, as will be detailed below.

5.2 Expression and purification of SHP2

We obtained a DNA plasmid encoding for the His-tagged catalytic domain (a.a. 237-529, 36.88 kDa) of SHP2 from the Structural Genomics Consortium. We transformed several different cell lines with the plasmid, and found that we had the maximum amount of overexpression of a protein that migrated around 37 kDa (compared

to the size standards) and hydrolyzed *p*-nitrophenyl phosphate, from the culture containing BL21 DE3 cells as judged by SDS-PAGE (Figure 5-1). Since our initial trials showed promise, we chose to continue with the BL21 DE3 cell line in order to express and purify SHP2.

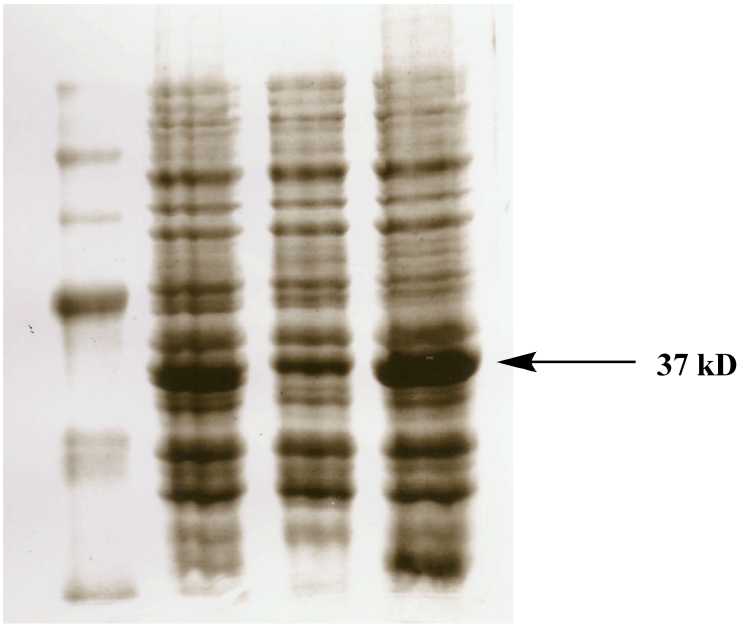

Figure 5-1. A whole cell extract of three different cell lines, after insertion of the DNA plasmid encoding for SHP2. As can be seen, we observed the most expression from BL21 DE3 cells (lane 3).

We then scaled up to a liter of cell culture, and expression of SHP2 was performed by autoinduction at 18°C and 250 rpm over the course of 4-6 days, depending on cell growth. Cells were harvested by centrifugation and lysed by a high-pressure cell disrupter. The protein was purified from the centrifugation-clarified cell lysates by nickel chelate, followed by a cation exchange column to >90% homogeneity as detailed in the Materials and Methods section at the end of this chapter (Figure 5-2).

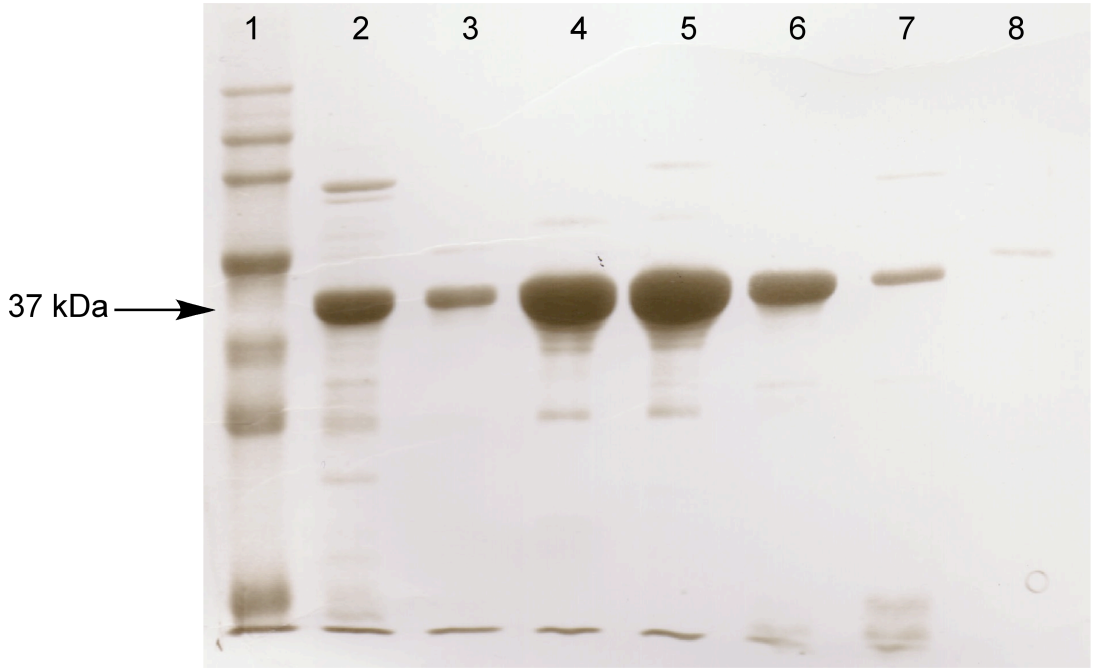

Figure 5-2. PAGE of the cationic exchange column aliquots. Lanes: 1, size marker, 2, protein sample after first column (Ni-NTA), 3-8, aliquots collected from cationic exchange column, which were pooled and used for all subsequent experiments.

5.3 Kinetic Analysis of SHP2

We utilized the common phosphatase substrate *p*-nitro phenylphosphate (pNPP) for monitoring the enzymatic activity of our tyrosine phosphatases, pNPP is hydrolyzed by PTPs to produce nitrophenol (easily detectable due to a yellow color change) and phosphate. (Scheme 5-1). Therefore, we needed to characterize the K_m and V_{max} of the freshly purified SHP2 with the substrate pNPP.

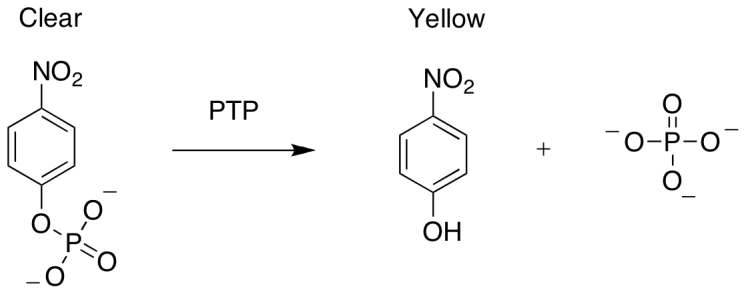

Scheme 5-1. The hydrolysis of the substrate pNPP by PTPs produces a yellow color that is easily followed by UV/Vis spectrometry.

We monitored the reaction of SHP2 with various concentrations of the substrate pNPP. The data was plotted with Prism (GraphPad Software, Inc.) as detailed in the Materials and Methods section, and is illustrated in Figure 5-3. We calculated the concentration of pNPP required to achieve half maximal velocity (K_m) to be 7.5 mM, and the maximum velocity of the enzyme to be 2.8 x 10^{-3} Au/sec (absorbance units per second).

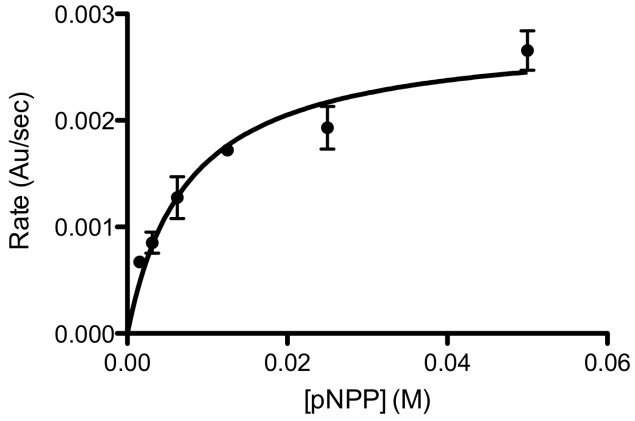

Figure 5-3. The plot of rate of para-nitro phenyl phosphate (pNPP) hydrolysis (in A.U./sec (absorbance units/sec)) versus the concentration of pNPP (Points represent mean with standard deviation, n=2).

Next, we explored the kinetics of inactivation of SHP2 by the endogenous PTP regulator of activity, hydrogen peroxide. SHP2, like PTP1B, has been shown to be regulated by hydrogen peroxide *in vivo*.[4, 5] Toward this end, we subjected the enzyme to various concentrations of hydrogen peroxide and followed the inactivation time courses using UV/Vis spectroscopy (Figure 5-4), as done previously.[6, 7]

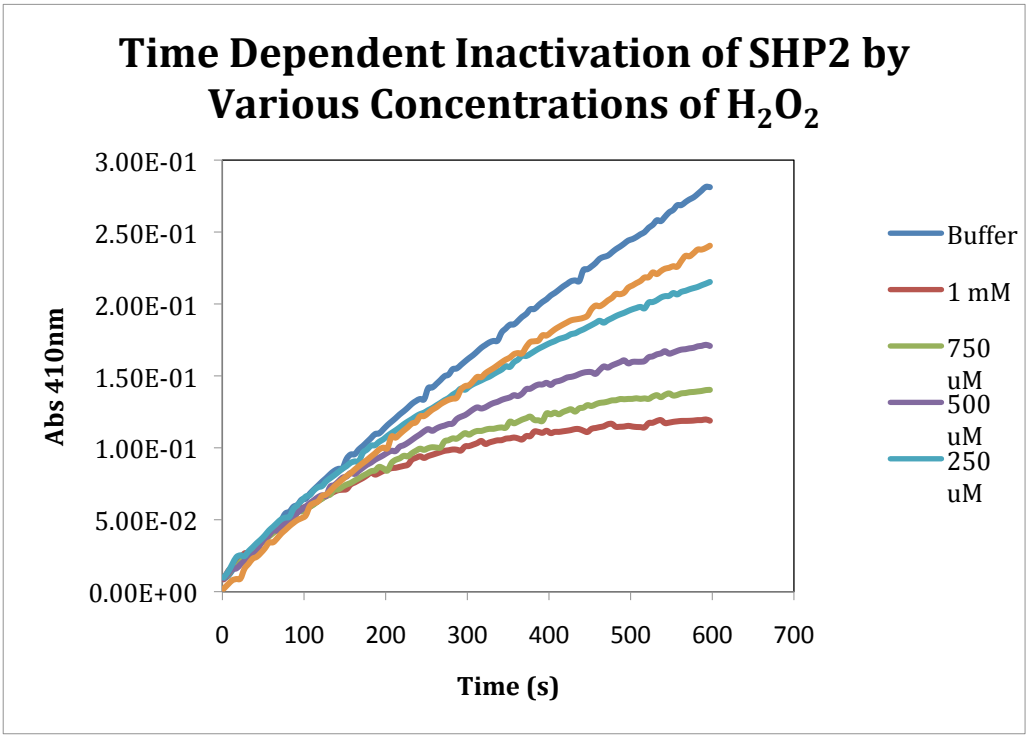

Figure 5-4. Time courses for the inactivation of SHP2 by various concentrations of hydrogen peroxide.

Utilizing the program Prism 5.0 (GraphPad Software), a nonlinear regression of the time course plots applying the equation, $Abs_{410nm} = (C - (e^{(\ln Vo - k't)}/k')$, yields the values for k'.[8] A replot of the inactivation time course data yields a rate of inactivation of SHP2 by H_2O_2 of 0.68 ± 0.02 $M^{-1}s^{-1}$ (Figure 5-5). It is worth noting that the rate calculated for the inactivation of SHP2 by hydrogen peroxide is comparable to the rate recently reported for SHP2 and hydrogen peroxide (8.8 $M^{-1}s^{-1}$).[9]

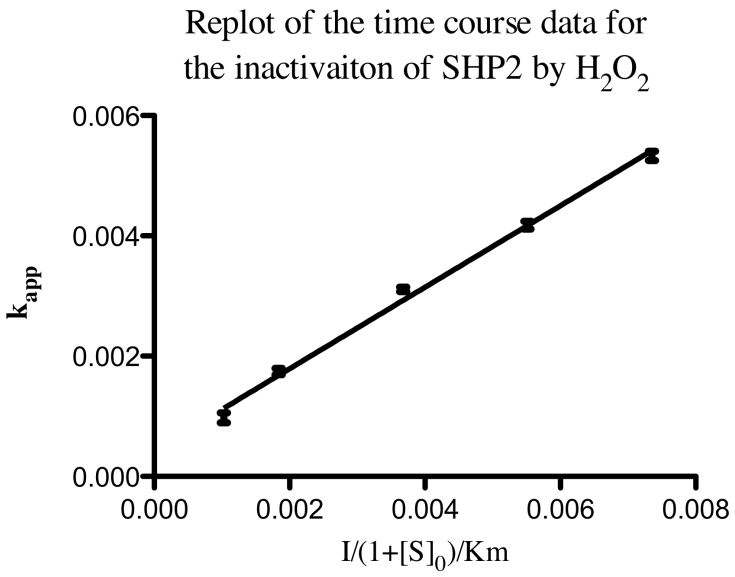

Figure 5-5. A replot of the time course data for the inactivation of SHP2 by H_2O_2. Points represent the mean with SD, n=3.

In the course of performing these experiments, we noticed something unusual about the inactivation of SHP2 by hydrogen peroxide. Whenever we added a sodium bicarbonate buffer to the inactivation reactions, the inactivation of SHP2 by hydrogen peroxide significantly increased. We also analyzed the kinetics of the inactivation of SHP2 in the presence of bicarbonate, to compare the two rates of inactivation. Toward this end, we repeated the previously discussed inactivation reactions with the addition of 25 mM sodium bicarbonate. Indeed, the inactivation of SHP2 in the presence of bicarbonate greatly increases the inactivation reaction (Figure 5-6).

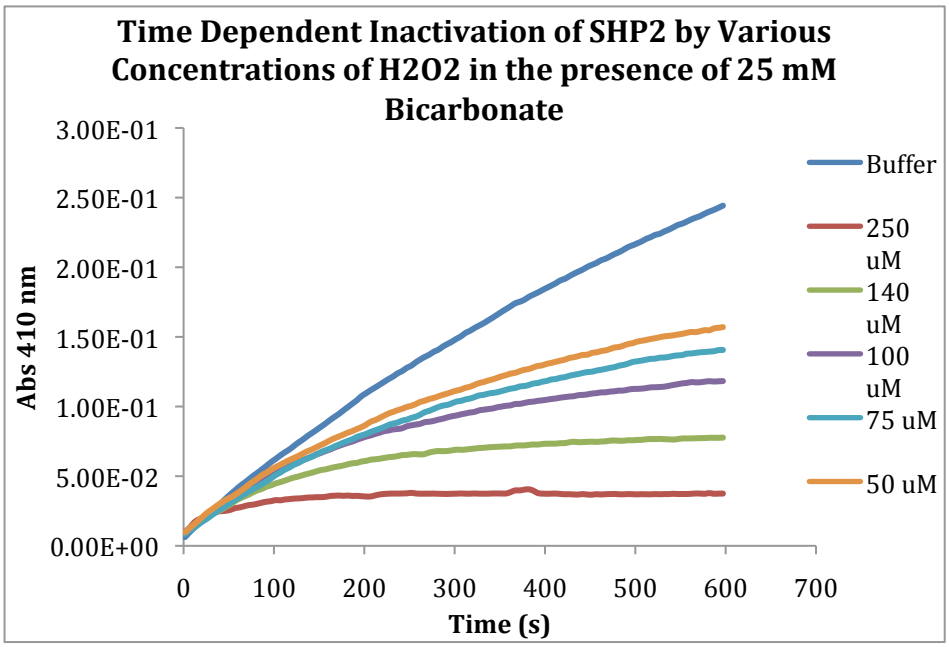

Figure 5-6. Time courses for the inactivation of SHP2 by hydrogen peroxide in the presence of 25 mM sodium bicarbonate.

A replot of this inactivation data, in an identical fashion as that done above, yields the graph seen below (Figure 5-7).

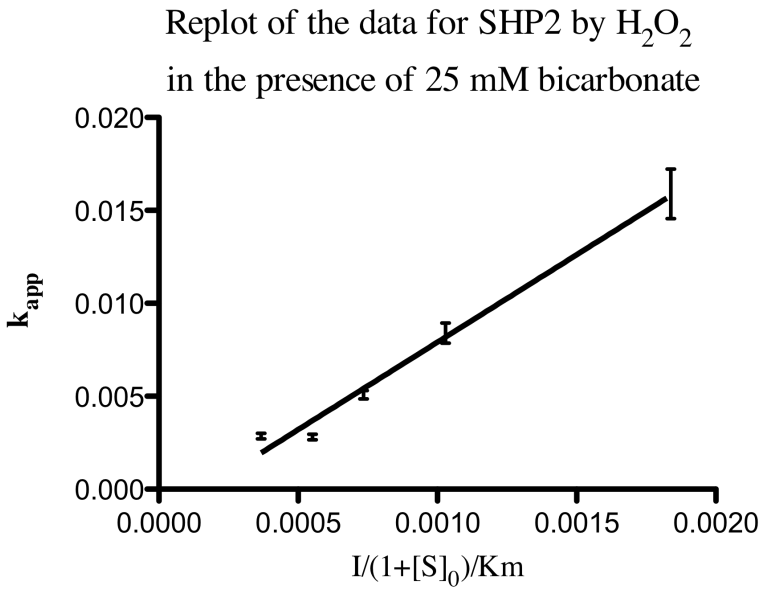

Figure 5-7. A replot of the time course data for the inactivation of SHP2 by hydrogen peroxid in the presence of 25 mM sodium bicarbonate. Points represent the mean with SD, n=3.

From the replot of the time course data (Figure 5-7), we estimate the rate of inactivation of SHP2 by hydrogen peroxide in the presence of 25 mM sodium bicarbonate to be 9.40 ± 0.59 $M^{-1}s^{-1}$. This represents a more than 10 fold increase in the rate of inactivation. Based on literature precedent, we propose that hydrogen peroxide could be reacting with carbonate *in situ* to produce the more reactive peroxycarbonate (Scheme 5-2).[10-12] Thus, generation of the more reactive peroxycarbonate could be the reason we observe an increase in the rate of inactivation of SHP2 in these experiments.

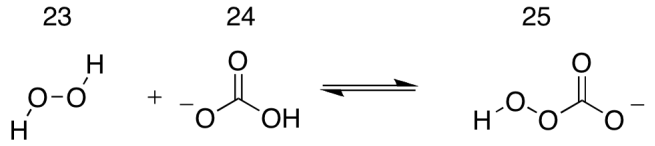

Scheme 5-2. Hydrogen peroxide reacts with bicarbonate to produce peroxycarbonate.[10-12]

5.4 Chapter Discussion and Conclusions

SHP2 is a ubiquitous enzyme involved in several different cellular signaling pathways. We needed to expand our current PTP studies with another phosphatase, for a multitude of reasons. Toward this end, we have expressed SHP2 by recombinant methods, and purified the protein to >90% homogeneity as judged by SDS-PAGE. We have determined the K_m (7.5 mM) and V_{max} (2.8 x 10^{-3} Au/sec) for the phosphatase with the substrate *p*-nitrophenyl phosphate.

We have also determined the rate of inactivation of SHP2 by the endogenous PTP regulator, H_2O_2 (0.68 ± 0.02 $M^{-1}s^{-1}$), and we found the rate to be similar to that reported for PTP1B.[9] Further, we calculated the rate constant for the inactivation of SHP2 by hydrogen peroxide in the presence of bicarbonate, and found it to be significantly increased (9.4 ± 0.59 $M^{-1}s^{-1}$). This could be due in part to formation of peroxycarbonate *in situ* from the reaction of hydrogen peroxide and bicarbonate. Haiying Zhou, from our goup, is currently exploring this kinetic conundrum with bicarbonate, and her initial work reveals concentration dependence with varying amounts of bicarbonate.[13] More work must be done to discover precisely what is causing the increase in the rate of inactivation.

We have attempted crystallizing SHP2, however, so far the crystallization trials have not been fruitful. Besides crystallization of SHP2, we will continue our studies of

this important enzyme through studying the inhibition/inactivation by several different molecules of interest.

5.5 Materials and Methods

5.5.1 Materials

Reagents were purchased from the following suppliers: Buffers, salts, *p*-nitrophenylphosphate (pNPP), thiols, and kanamycin (# K1876) were obtained from Sigma Aldrich (St. Louis, MO). BL21 DE3 competent cells (# 11665-015) were obtained from Invitrogen (Carlsbad, CA). Overnight Express Autoinduction System 1 (# 71300-4) was obtained from Novagen (Darmstadt, Germany). Zeba mini centrifugal buffer exchange columns (#89882) were obtained from Pierce Biotechnology (Rockford, IL). SnakeSkin Pleated Dialysis Tubing (10,000 MWCO, #68100) was obtained from Thermo Scientific (Rockford IL). Amicon Ultra centrifugal filter devices (# UFC901008) were purchased from Millipore (Milford, MA). Ni-NTA Superflow columns (5 mL, # 30761) were obtained from Qiagen.

5.5.2 Recombinant Expression of SHP2

DNA plasmid encoding for a His-tagged catalytic subunit (a.a. 237-529, 36.88 kDa) of SHP2 was obtained from the Structural Genomics Consortium. BL21 DE3 cells (# 11665-015) were transformed with the plasmid according to manufacturers protocol. Cells were selected on LB agar fortified with kanamycin (50 μg/ml) and placed in 1 L of freshly prepared Autoinduction media (Overnight Express Autoinduction System). The liter was split into four cultures of 250 mL, and grown at 18°C and 250 rpm for 5 days. Cells were harvested by centrifugation at 5000 x g for 10 minutes. Cell pellets were resuspended in 50 mM HEPES pH 7.5, 500 mM NaCl, 20 mM imidazole, 5% glycerol, and 1 mM DTT. Cells were lysed by a French press and the lysate was clarified by centrifugation at 16,000 rpm for 10 minutes, then at 50,000 rpm for 50 minutes at 4°C.

Supernatant was applied to a 5 mL Ni-NTA Superflow column and the column was washed with 20 mL of lysis buffer. Protein was eluted with a linear gradient of imidazole of 20 mM to 1M at a rate of 2 mL/min. 2 mL fractions were collected and tested for phosphatase activity with pNPP. Aliquots containing enzymatic activity were pooled and dialyzed with 50 mM Tris pH 8.5, 50 mM NaCl, and 1 mM DTT. The dialyzed protein was applied to a 5 mL cation exchange column at a flow rate of 1 mL/min. The column was washed with 20 mL of dialysis buffer, then a gradient of NaCl was ran at 2 mL/min from 50 mM to 1M, and eluted 2 mL fractions were collected and tested for enzymatic activity with pNPP. Active fractions were >90% pure as judged by SDS-PAGE. Fractions were pooled and dialyzed with 100 mM Bis Tris pH 7.0, 250 mM NaCl, 10 mM DETAPAC, and 1 mM DTT. Dialyzed protein was concentrated with an Amicon Ultra centrifugal filter (10,000 MW cut off) to about 10 mg/mL.

5.5.3 Calculation of K_m and V_{max} of SHP2 with *p*-Nitro Phenyl Phosphate (pNPP)

Free thiols were removed from a stock solution of purified SHP2 using Zeba mini centrifugal buffer exchange columns (Pierce, catalog number 89882) according to manufacturer's protocol. The exchange buffer contained 100 mM Tris-HCl pH 7.0, 10 mM DTPA, 0.05% Tween 80. SHP2 (30-50 pmol, 10 μL) diluted in exchange buffer was added to a cuvette containing a three-component assay buffer (100 mM NaOAc, 50 mM Bis-Tris, and 50 mM Tris pH 7.0) with various concentrations of pNPP substrate (50 mM, 25 mM, 12.5 mM, 6.25 mM, 3.1 mM, and 1.6 mM). Upon addition of enzyme, the reaction was mixed by repeated inversion and the enzyme-catalyzed release of *p*-

nitrophenol (from *p*-nitrophenyl phosphate) was monitored with a Hewlett Packard model 8453 spectrophotometer at 410 nm, and 25 °C. Data points were taken every 2 s. The rate of the reaction in Absorbance units (A.U.) per second versus substrate concentration was graphed and used to determine the V_{max} and K_m for SHP2 with pNPP in Prism 5.0 (GraphPad Software, Inc.)

5.5.4 Continuous Assay for Time Dependent Inactivation of SHP2 by H_2O_2

Free thiols were removed from a stock solution of purified SHP2 using Zeba mini centrifugal buffer exchange columns (Pierce, catalog number 89882) according to manufacturer's protocol. The exchange buffer contained 100 mM Tris-HCl pH 7.0, 10 mM DTPA, 0.05% Tween 80. To measure either enzymatic activity, or time dependent inactivation of SHP2 by H_2O_2, 10 μL of enzyme (30-50 pmol) diluted in exchange buffer was added to a cuvette containing a three component assay buffer (100 mM NaOAc, 50 mM Bis-Tris, and 50 mM Tris pH 7.0) with substrate (pNPP, 20 mM) and various concentrations of hydrogen peroxide in a total volume of 1 mL. Immediately following addition of enzyme to the cuvette, the reaction was mixed by repeated inversion, and enzyme-catalyzed release of *p*-nitrophenol (from *p*-nitrophenyl phosphate) was monitored with a Hewlett Packard model 8453 spectrophotometer at 410 nm, and 25 °C. Data points were taken every 2 s.

In the case of the inactivation of SHP2 by H_2O_2 in the presence of bicarbonate, freshly prepared sodium bicarbonate (30 μL of a 833 mM stock solution, final concentration, 25 mM) was added to the cuvette and the inactivation assays were run

identical to those as previously described. The rate constant of the inactivation of SHP2 was calculated from the time course data utilizing the methods described in Duranton et. al.[14], Hart et. al.[15], and Kraut, et. al.[8] The rates of inactivation (k') were calculated by fitting the time dependent inactivation curves to the equation $y = C - (e^{lnVo-k't})/k'$ in Prism 5.0 (GraphPad Software). A replot of the k' versus $I/(1+[S]_0)/Km$, where I is the concentration of hydrogen peroxide, S equals the concentration of substrate at time zero (20 mM), and K_m is 7.5, as has been determined experimentally. The equation yields a straight line where the slope equals the rate of the reaction.[14]

5.6 References

1. Neel, B. G.; Gu, H.; Pao, L., The Shp'ing news: SH2 domain-containing tyrosine phosphatases in cell signaling. *Trends Biochem. Sci.* **2003,** 28 (6), 284-293.

2. Chan, G.; Kalaitzidis, D.; Neel, B. G., The tyrosine phosphatase Shp2 (PTPN11) in cancer. *Cancer Metastasis Rev.* **2008,** 27 (2), 179-192.

3. Wang, S.; Yu, W.-M.; Zhang, W.; McCrae, K. R.; Neel, B. G.; Qu, C.-K., Noonan Syndrome/Leukemia-associated Gain-of-function Mutations in SHP-2 Phosphatase (PTPN11) Enhance Cell Migration and Angiogenesis. *J. Biol. Chem.* **2009,** 284 (2), 913-920.

4. Kwon, J.; Qu, C.-K.; Maeng, J.-S.; Falahati, R.; Lee, C.; Williams, M. S., Receptor-stimulated oxidation of SHP-2 promotes T-cell adhesion through SLP-76-ADAP. *Embo J.* **2005,** 24 (13), 2331-2341.

5. Chen, C.-Y.; Willard, D.; Rudolph, J., Redox Regulation of SH2-Domain-Containing Protein Tyrosine Phosphatases by Two Backdoor Cysteines. *Biochemistry* **2009,** 48 (6), 1399-1409.

6. Bhattacharya, S.; LaButti, J. N.; Seiner, D. R.; Gates, K. S., Oxidative inactivation of protein tyrosine phosphatase 1B by organic hydroperoxides. *Bioorg. Med. Chem. Lett.* **2008,** 18 (22), 5856-5859.

7. LaButti, J. N.; Chowdhury, G.; Reilly, T. J.; Gates, K. S., Redox regulation of protein tyrosine phosphatase 1B by peroxymonophosphate. *J. Am. Chem. Soc.* **2007,** 129, 5320-5321.

8. Kraut, D.; Goff, H.; Pai, R. K.; Hosea, N. A.; Silman, I.; Sussman, J. L.; Taylor, P.; Voet, J. G., Inactivation studies of acetylcholinesterase with phenylmethylsulfonyl fluoride. *Mol. Pharmacol.* **2000,** 57 (6), 1243-1248.

9. Denu, J. M.; Tanner, K. G., Specific and reversible inactivation of protein tyrosine phosphatases by hydrogen peroxide: evidence for a sulfenic acid intermediate and implications for redox regulation. *Biochemistry* **1998,** 37, 5633-5642.

10. Balagam, B.; Richardson, D. E., The Mechanism of Carbon Dioxide Catalysis in the Hydrogen Peroxide N-Oxidation of Amines. *Inorg. Chem. (Washington, DC, U. S.)* **2008,** 47 (3), 1173-1178.

11. Maetzke, A.; Knak Jensen, S. J.; Csizmadia, I. G., Putative mechanisms of peroxybicarbonate formation. *Chem. Phys. Lett.* **2007,** 448 (1-3), 46-48.

12. Regino, C. A. S.; Richardson, D. E., Bicarbonate-catalyzed hydrogen peroxide oxidation of cysteine and related thiols. *Inorg. Chim. Acta* **2007,** 360 (14), 3971-3977.

13. Zhou, H., Unpublished results. In Columbia, MO, 2009.

14. Duranton, J.; Adam, C.; Bieth, J. G., Kinetic Mechanism of the Inhibition of Cathepsin G by Œ±1-Antichymotrypsin and alpha-Proteinase Inhibitor. *Biochemistry* **1998,** 37 (32), 11239-11245.

15. Hart, G. J.; O'Brien, R. D., Recording spectrophotometric method for determination of dissociation and phosphorylation constants for the inhibition of acetylcholinesterase by organophosphates in the presence of substrate. *Biochemistry* **1973,** 12 (15), 2940-5.

EFFECT OF SEQUENCE CONTEXT ON RATE AND YIELD OF INTERSTRAND CROSSLINKS GENERATED FROM ABASIC SITES IN DNA

6.1 Abasic sites

Abasic sites (apurinic or apyrimidinic or AP-sites, resulting fromthe loss of a base) are the most common lesions to cellular DNA.[1, 2] Abasic sites are formed from the hydrolytic cleavage of the glycosidic bond, leaving deoxyribose residues in the DNA strand.[3, 4] The cleavage of the glycosidic bond can result from a variety of factors. For example, the exposure of DNA to some anticancer agents, radiation, mutagens, or from acidic conditions can cause cleavage of this bond and subsequent formation of an abasic site (Scheme 6-1).[3-5]

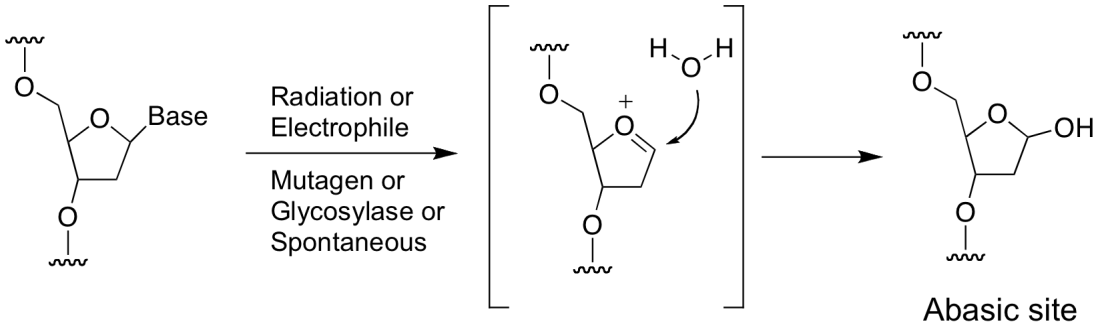

Scheme 6-1. Formation of an abasic site.[6]

Spontaneous formation of abasic sites in duplex DNA also occurs at a significant rate.[3] It has been estimated that cellular DNA has 10,000 abasic sites, per cell, per day.[3, 6] Further, some cellular DNA repair enzymes catalyze the hydrolysis

of the N-glycosidic bond. The DNA repair enzyme Uracil DNA Glycosylase (UDG) removes uracil residues in duplex DNA, caused from either deamination or misincorporation by polymerase, and leaves an abasic site in the duplex.[1, 7]

6.2 Brief discussion of the toxicity of Abasic sites

The toxicity of abasic sites can be derived from many different sources. Since abasic sites are essentially a 'blank' in the DNA template for DNA polymerase, they can potentially be mutagenic. Abasic sites have been shown to stall both DNA and RNA polymerase.[8] In addition, abasic sites can cause frameshit mutations and substitutions by DNA polymerase.[9]

Repair pathways exist for abasic sites. In mammalian cells, several enzymes are involved in their repair, including apurinic/apyrimidinic endonucleases.[10-12] Human apurinic-endonuclease (APE1) is one such enzyme, and our work with this enzyme will be discussed in more detail later in this chapter.

6.3 Overview of the chemical properties of abasic sites

Abasic sites are known to exist in equilibrium between two main forms (Scheme 6-2), the cyclic hemiacetal, is the predominant form totaling about 99%. The open chain aldehyde exists as about 1% of the mixture.

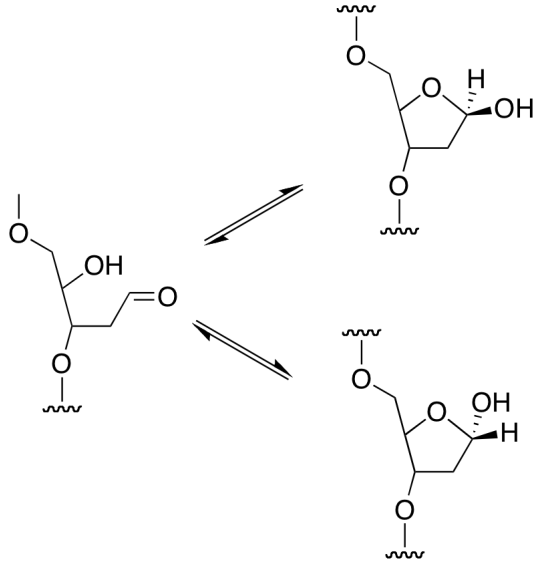

Scheme 6-2. Abasic sites exist as a mixture of ring closed and ring open form.

The ring open aldehyde imparts reactivity to the abasic site. Abasic sites have been shown to react with amines, to form an imine, or Schiff's base.[13] The imine can be stabilized through reduction by $NaCNBH_3$ or $NaBH_4$, as will be shown later (Scheme 6-3).

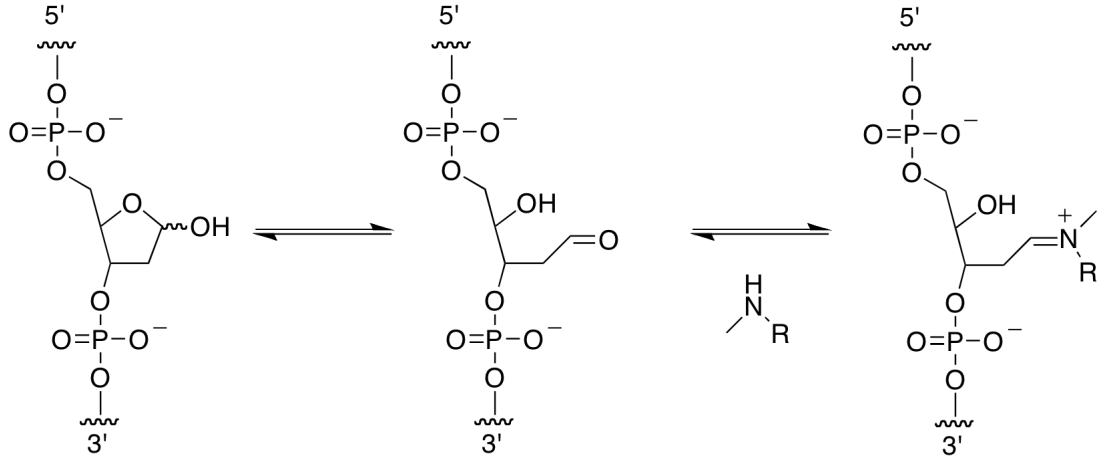

Scheme 6-3. Abasic sites react with amines to produce imines, or a Schiff's base.[13]

Abasic sites can also generate single strand cleavage in duplex DNA, via a β-elimination reaction (Scheme 6-4). The β-elimination reaction is quite slow at

physiological conditions, with a $t_{1/2}$ of about 190 hours; however, the reaction has been shown to be catalyzed by some proteins, peptides, amino acids, and amines.[10, 14]

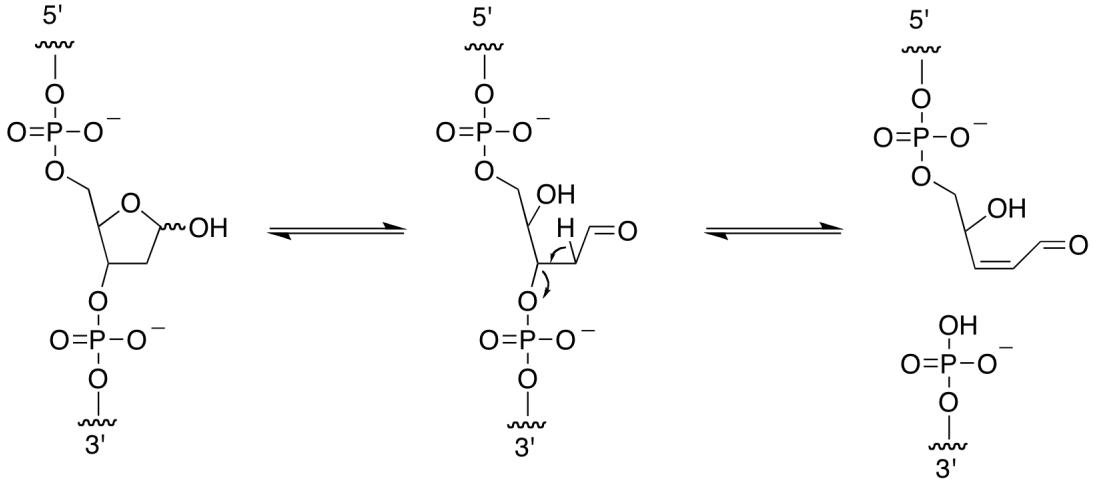

Scheme 6-4. The mechanism of the β-elimination reaction of an abasic site.[3]

The β-elimination product, besides generating a single strand break, also introduces new reactivity into DNA. As shown in Scheme 6-5, the β-elimination product is a Michael acceptor, and can react with nucleophiles, like cellular thiols and amines.[13, 15]

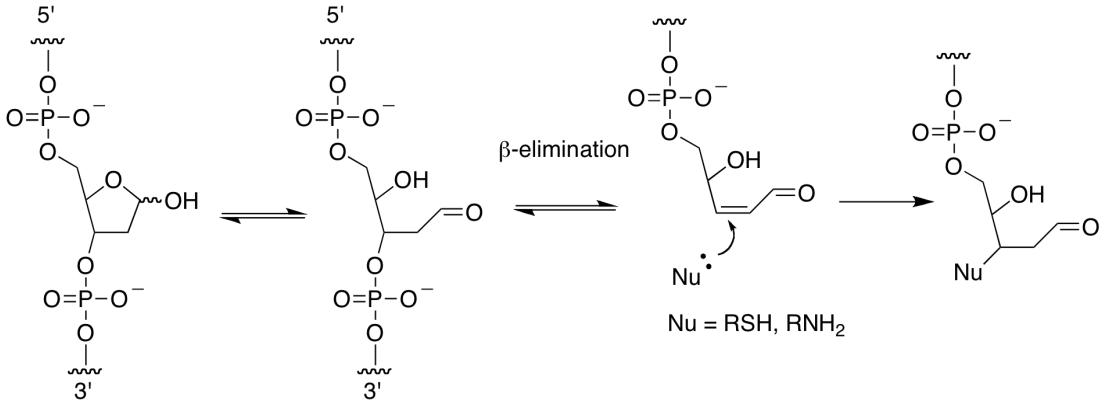

Scheme 6-5. The β-elimination from an abasic site is reactive towards amines and thiols.[13, 15]

It is important to note here, that abasic sites react quantitatively with methoxyamine at physiological pH to produce a stable linkage that does not yield strand cleavage (Scheme 6-6).[16] We have used methoxyamine to quench the reactivity of the abasic sites in control experiments, as will be discussed later.

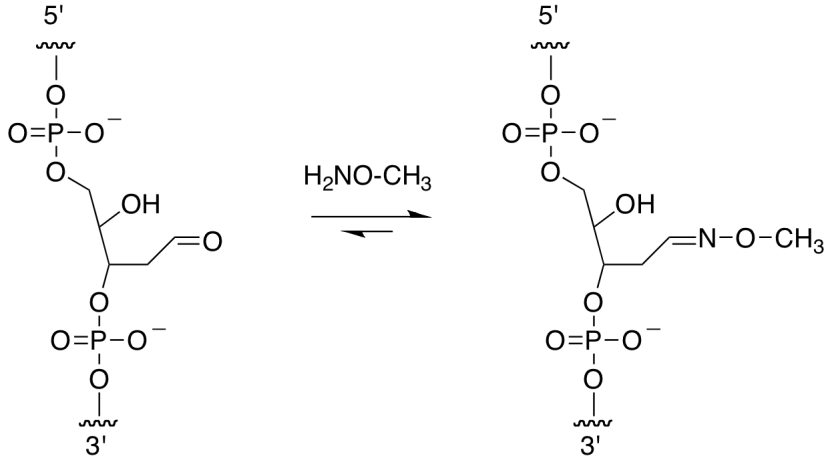

Scheme 6-6. Reaction of methoxyamine with an abasic site.[16]

6.4 Our early work

Our laboratory has explored the chemical reactivity of abasic sites for some time. Specifically, we have studied the ability of abasic sites to form interstrand crosslinks in duplex DNA. In 2007, Dr. Sanjay Dutta, from this laboratory, published a seminal paper on the reactivity of abasic sites in duplex DNA.[17] In the next few paragraphs, I will provide a brief overview of what has been done in the past, so we can have a better understanding of what was done more recently.

First, it is worth mentioning that abasic sites had, long ago, been shown to produce interstrand crosslinks in duplex DNA, however, the exact nature of the crosslink was not known.[18] The authors speculated that the crosslink could be

derived from a reaction between the open-chain aldehdye, and an amine from the opposing strand.

We were aware that the exocyclic *N*2-amino group of guanine is reactive towards aldehydes like formaldehyde, acetaldehyde, and crotonaldehyde (Scheme 6-7).[19, 20]

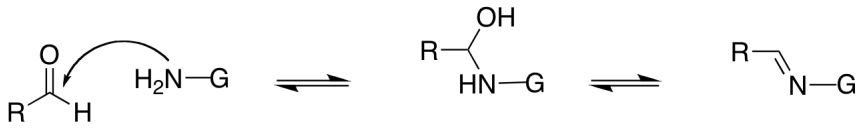

Scheme 6-7. Simple aldehydes have been shown to covalently modify the the exocyclic amino group of guanine in DNA. (G = guanine).[19]

We thought it was possible that interstrand crosslinks could be derived from the exocyclic *N*2 amino group of guanine reacting with the open chain aldehyde of the abasic site. Initially, molecular model building experiments were undertaken to identify the best sequence scenario to produce an interstrand crosslink in B-DNA. As reported in 2007, several different sequences were investigated, but the best candidate was found to be a guanine one base away from the abasic site in the 3' position (Figure 6-1).[17]

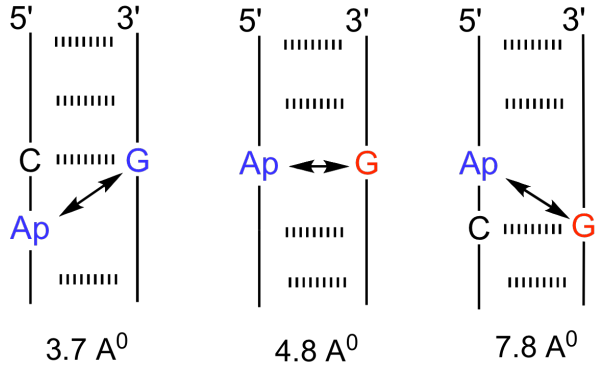

Figure 6-1. The calculated distances between the exocyclic *N*2 amino group of guanine and the open chain aldehyde of the abasic site.[17]

Abasic sites were introduced into DNA by treatment of 2'-deoxyuridine-containing duplexes with uracil deglycosylase (UDG). This enzyme hydrolytically cleaves the uracil out of the backbone of the duplex, leaving the desired abasic site (Scheme 6-8). This process is extremely efficient, generating abasic sites at greater than 99% in all oligonucleotides.[21]

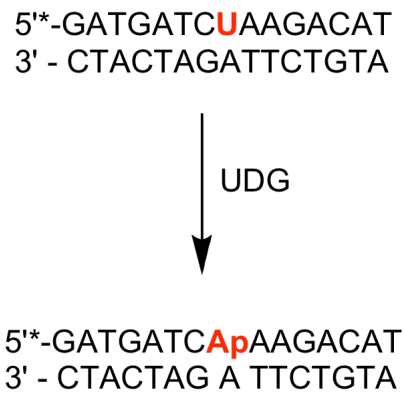

Scheme 6-8. Generation of abasic sites from uracil containing oligonucleotide with the enzyme UDG.

Indeed, Dutta found that whenever these duplexes were incubated in MES buffer (pH 5.5) in the presence of $NaCNBH_3$, a slow moving band was observed in the gel where DNA interstrand crosslinks would be expected to migrate.[17] To provide further evidence of crosslink formation, extension of the 5' or 3' side of both the abasic site containing, and guanine containing strand retards movement of the crosslink band on the gel. Moreover, the addition of methoxyamine to the crosslinking reaction completely quenched the crosslink band. Similarly, replacement of the guanine residue expected to be involved in the crosslink reaction with inosine, which lacks the exocyclic *N*2 amino group of guanine, also quenched formation of the crosslink.

Furthermore, the expected crosslink band was cut out of the gel and subjected to mass spectrometry, and the results indicated formation of a reduced, interstrand crosslink. The proposed mechanism of crosslink formation is presented in Scheme 6-9 below.

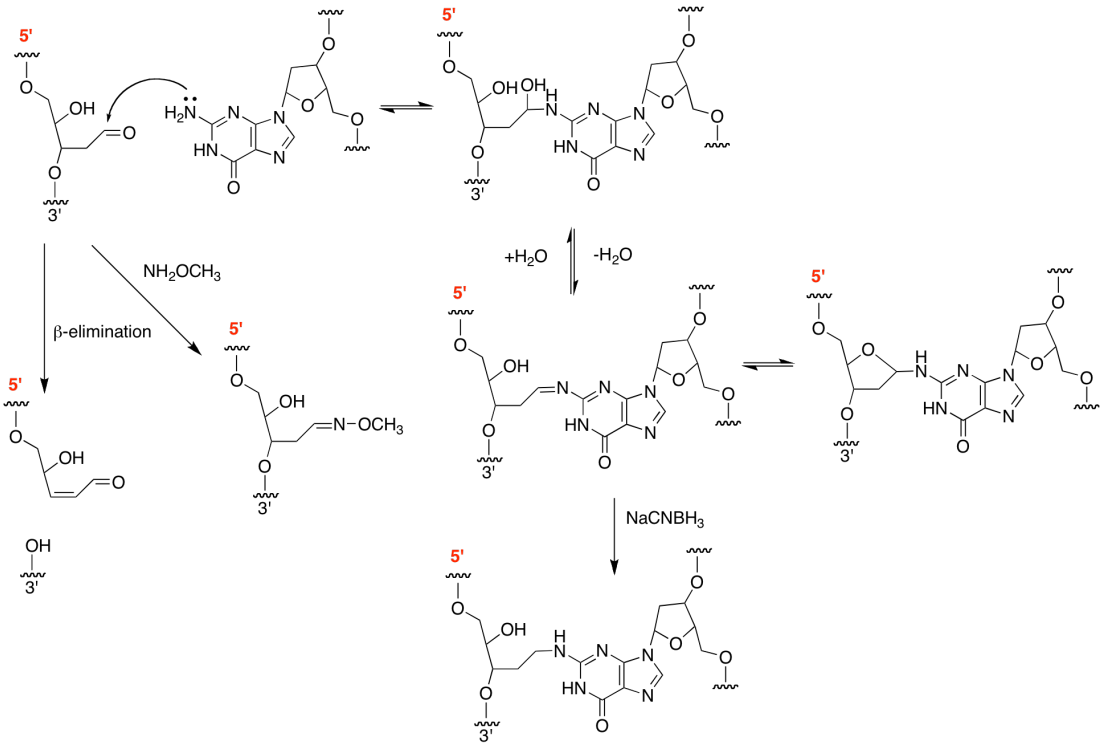

Scheme 6-9. The proposed mechanism of crosslink formation.[17] The exocyclic *N*2-amino group of guanine reacts with the open chain aldehyde form to produce an interstrand crosslink, loss of water and reduction by $NaCNBH_3$ yields the stable species in the duplex.

Lastly, we have shown that the DNA interstrand crosslink in this sequence inhibits the repair action of the human abasic endonuclease enzyme (APE1).[22] APE1 was virtually completely inhibited from cleaving the DNA at the abasic site whenever the interstrand crosslink was present in the duplex.[22] This data provides more evidence of the toxicity of Ap sites could be associated with the formation of these interstrand crosslinks in cellular DNA.

6.5 Calculation of the rate of crosslink formation.

After establishing that the crosslink forms, many questions remained about its structure and formation. First, we explored the kinetics of the reaction at both physiological pH and at pH 5.5, the reducing pH. For these experiments 5'^{32}P-radiolabelled duplex **A** (Figure 6-4) was incubated in 50 mM MOPS (3-(N-Morpholino)propanesulfonic acid) pH 7.0 and 100 mM NaCl at 30°C, and at each time point, an aliquot was taken and frozen at -20°C. The samples were desalted by Sephadex G-25 spin column and dried under vacuum. The dried aliquots were resuspended in formamide loading buffer and run in 20% polyacrylamide gel. We observed an increase in intensity of the crosslink band over time. The resulting fractional increase in crosslink band was fitted to the equation for a first-order reaction ($P_t = A_0(1-e^{-kt})$) as detailed in the Materials and Methods section. The rate of the reaction at pH 7.0 was found to be $k = 0.079\ hr^{-1}$, which corresponds to a half-life of 8.8 hours.

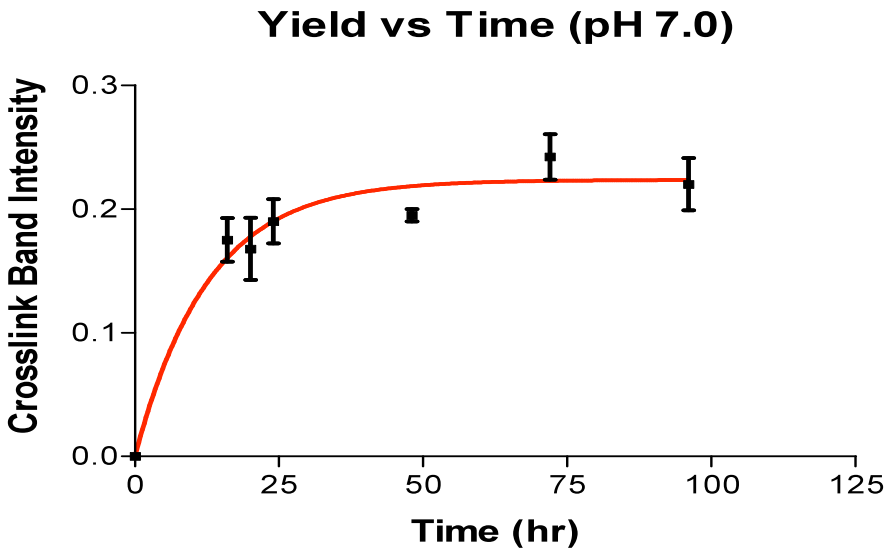

Figure 6-2. Plot of fractional increase in the slower migrating crosslink band versus time. Points represent mean with SD, n = 3.

We also explored the kinetics of the crosslink reaction at pH 5.5, since we are using those conditions to reduce with $NaCNBH_3$ to stabilize the crosslink. We performed the same kinetics experiment, as done above with the pH 7 experiments, and followed the increase in crosslink band with time (Figure 6-2).

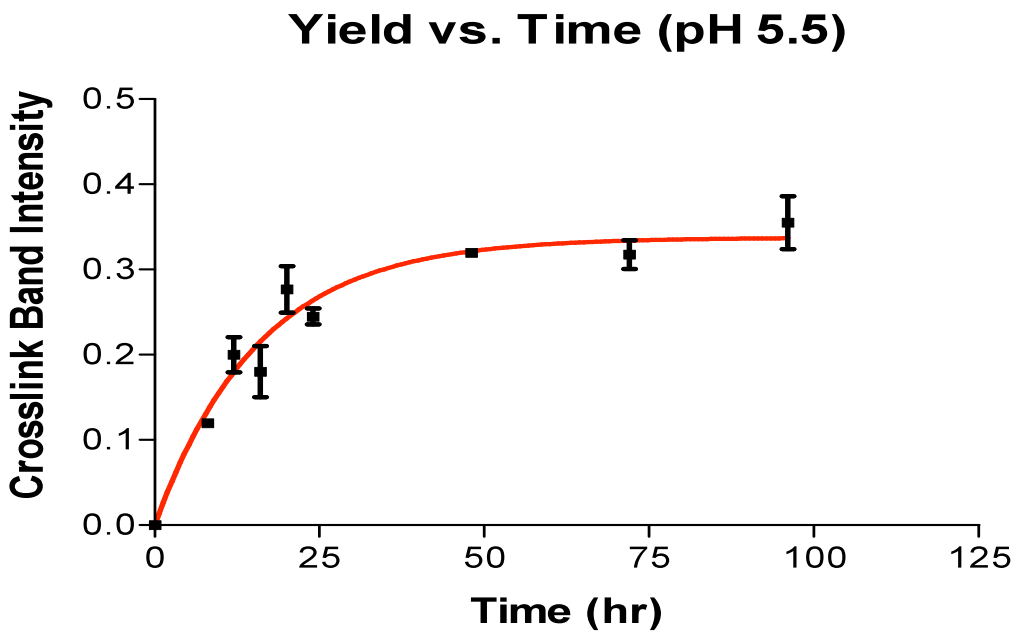

Figure 6-3. The plot of the fractional increase of the slower migrating crosslink band versus time. Points represent mean with SD, n = 3.

The rate constant for the formation of crosslink at pH 5.5 calculates to be k = 0.063 hr^{-1}, which corresponds to a half-life of 10.9 hours. This data signals that the crosslink reaction is a feasible process on a physiological time scale. DNA interstrand crosslinks are one of the most deleterious lesions known to cellular DNA. For this reason, a single unrepaired DNA crosslink is sufficient to kill a yeast or bacterial cell, and furthermore, it takes somewhere between 20-40 interstrand crosslinks to kill a repair-deficient mammalian cell.[23] Our kinetic calculations indicate that part of abasic sites widely reported toxicity could, in fact, be derived from interstrand crosslinks.

6.6 Sequence effect on formation of Interstrand Crosslinks

Next, we chose to explore the effect of sequence context on the yield of the interstrand crosslinks. There are several reports in the literature about how the base opposite an abasic site affects the overall structure and thermodynamics of duplex DNA.[24-27]

A	5'^{32}P-GATGATCApAAGACAT 3'-CTACTAG **A** TTCTGTA
B	5'^{32}P-GATGATCApAAGACAT 3'-CTACTAG **G** TTCTGTA
C	5'^{32}P-GATGATCApAAGACAT 3'-CTACTAG **T** TTCTGTA
D	5'^{32}P-GATGATCApAAGACAT 3'-CTACTAG **C** TTCTGTA
E	5'^{32}P-GATGATCApAAGACAT 3'-CTACTAG **G** TTCTGTA
F	5'^{32}P-GATGATCApAAGACAT 3'-CTACTAG **I** TTCTGTA
G	5'^{32}P-GATGATCApAAGACAT 3'-CTACTA I **I** TTCTGTA
H	5'^{32}P-GATGATCApAAGACAT 3'-CGATACTACTAG **C** TTCTGTA

Figure 6-4. Sequences of oligonucleotides used for the seqence effect experiments.

Originally, we had an adenine opposite the abasic site (duplex **A**, Figure 6-4**)**, and we wanted to explore the effect of substituting this adenine with the different bases to explore the effect of the 'base in the gap' (Figure 6-4).

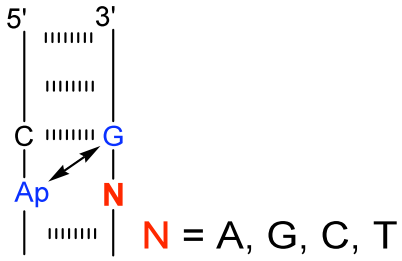

Figure 6-5. The base in the gap, or the base opposite the abasic site, was changed to explore the effect on the crosslink reaction.

Based on literature precedent, we expected the purines (guanine and, our standard, adenine) to produce an interstrand crosslink, however, we did not expect the pyrimidines (cytosine and thymidine) to produce a crosslink. This is due to literature reports that state that the pyrimidines either flip out of the double helix or exist in an equilibrium mixture of extrahelical and intrahelical conformers, whenever opposite an abasic site, resulting in collapse of the overall structure of the DNA surrounding the abasic site.[1] We proposed this "flipping out" of the double helix would quench the formation of the crosslink because the exocyclic *N*2 amino group of guanine would no longer be in the correct position to attack the open chain aldehyde of the abasic site.

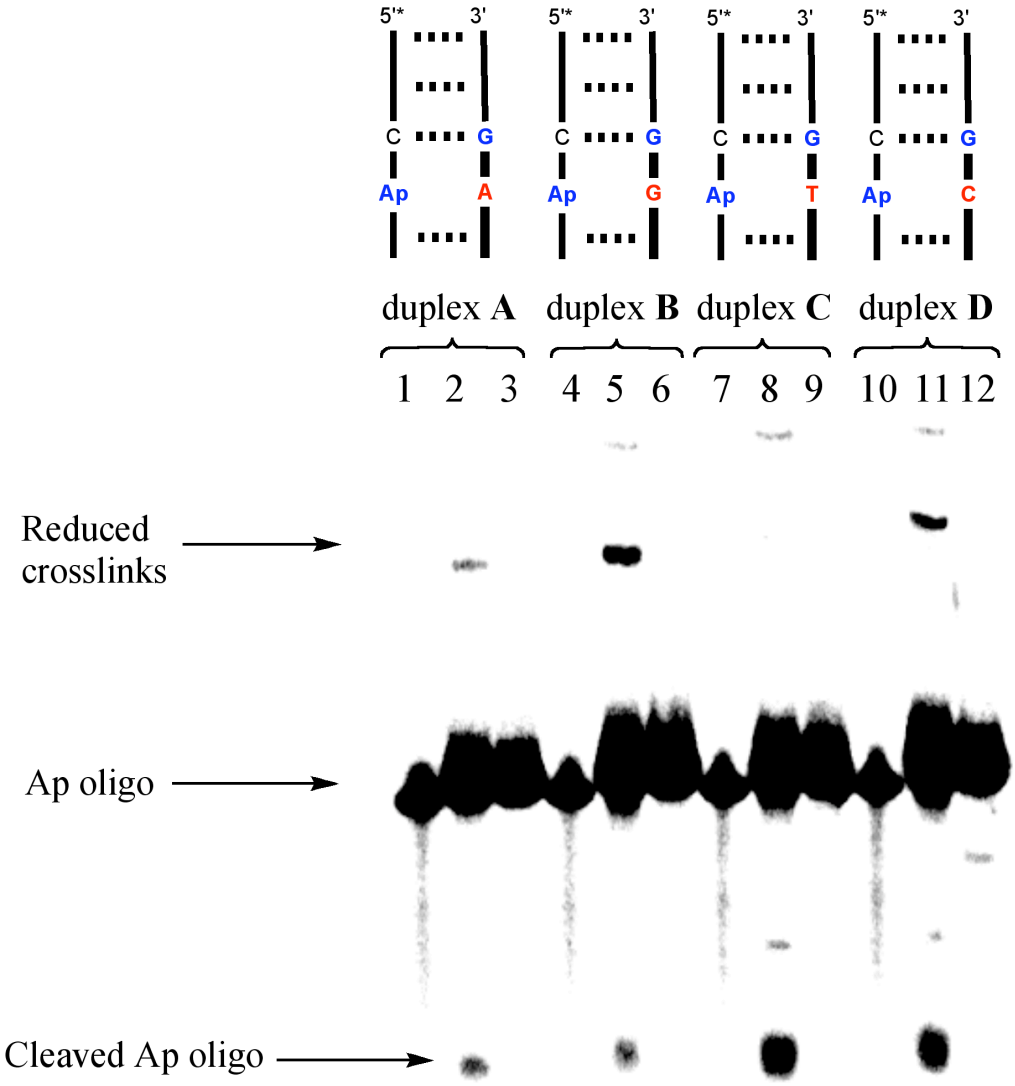

Figure 6-6. Lanes 1, 4, 7, 10, Abasic duplexes; Lanes 2, 5, 8, 11, Reduced duplexes; Lanes 3, 6, 9, 12, Reduced duplexes in presence of 20 mM methoxyamine; Reducing conditions: $NaCNBH_3$, 50 mM MES, pH 5.5 at 30 ^{0}C, 7 d, 100 mM NaCl

As can be seen in Figure 6-6 above, the base in the gap had a significant effect on the formation of the interstrand crosslink. Duplex **A**, with adenine as the base in the gap, is the standard crosslink reaction performed previously, and as expected we observed the crosslink band. Interestingly, whenever we replaced the adenine with

guanine (duplex **B**), we see an increase in the overall yield of the interstrand crosslink.

It is worth mentioning, whenever methoxyamine is added to all these crosslink reactions, we see a complete quenching of the formation of the interstrand crosslink. Methoxyamine reacts quantitatively with the open chain aldehyde of the abasic site, as mentioned previously. This provides us evidence that the open chain aldehyde is required for formation of the interstrand crosslink in all of these reactions.

As stated above, we expected the pyrimidines in the gap to quench formation of the crosslink, and indeed, whenever we replaced the adenine with thymidine (duplex **C**) the crosslink is abrogated (Figure 6-6). However, contrary to our original hypothesis, replacement of adenine with cytosine (duplex **D)** does indeed produce a crosslink band. These unexpected results were surprising, but after looking more closely at the literature we found some explanations. Chen and colleagues reported in 2008 a new study looking at the effect of the base opposite the abasic site on the overall topology of the DNA.[28] In that study, they looked at the purine, guanine, and both the pyrimidines. They found that the pyrimidines did not flip out into solvent as reported previously, but instead adopted a intrahelical conformation, within the duplex.[28] However, they did observe a perturbation of the local duplex whenever either pyrimidine was opposite the abasic site.[28] More work, including molecular dynamics calcultions and/or solution NMR must be done with our particular sequences in order to better understand the results more fully.

6.7 Sequence effect on yield of interstrand crosslink

As already noted about the guanine opposite the gap, we noticed something interesting about the sequence substitution interstrand crosslink reactions. The base opposite the abasic site affected the yield of the interstrand crosslink (Figure 6-7). Using our standard crosslink Duplex **A**, as the standard, we observe that changing the adenine to a guanine (Duplex **B**), more than doubles the yield of the crosslink. Furthermore, whenever we use a cytosine opposite (Duplex **D**), we also saw an increase in the yield of the crosslink, when compared to our standard (duplex **A**) crosslink.

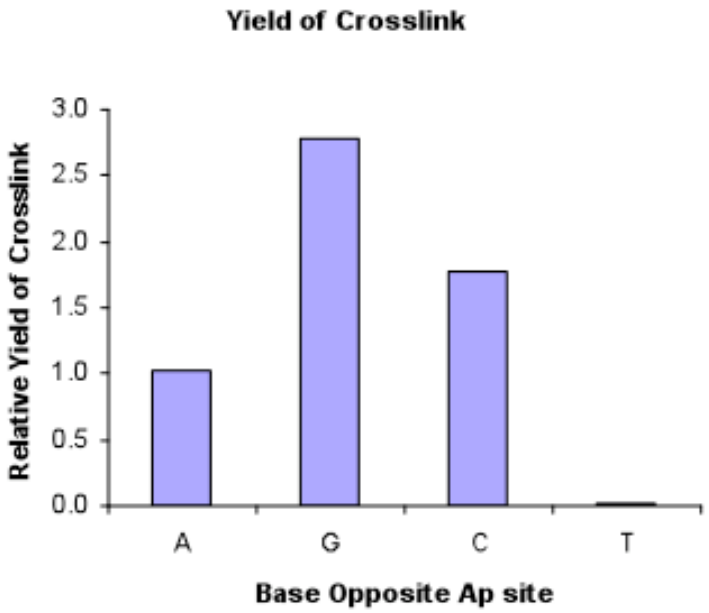

Figure 6-7. The relative yield of the crosslink band compared to our standard crosslink reaction (Duplex **A**). This experiment was performed one time only and therefore error bars cannot be calculated.

Next, in order to expand our understanding of the sequence effect on the formation of DNA interstrand crosslinks from abasic sites, we needed to do a few control experiments. In the first of several control reactions, we used inosine in place of guanine, as done previously. As mentioned above, whenever guanine is replaced with inosine (Duplex **F**) in the duplex, we see complete disappearance of the crosslink band, providing evidence that the crosslink requires the *N*2-exocyclic amino group of guanine to form a crosslink in these conditions. The structure of inosine, compared to the structure of guanine, can be seen in Figure 6-8.

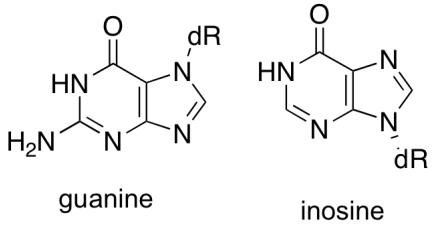

Figure 6-8 The structures of inosine and guanine. Inosine lacks the exocyclic amine of guanine.

First, we were interested in the increased yield of interstrand crosslink we observed whenever we changed the base in the gap from an adenine (duplex **A**) to a guanine (duplex **B**) in our initial sequence effect experiments. It is possible that the guanine in the gap could be reacting with the abasic site opposite it to produce a similar crosslink, one base removed. Therefore, we replaced the guanine responsible for the interstrand crosslink (in duplex **A**) with an inosine, which lacks the necessary *N*2 exocyclic amino group (Figure 6-8). Replacement of the 3' guanine (duplex **E**) with inosine completely quenched formation of the crosslink under our conditions. This provided us evidence that the 3' guanine was completely responsible for the crosslink formation observed in duplex **B**. To further confirm this, whenever we

replace the 5' guanine with inosine (duplex **F**, inosine opposite the abasic site) we observed a return of the crosslink band, as expected.

As a further control experiment, whenever we replace both the 3' and 5' guanine with inosine (duplex **G**), we see complete disappearance of crosslink formation, as we had expected. These control experiments provide even further evidence the opposite 3' guanine's *N*2-exocyclic amino group is responsible for the formation of the interstrand crosslink with the abasic site.

We chose to perform one more experiment, in order to further validate the crosslink formation in duplex **D**. We noticed the crosslink band was slightly slower moving than the crosslinks in other sequence contexts. We wanted to provide more evidence that this band was in fact a band from an interstrand crosslink. We attached a 'tail' to the 3' end of the opposing strand and subjected it to the same crosslinking conditions. Indeed, we observed a retardation of the crosslink band (Figure 6-9).

This result provides further evidence that an interstrand crosslink is forming. It is possible that the cytosine is flipping out of the duplex, causing a collapse of one side of the double helix, which might cause the crosslinked duplex to move slower through the gel. More evidence, including, but not limited to, molecular modeling of the crosslinked structure is required to form a better hypothesis.

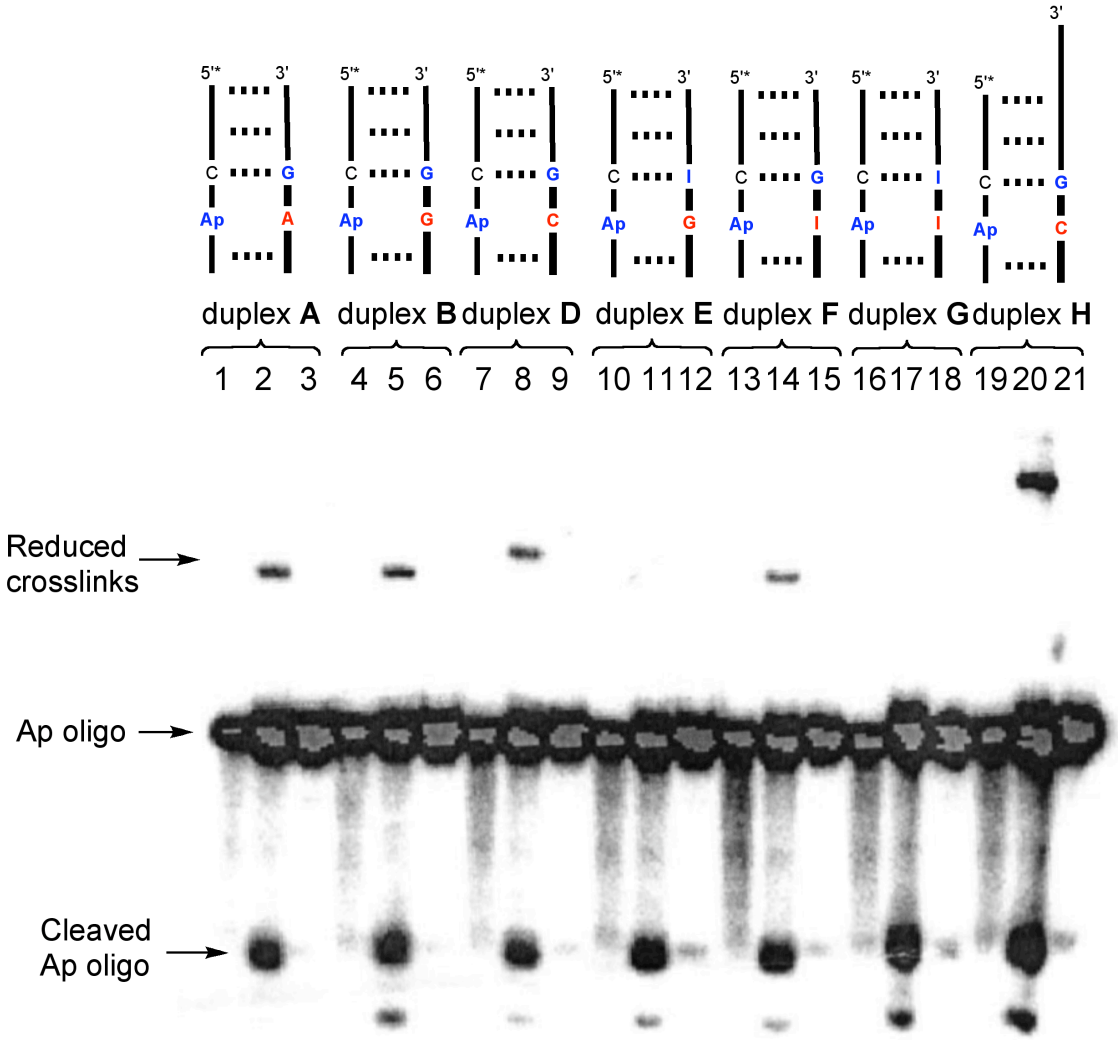

Figure 6-9. Lanes 1, 4, 7, 10, 13, 16, 19, Abasic duplexes; Lanes 2, 5, 8, 11, 14, 17, 20, Reduced duplexes; Lanes 3, 6, 9, 12, 15, 18, 21, Reduced duplexes in presence of 20 mM methoxyamine; Reducing conditions: $NaCNBH_3$, 50 mM MES, pH 5.5 at 30 ^{0}C, 7 d, 100 mM NaCl

6.8 Discussion and Conclusions

In this work, we further characterized the interstrand crosslink formed from an abasic site residue in duplex DNA. As reported previously, certain duplex sequences are capable of forming a bond between the *N*2-exocyclic amino group of guanine, and the open chain aldehyde of an abasic site. In our latest work reported here, we have calculated the rate of crosslink formation under two separate sets of conditions. In the pH 5.5 conditions, we found the half-life of crosslink formation to be 10.93 hours. Moreover, we also calculated the rate of crosslink formation under the more physiologically relevant conditions of pH 7.0, and we found the half-life of crosslink formation to be 8.76 hours, or just slightly faster than pH 5.5, our original conditions.

Next, we explored the effect of sequence context on the rate and yield of interstrand crosslink formation. Whenever the adenine opposite the abasic site was replaced with guanine (duplex **B**) we saw an increase in the yield of crosslink under the same conditions. We verified that the 3' guanine was the only guanine involved in crosslink formation by performing a series of control reactions, replacing the 3' guanine with inosine, and observing complete disappearance of crosslink formation. Furthermore, whenever the 5' guanine (opposite the abasic site) is replaced with inosine, we still observed the crosslink band in the gel. This data provides evidence that the *N*2-exocyclic amino group of the 3' guanine is involved in crosslink formation. Importantly, whenever methoxyamine was added to these reactions, we see complete quenching of the crosslink band, showing the involvement of the open chain aldehyde of the abasic sites involvement in formation of the crosslink.

In addition, whenever we changed our standard base in the gap of adenine to the pyrimidines, we experienced an unusual result. In the duplex with thymidine opposite the abasic site (duplex **C**) we observed the expected quenching of crosslink formation. We expected this result because several reports exist in the literature that state that pyrimidines opposite an abasic site flip out into solvent and cause an overall collapse of the duplex structure.[24-26] However, whenever the pyrimidine cytosine was placed opposite the abasic site (duplex **D**) we observed a slower moving crosslink band in the gel. We also observed quenching of this crosslink region band upon the addition of methoxyamine to the reaction, showing that the open chain aldehyde is likely involved in the formation of this crosslink species. We provided further verification that this band is indeed a DNA interstrand crosslink by extending the 3' end of the opposing strand with a 'tail' of residues (duplex **H**) in a separate control experiment. Indeed, the 3' tail further decreases the mobility of the crosslink species, providing further evidence an interstrand crosslink is taking place between the abasic site containing oligonucleotide and the opposing strand.

Overall, we have calculated the rates of formation of the crosslink species, and found them to be reasonable on a physiological time scale. We have also greatly increased our understanding of the effect that sequence surrounding the abasic site has on the formation of an interstrand crosslink. In our studies, clearly the best sequence context for formation of an interstrand crosslink, involves a guanine opposite the abasic site, with a guanine in the opposing 3' position (duplex **B**).

In conclusion, we have shown that sequence context is essential to the formation of interstrand DNA crosslinks from abasic sites. Future studies are

required to increase our understanding of these very toxic lesions in cellular DNA. By increasing our understanding of the formation of these interstrand crosslinks, we can better explain the toxicity of abasic sites, and their consequences.

6.9 Materials and Methods

6.9.1 Chemicals and Reagents

Reagents were purchased from the following suppliers and were of the highest purity available at the time of purchase: N,N,N',N'-tetraethylenediamine (TEMED), sodium cyanoborohydride $NaCNBH_3$, G-25 Sephadex, and 4-morpholineethanesulfonic acid (MES) were purchase from Aldrich Chemical; 3-(N-morpholino)propanesulfonic acid (MOPS), sodum acetate, methoxyamine hydrochloride, and phenol:chloroform:isoamyl alcohol (25:24:1), Sigma Chemical Company; sodium cholride, Fischer Scientific, Inc.; ethanol, Aaper Alcohol & Chemical Company; xylene cyanol, bromophenol blue, formamide, acrylamide, and urea, United States Biochemical; ammonium persulfate and *N,N'*-bisacrylamide, Boehringer Mannheim; T4 polynucleotide kinase and uracil DNA glycosylase (UDG), New England Biolabs; [γ-^{32}P]-dATP, Perkin-Elmer Life Sciences. All solvents were HPLC grade or higher and were purchase through Fischer Scientific, Inc. Oligonucleotides were purchased from Integrated DNA Technologies and were standard desalted.

6.9.2 Preparation of 5'-^{32}P-labeled abasic-site-containing DNA duplexes from uracil-containing precursor duplexes.

We prepared the ^{32}P-labeled abasic-site-containing DNA duplex, as has been reported previously.[17] The single-stranded 2'deoxyoligonucleotides were labeled using [ϒ-^{32}P]dATP and T4 polynucleotide according to established protocols.[29] The labeled oligonucleotides were purified by 20% denaturing Polyacrylamide gel electrophoresis. The resulting radiolabelled oligonucleotides were hybridized with 1.5 equivulant of the complementary strand by heating at 95°C for 5 min in MOPS (25 mM, pH 7.0), and NaCl (100 mM), then allowed to cool to room temperature (~25°C) by slow-cooling for 20 hrs. In our standard uracil deglycosylase reaction, the hybridized, uracil-containing, 5'-^{32}P labeled oligonucleotide duplex (50 μL, approximately 1,000,000 cpm) was mixed with uracil DNA glycosylase buffer (10 μL of the 10X solution from New England Biolabs), uracil DNA glycosylase (5 μL of a 1,000 units/mL solution), and 35 μL water. The resultant solution (final volume 100 μL) was incubated at 37°C for 1.5 hrs. After incubation, the protein was removed from the mixture by performing a phenol-chloroform work up (100 μL of phenol-chloroform was added, followed by vortex-mixing and centrifugation at 14,000 rpm for 5-10 min to separate the layers) was performed. The resultant aqueous supernatant containing the ^{32}P-labeled abasic oligonucleotide was passed through a Sephadex G-25 spin column (1.5 mL) and the flow through solution was stored at -20°C until use.

6.9.3 Interstrand crosslink reactions and PAGE analysis.

In a typical crosslinking reaction, the abasic-site-containing 2'-deoxyoligonucleotide duplex (~100,000 cpm, ~15 μL) was mixed with $NaCNBH_3$ (25 μL of a 535 mM solution freshly dissolved in 100 mM MES, pH 5.5; final concentrations: 50 mM MES; 270 mM $NaCNBH_3$), NaCl (5 μL of a 1M solution in water; final concentration: 100 mM NaCl), and water (5 μL; final volume, 50 μL), and the resultant solution was then incubated at 30°C for 4-7 days. Filtering through a Sephadex G-25 quenched the reaction and the resulting flow-through dried under vacuum. The dried oligonucleotides were resuspended in formamide loading buffer and an equal amount of radioactivity was loaded into each lane of a 20% denaturing polyacrylamide gel.[17, 29] The loaded gel was then subjected to electrophoresis until the bromophenol blue marker dye had migrated ~20 cm from the top of the gel (1000 V for ~3.5 hrs). The radiolabelled DNA fragments were then visualized and/or quantitated by phosphorimager analysis (Molecular Imager®FX, Imaging Screen-K, catalog number 170-7841, Bio-Rad, utilizing the program Quantity One® Version 4.2.3, Bio-Rad). The methoxyamine-containing reactions were carried out in an identical fashion as those described above with the exception of 5 μL of a 200 mM solution, in water) was added to the crosslinking reaction in place of water.

6.9.4 Calculating the Rates of Interstrand-Crosslink Formation.

In the crosslinking rate experiments, the single stranded oligonucleotide was radiolabelled, purified, and annealed with the complementary strand, to form duplex **A**, as described previously in this document. An abasic site was introduced to the duplex as described earlier. Phenol-chloroform workup and Sephadex G25 purified the oligonucleotide as described previously. In a typical reaction, about 1,000,000 cpm (50 μL) of radiolabelled duplex **A**, was incubated in 50 mM MOPS (10 μL of 500 mM MOPS, pH 7.0), 100 mM NaCl (10 μL of a 1M stock NaCl solution), and 30 μL of water (final reaction volume of 100 μL) at 30°C. At specified time points, an aliquot (10 μL) was removed and frozen at -20°C. The aliquots were filtered through Sephadex G-25 and dried under vacuum. The dried oligonucleotides were dissolved in formamide loading buffer and an equal number of counts were loaded in each lane of a 20% denaturing polyacrylamide gel. The gel was then electrophoresed at 1000 V for approximately 3.5 hrs. The radio DNA oligonucleotides in the gel were observed and quantitated by a phosphorimager as described previously in this document.

The rate of formation of the crosslink was measured by fitting the fractional increase of the crosslink band to the integrated rate expression for a first-order process: $P_t = A_0(1\text{-}e(^{-kt}))$. P_t is the fractional increase of the crosslinked band at time t. A_0 is the concentration of starting material at time zero, which is equal to P, at

infinite time. Fitting was performed using Prism version 5.0 (GraphPad Software, Inc.) Reaction half-lives were calculated using the equation $t_{1/2} = (\ln 2)/k$.

6.10 References

1. Lhomme, J.; Constant, J.-F.; Demeunynck, M., Abasic DNA structure, reactivity, and recognition. *Biopolymers* **2000,** 52 (2), 65-83.

2. Evans, A. R.; Limp-Foster, M.; Kelley, M. R., Going APE over ref-1. *Mutation Res.* **2000,** 461, 83-108.

3. Lindahl, T.; Andersson, A., Rate of chain breakage at apurinic sites in double-stranded deoxyribonucleic acid. *Biochemistry* **1972,** 11, 3618-3623.

4. Lawley, P. D.; Brookes, P., Further studies on the alkylation of nucleic acids and their constituent nucleotides. *Biochem. J.* **1963,** 89, 127-138.

5. Lindahl, T., DNA repair enzymes. *Annu. Rev. Biochem.* **1982,** 51, 61-87.

6. Loeb, L. A.; Preston, B. D., Mutagenesis by apurinic/apyrimidinic sites. *Ann. Rev. Genet.* **1986,** 20, 201-230.

7. Varshney, U.; van de Sande, J. H., Specificities and kinetics of uracil excision from uracil-containing DNA oligomers by Escherichia coli uracil DNA glycosylase. *Biochemistry* **1991,** 30, 4055-4061.

8. Wilson III, D. M.; Barsky, D., The major human abasic endonuclease: formation, consequences and repair of abasic sites in DNA. *Mutation Res.* **2001,** 485, 283-307.

9. Otterlei, M.; Kavli, B.; Standal, R.; Skjelbred, C.; Bharati, S.; Krokan, H. E., Repair of chromosomal abasic sites in vivo involves at least three different repair pathways. *EMBO J.* **2000,** 19 (20), 5542-5551.

10. McCullough, A. K.; Sanchez, A.; Dodson, M. L.; Marapaka, P.; Taylor, J.-S.; Lloyd, R. S., The Reaction Mechanism of DNA Glycosylase/AP Lyases at Abasic Sites. *Biochemistry* **2001,** 40 (2), 561-568.

11. McKenzie, J. A.; Strauss, P. R., Oligonucleotides with Bistranded Abasic Sites Interfere with Substrate Binding and Catalysis by Human Apurinic/Apyrimidinic Endonuclease. *Biochemistry* **2001,** 40 (44), 13254-13261.

12. Izumi, T.; Schein, C. H.; Oezguen, N.; Feng, Y.; Braun, W., Effects of Backbone Contacts 3' to the Abasic Site on the Cleavage and the Product Binding by Human Apurinic/Apyrimidinic Endonuclease (APE1). *Biochemistry* **2004,** 43 (3), 684-689.

13. Mazumder, A.; Gerlt, J. A.; Absalon, M. J.; Stubbe, J.; Cunningham, R. P.; Withka, J.; Bolton, P. H., Stereochemical studies of the b-elimination reactions at aldehydic abasic sites in DNA: endonuclease III from Escherichia coli, sodium hydroxide, and Lys-Trp-Lys. *Biochemistry* **1991,** 30 (4), 1119-26.

14. McHugh, P. J.; Knowland, J., Novel reagents for chemical cleavage at abasic sites and UV photoproducts in DNA. *Nucleic Acids Res.* **1995,** 23 (10), 1664-1670.

15. Bailly, V.; Verly, W. G., Importance of thiols in the repair mechanisms of DNA containing AP (apurinic/apyrimidinic) sites. *Nucleic Acids Res.* **1988,** 16 (20), 9489-9497.

16. Talpaert-Borle, M.; Liuzzi, M., Reaction of apurinic/apyrimidinic sites with [14C]methoxyamine. A method for the quantitative assay of AP sites in DNA. *Biochim. Biophys. Acta* **1983,** 740 (4), 410-16.

17. Dutta, S.; Chowdhury, G.; Gates, K. S., Interstrand crosslinks generated by abasic sites in duplex DNA. *J. Am. Chem. Soc.* **2007,** 129, 1852-1853.

18. Goffin, C.; Bricteux-Gregoire, S.; Verly, W. G., Some properties of the interstrand crosslinks in depurinated DNA. *Biochim. Biophys. Acta, Gene Struct. Expression* **1984,** 783 (1), 1-5.

19. Riggins, J. N.; Daniels, J. S.; Rouzer, C. A.; Marnett, L. J., Kinetic and Thermodynamic Analysis of the Hydrolytic Ring-Opening of the Malondialdehyde-Deoxyguanosine Adduct, 3-(2'-Deoxy-β-D-erythro-pentofuranosyl)- pyrimido[1,2-α]purin-10(3H)-one. *J. Am. Chem. Soc.* **2004,** 126 (6), 8237-8243.

20. Wang, M.; McIntee, E. J.; Cheng, G.; Shi, Y.; Villalta, P. W.; Hecht, S. S., Identification of DNA Adducts of Acetaldehyde. *Chem. Res. Toxicol.* **2000,** 13 (11), 1149-1157.

21. Lindahl, T.; Ljungquist, S.; Siegert, W.; Nyberg, B.; Sperens, B., DNA N-glycosidases. Properties of uracil-DNA glycosidase from Escherichia coli. *J. Biol. Chem.* **1977,** 252 (10), 3286-94.

22. Dutta, S. Novel Chemical Mechanisms of DNA Damage by Natural Products. University of Missouri, Columbia, MO, 2007.

23. Schärer, O. D., DNA interstrand crosslinks: natural and drug-induced DNA adducts that induce unique cellular responses. *ChemBioChem* **2005,** 6, 27-32.

24. Ayadi, L.; Coulombeau, C.; Lavery, R., Abasic sites in duplex DNA: molecular modeling of sequence-dependent effects on conformation. *Biophys. J.* **1999,** 77 (6), 3218-3226.

25. Gelfand, C. A.; Plum, G. E.; Grollman, A. P.; Johnson, F.; Breslauer, K. J., Thermodynamic Consequences of an Abasic Lesion in Duplex DNA Are Strongly Dependent on Base Sequence. *Biochemistry* **1998,** 37 (20), 7321-7327.

26. Ayadi, L.; Forget, D.; Martelli, A.; Constant, J.-F.; Demeunynck, M.; Coulombeau, C., Molecular modeling study of DNA abasic sites. *Theor. Chem. Acc.* **2000,** 104 (3-4), 284-289.

27. Singh, M. P.; Hill, G. C.; Peoc'h, D.; Rayner, B.; Imbach, J.-L.; Lown, J. W., High-Field NMR and Restrained Molecular Modeling Studies on a DNA Heteroduplex Containing a Modified Apurinic Abasic Site in the Form of Covalently Linked 9-Aminoellipticine. *Biochemistry* **1994,** 33 (34), 10271-85.

28. Chen, J.; Dupradeau, F.-Y.; Case, D. A.; Turner, C. J.; Stubbe, J., DNA oligonucleotides with A, T, G or C opposite an abasic site: structure and dynamics. *Nucl. Acids Res.* **2008,** 36 (1), 253-262.

29. Sambrook, J.; Fritsch, E. F.; Maniatis, T., *Molecular Cloning: A Lab Manual*. Cold Spring Harbor Press: Cold Spring Harbor, NY, 1989.

Protein tyrosine phosphatases control a number of functionally critical mammalian signal transduction pathways. The understanding of PTP function and regulation is critical in the search for new molecules to treat a variety of disease states. We have sought to explore the mechanisms by which small molecules from the diet or the environment may interact with PTPs to yield their respective biological consequences.

I found that the dietary aldehyde acrolein is a potent irreversible inactivator of PTP1B and explored the mechanism of inactivation of the enzyme by mass spectrometry and structure activity studies. This work suggests that some of acroleins widely reported biological effects could stem from modulation of signal transduction pathways by the inactivation or inhibition. It would be beneficial to extend these studies to cell culture, by exploring the modification of cellular PTPs from exposure to acrolein.

I also explored the mechanism of inactivation of PTP1B by the dietary isothiocyanates. Isothiocyanates have been reported to have a number of biological effects. We thought it was possible that some of these reported activities could be the direct or indirect result of modification of cellular PTP activity. We found the kinetics and mechanism of the inactivation of PTP1B by a few isothiocyanates. We plan on extending this work directly into a number of different cellular studies with these compounds in the near future. We are starting collaborations with a number of different groups on campus to explore the effects of these compounds on cellular phosphorylation pathways.

The great deal of knowledge of protein function would not be nearly as vast without the significant contributions of crystallographers. I have started a new

collaboration with another group in the department that has produced crystals of PTP1B, and will hopefully produce crystals of a multitude of different PTPs in the near future. This work shows significant promise to produce a vast amount of information about PTP mechanism, as well as inactivation by our small molecules.

Toward expanding our PTP library, I have expressed and purified another phosphatase, SHP2. I have explored the kinetics of inactivation by hydrogen peroxide with SHP2, and started crystallization trials. This work is likely to produce a significant amount of information for our laboratory. Others in the lab will continue this project and will express, purify and crystallize a number of PTPs that will have a major impact on our PTP studies.

I have also done work outside of the realm of phosphatase research. We have been interested in the chemistry of abasic sites in DNA for some time. Specifically, we have discovered abasic sites are able to form interstrand crosslinks in duplex DNA. I have investigated the kinetics and the effect of sequence context on this reaction in DNA. Future work will be aimed at expanding our understanding of the sequence context effect as well as attempting to find evidence of interstrand crosslink formation inside cells.

Overall, I feel lucky to have been apart of these exciting and interesting scientific pursuits. I look forward to seeing how future young scientists in this laboratory solve the many mysteries that have not been solved.

VITA

Derrick Russell Seiner was born on February 14, 1981 to Brent and Vesta Seiner. Derrick was preceded by a brother, Heath, and followed by another brother, Nick. He attended K-12 at Bolivar R1 public schools. Following graduation from High school, Derrick attended Southwest Missouri State University (later to be renamed Missouri State University) and received his Bachelors of Science in Chemistry in May 2004. The fall of that same year, Derrick started graduate school in Chemistry at the University of Missouri-Columbia. He obtained his PhD in Chemistry in May of 2009.

Derrick will begin his postdoctoral studies at The Albert Einstein College of Medicine under the tutelage of John Blanchard starting June 1st. Derrick will be marrying Brienne Bottenus in September of 2009.